Self-compacting concrete for submerged repair of harbours or water power plant dams

Persson, Bertil

2003

LUND INSTITUTE OF TECHNOLOGY
LUND UNIVERSITY

Division of Building Materials

Self-compacting concrete for submerged repair of harbours or water power plant dams

Bertil Persson

Report TVBM-3113, 2nd edition Lund 2003

ISRN LUTVDG/TVBM--03/3113--SE(1-67)
ISSN 0348-7911 TVBM
ISBN 91-631-4006-3

Lund Institute of Technology
Division of Building Materials
Box 118
SE-221 00 Lund, Sweden

Telephone: 46-46-2227415
Telefax: 46-46-2224427
www.byggnadsmaterial.lth.se

PREFACE

Self-Compacting Concrete, SCC, that does not require any energy for compacting in order to cover the reinforcement or fill out the mould has attracted a great deal of interest internationally and in Sweden. Nineteen full-scale bridges and other full-scale projects now exist from SCC. The technique has also been introduced for dwelling houses, tunnels and office buildings. SCC has been introduced for the production of poles, piles and pillars. Regarding concrete under severe circumstances for construction of bridges, dams, tunnels and so forth, the requirements of durability are higher and a higher level of documentation is required than for concrete that is used for dwelling houses or office buildings. The primary durability properties are chloride ingress, fire resistance, internal freezing and thawing resistance, salt freezing and thawing scaling and sulphate resistance for concrete under severe situations. All mentioned properties of a typical construction concrete were studied at our department. Salt freezing and thawing scaling, internal freezing and thawing resistance and sulphate resistance did not differ much from the corresponding properties of normal compacting concrete. Chloride ingress was larger in SCC than in normal concrete, NC. It is known from the Great Bält railway tunnel and also from the Channel railway tunnel that large scale spalling of the concrete may occur during catastrophic fire especially in concrete at low water to cement ratio, w/c. Such scaling is avoided by including polypropylene fibre also in SCC or by avoiding large quantities of filler in SCC, i.e. by the use of a cement-powder ratio, c/p, high enough. A water-binder ratio, w/b, was also important for avoiding fire spalling.

In this project the objectives were to investigate freezing and thawing resistance (internal frost resistance and salt frost scaling) of submerged cast SCC at different w/c and different air content for repair of concrete for water power plant dams and harbours in severe conditions. The objective was also to compare the result with the corresponding properties of normal submerged cast concrete, NC. w/c of the NC varied between 0.45 and 0.78. The air content of NC varied between 1 and 11% vol. For SCC the w/c varied between 0.35 and 0.49 with an air content varying between 1 and 8%. Finally the objective was to give recommendations how to produce SCC for repair of water power plant dams and harbours in severe conditions durable to freezing and thawing attack. An associated project within Vattenfall Utveckling has given valuable input to the project and also delivered a lot of specimens for tests within the project. Financial support from the Development Fund of the Swedish Construction Industry, SBUF and from Skanska Asfalt & Betong LTD, Concrete Technical Centre, BTC, is gratefully acknowledged. Furthermore gratitude is expressed to Iad Saleh, who coordinated the project. I am also most grateful to Jan Alemo and to Emma Björkenstam who offered many comments from the practical point of view. Finally, thanks are due to Stefan Backe, Ingemar Larsson and Bengt Nilsson who carried out most of the laboratory experiments.

It must be underlined that this scientific report only emphasis a description of experimental and analytical studies of workability and freezing and thawing resistance (internal frost resistance and salt frost scaling) of SCC with different w/c and increased amount of air content including a comparison with the corresponding properties of normal submerged cast concrete, NC, both concrete types intended for submerged repair of dams, foundations and columns in severe conditions.

Lund 11 November 2003

Bertil Persson

SUMMARY AND CONCLUSIONS

General

It must be underlined that this scientific report only emphasis a description of experimental and analytical studies of workability and freezing and thawing resistance (internal frost resistance and salt frost scaling) of Self Compacting Concrete, SCC, with different water-binder ratio, w/b, and increased amount of air content including a comparison with the corresponding properties of normal submerged cast concrete, NC, both concrete types intended for submerged repair of dams, foundations and columns in severe conditions. w/b of the NC varied between 0.45 and 0.78. The air content of NC varied between 1 and 11% vol. For SCC w/b varied between 0.35 and 0.49 with an air content varying between 1 and 8%. Recommendations are given how to produce SCC for repair of water power plant dams and harbours durable to freezing and thawing attack. About 3 months age applied at the start of testing. The strength development was followed in parallel. Twelve SCC with w/b = 0.35, 0.40 or 0.45 and 12 NC with w/b varying between 0.45 and 0.78 were studied related to strength and freezing and thawing resistance. The tests were carried out in fresh water (internal frost resistance) or in water with 3% of sodium chloride (salt frost scaling). The temperature during testing varied between +/- 20 °C, twice a day.

Tested concrete

Studies of the grading curves of the fresh concrete clearly showed that more fines were required in submerged cast SCC than in NC and normal SCC in order to obtain stability of the concrete in the fresh state. With a 1 mm sieve about 38% of the material in the NC mix proportions passed, about 47% of the material of the mix proportions passed 1 mm sieve width with normal SCC and about 53% of the material in the mix proportions passed 1 mm sieve width with submerged cast SCC. It became clear that a large content of air in the concrete in order to avoid frost damage to submerged cast concrete affected the strength results substantially. Increase of the air content (> 8%) as a method to avoid frost damage in concrete with w/b > 0.45 was not feasible as strength became unacceptably low. For concrete cast in the laboratory and in the field with w/b varying between w/b = 0.35 and w/b = 0.45 the strength varied between 100 and 55 MPa at 4% air content. Some effect of the position of the casting on strength was observed in the field, i.e. strength at the crest of the casting became up to 4 MPa lower than average strength and up to 4 MPa higher at the foot of the casting than average strength. The difference in strength due to the position of casting was probably dependent on segregation of aggregate in the fresh mix proportions. Some loss of air also affected strength, i.e. lower air content at the far end of submerged casting increased strength, which acted contrary to a decrease of the aggregate content.

Internal freezing and thawing resistance

Submerged cast SCC with w/b = 0.40 and $\geq$ 4% air content fulfilled the requirements (7.5% silica fume) of internal freezing and thawing resistance. The freezing rates of the specimens, which were recommended to be 14 °C/h (ASTM 666-92), varied between 6 and 9 °C/h (internal frost resistance) and between 8 and 11 °C/h (salt frost resistance). Still, the freezing rates by far exceeded the maximum values obtained in reality, 3 °C/h. Practical concrete with w/b > 0.45 and anti-washout powder did not fulfil the ASTM 666 requirements for internal loss of FRF, i.e. elastic modulus to be larger than 40% after 300 cycles. Concrete cast in the laboratory exhibited less internal frost resistance at the remote end of the L-box than near the place of casting, Fig. 1.

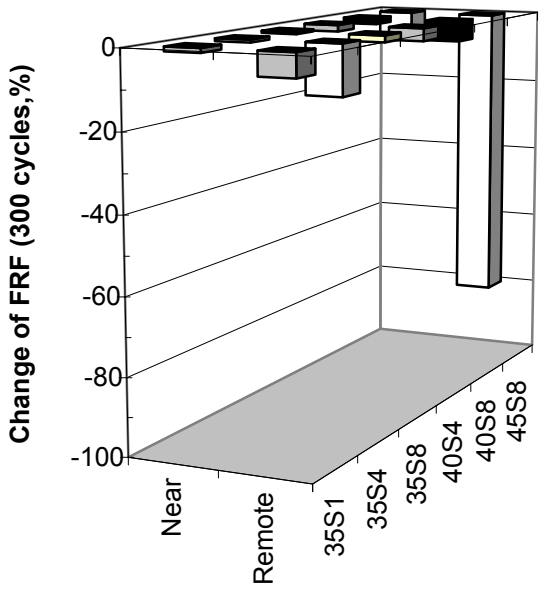

Fig. 1 – Alteration of FRF of concrete cast in a L-box. 8 = air content (%), 35 = w/b.

The difference between the frost resistance at the near and the remote end of casting in the L-box clearly indicates that either some segregation took place during the casting or that some air content was washed out during the movement of the concrete in the water. Concrete with w/b = 0.45 was not acting acceptably at the remote end at casting in the L-box (80% loss of FRF). Still, all concrete with w/b = 0.35 and w/b = 0.40 showed good internal frost resistance related to FRF (less than 13% losses of FRF after 300 cycles). Concrete cast in the field with w/b = 0.35 showed poor performance of internal frost resistance of concrete at the remote position of casting (70% loss of FRF at the crest and 40% loss of weight at the foot of casting after 300 cycles), Fig. 2. This may be a confirmation of segregation of the aggregate during the casting process of the concrete or may indicate that air was leaving the concrete. Also at the near end a tendency of larger loss of elastic modulus was observed in concrete with w/b = 0.35 than in the other concrete. Concrete with w/b = 0.40 and w/b = 0.45 in the field acted well to internal frost.

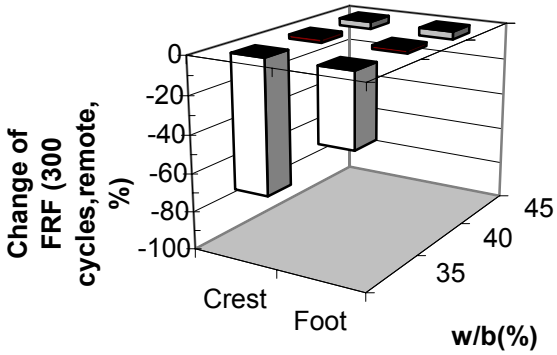

Fig. 2 – Alter of FRF of concrete. 35 = w/b. Crest and foot of mould indicated.

Salt freezing and thawing resistance

Submerged cast SCC with w/b = 0.40 (7.5% silica fume) with ≥ 4% air content fulfilled the requirements of less than 0.5 kg/m² of salt frost scaling. Salt freezing and thawing resistance is normally not required for dams, foundations and pillars in fresh water. SCC may probably not be cast submerged in seawater since cast-in chloride may cause reinforcement corrosion. Too large salt frost scaling for all practical concrete with w/b > 0.45 and anti-washout powder was observed. Concrete with w/b > 0.45 and anti-washout powder was not durable to salt freezing and thawing scaling even though as much as 8% air content was studied. SCC with w/b = 0.35 and w/b = 0.45, submerged cast in the laboratory, showed large salt frost scaling at the remote end of the L-box, Fig. 3. Air was probably washed out during the casting process, which reduced the salt freezing and thawing resistance substantially, or aggregate segregation also affected the salt frost scaling. Eight percent of air content was required for SCC with w/b = 0.35 and 4% of air content for SCC with w/b = 0.40 in order to fulfil the requirements. For w/c = 0.45 not even an air content of 8% was sufficient to obtain salt frost scaling of less than 0.5 kg/m² in the laboratory.

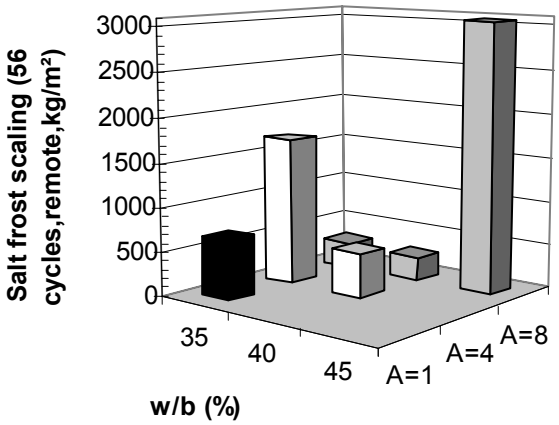

Fig. 3 – Salt frost scaling of concrete cast in the laboratory. A = air content (%).

Density, segregation and strength

A clear effect of the air content on the density of the concrete was observed. Segregation at the crest near the pump, which was almost independent of w/b, was observed in the field concrete. Some coarse aggregate probably segregated both at the near and at the remote end of casting. On the other hand results on frost resistance showed that some of the air content was lost at the remote end of casting, which caused a comparative increase of the density. With larger loss of internal frost resistance almost no change of density was observed at the far end of casting since the segregation of aggregate just compensated for the density change due to the loss of air. Still the difference in density was small and the effect on strength minor, ±4 MPa, Fig. 4.

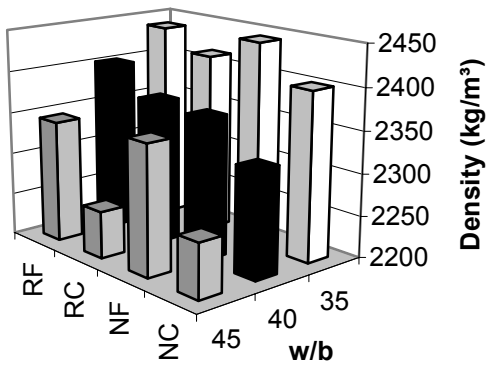

Fig. 4 – Concrete density in the field. C = crest, F = foot, N = near end of casting, R = remote end, 35 = w/b.

Recommendations

Based on previous results, results from the laboratory experiments and from experiments in the field, SCC with w/b = 0.40 (7.5% silica fume) and air content $\geq$ 4% may be used to fulfil both requirements of internal frost resistance and salt frost scaling.

SAMMANFATTNING OCH REKOMMENDATIONER

Allmänt

Det bör understrykas att denna vetenskapliga rapport bara omfattar en redogörelse för experimentella och analytiska studier av gjutbarhet och frostbeständigheten (inre frostbeständighet och saltfrostavskalning) hos självkompakterande betong, SKB, vid olika vattenbindmedelstal, vbt, med ett ökat innehåll av luft och en jämförelse av resultaten med motsvarande egenskaper hos normal undervattensbetong, NB, bägge betongtyperna avsedda för undervattensreparation av dammar, fundament och pelare. Vbt för de normal betong varierade mellan 0.45 och 0.78. Tretton SKB med vbt = 0.35, 0.40 eller 0.49 och tolv NB med vbt varierande mellan 0.45 och 0.78 studerades i fråga om hållfasthet och frostbeständighet. Lufthalter varierande mellan 1% och 11% användes i normal betong. För självkompakterande betong varierade vbt mellan 0.35 och 0.49 med en lufthalt varierande mellan 1 och 8%. Rekommendationer ges för hur frostbeständig SKB för reparation av vattenkraftsdammar och hamnar skall kunna produceras. Ungefär 3 månaders ålder användes vid försöksstart. Hållfasthetsutvecklingen hos betongen följdes parallellt. Provning ägde rum endera i destillerat vatten (inre frostbeständighet) eller i destillerat vatten med 3% koksalt (saltfrostavskalning). Temperaturen varierade mellan +/- 20 °C, två gånger per dygn.

Provad betong

Studier av partikelfördelningen hos färsk betong visade att mer finpartiklar krävdes i undervattensgjuten SKB än i normal SKB och NB i syfte att bibehålla stabiliteten i betongen i färskt tillstånd. Vid 1 mm siktvidd passerade ca 38% av material hos NB, ca 47% av materialet siktvidden 1 mm hos normal SKB och ca 53% av materialet hos färsk undervattensgjuten SKB, siktvidden 1 mm. Det klargjordes att stor tillsats av luftporbildare i syfte att göra undervattengjuten SKB frostbeständig, påverkade hållfastheten avsevärt. Ökning av lufthalten hos betong med vbt > 0.45 var inte lämplig med hänsyn till att hållfastheten då blev för låg. För betong som göts i laboratorium och i fält med vbt varierande mellan 0.35 och 0.45 erhölls hållfastheter varierande mellan 100 MPa och 55 MPa vid 4% lufthalt. En viss effekt på hållfastheten hos den fältgjutna betongen erhölls beroende av gjutningens läge, dvs. vid krönet erhölls upp till 4 MPa lägre hållfasthet än i genomsnitt och i underkant av gjutningen upp till 4 MPa högre hållfasthet än genomsnittligt. Skillnad i betonghållfasthet beroende på gjutningens läge berodde antagligen på stenseparation eller på att luft vaskades ur betongen i samband med undervattensgjutningen.

Inre frostbeständighet

Undervattensgjuten betong med vbt = 0.40 (7.5% silikastoft) och $\geq$ 4% luftinnehåll uppfyllde kraven på inre frostbeständighet. Fryshastigheten hos proverna, som rekommenderas vara 14 °C/h (ASTM 666-92), varierade mellan 6 and 9 °C/h (inre frost beständighet) och mellan 8 and 11 °C/h (saltfrostbeständighet). Fryshastigheten översteg dock de värden som uppmätts i verkligheten, 3 °C/h. Praktisk betong med vbt > 0.45 och antiutvaskningsmedel uppfyllde inte inre frostbeständigheten enligt ASTM 666-92 i fråga om inre förlust av egenfrekvens dvs. att elasticitetsmodulen, mätt som fundamentala resonansfrekvensen, FRF, efter 300 fryscykler skall vara större än 40% av utgångsvärdet. Lägre inre frostbeständighet hos betong gjuten i L-box i laboratorium observerades i den bortre delen av L-boxen än nära gjutplatsen, figur 1.

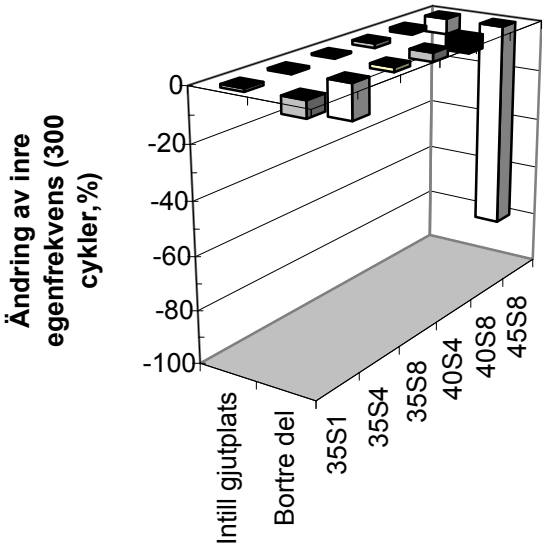

Figur 1 – Ändring av inre egenfrekvens hos betong gjuten i L-box i laboratorium. 8 = lufthalt (%), 35 = vbt.

Betong med vbt = 0.35 och vbt = 0.40 gjuten i laboratorium uppvisade ändock mycket god frostbeständighet ifråga om inre egenfrekvensen (mindre än 13% minskning efter 300 frys-cykler). Betong med vbt = 0.45 erhöll så mycket som 80% förlust av inre egenfrekvensen vid 300 cykler även med 8% lufthalt. Skillnaden i inre frostbeständighet mellan bortre och hitre delen av betong som gjutits i L-box visade att endera en viss separation inträffade eller att en del av lufthalten vaskades ur betongen under gjutningen. Betong som göts i fält visade dålig inre frostbeständighet för vbt = 0.35, figur 2. Försöken i fält visade också mycket större förlust av inre frostbeständighet i bortre delen av provkroppen i förhållande till hitre delen av provkroppen samt större förluster av inre frostbeständigheten i övre delen av provet än i undre delen. Denna indikation kan vara en bekräftelse på att betongen segregerade under gjutprocessen och att inblandad luft lämnade betongen under gjutförloppet.

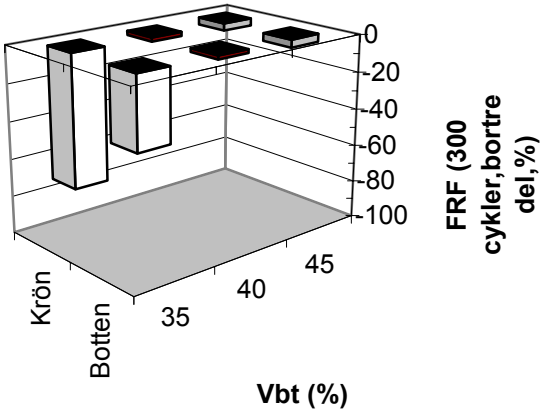

Figur 2 – Ändring av inre egenfrekvens i bortre delen av betongen.

Saltfrostbeständighet

För undervattengjuten betong krävdes vbt = 0.40 (7.5% silikastoft) med $\geq$ 4% lufthalt för att uppfylla kraven på god saltfrostbeständighet < 0.5 kg/m². Saltfrostbeständighet krävs normalt inte för dammar, fundament och pelare i sötvatten. SKB kan förmodligen inte gjutas under vatten i havet eftersom klorider då kan blandas in i betongen och förorsaka korrosion av eventuell ingjuten armering. För betong med vbt > 0.45 och antiutvaskningsmedel erhölls alltför hög saltfrostavskalning. Betong med vbt > 0.45 och antiutvaskningsmedel var inte saltfrostbeständig ens med 8% luftinnehåll vid vbt = 0.45. Betongen i bortre delen vid gjutning i L-box, där inblandad luft troligen vaskades ur under gjutningen, uppvisade en dålig saltfrostbeständighet för vbt = 0.35 och 4% lufthalt samt för vbt = 0.45 och 8% lufthalt, figur 3. För betong i bortre änden av L-boxen erfordrades 8% lufthalt för betong med vbt = 0.35 i syfte att uppfylla kraven på god saltfrostbeständighet (< 0.5 kg/m² avskalning). För betong med vbt = 0.45 uppfylldes inte kraven på god saltfrostbeständighet vid gjutning i bortre änden av L-boxen ens med 8% lufthalt.

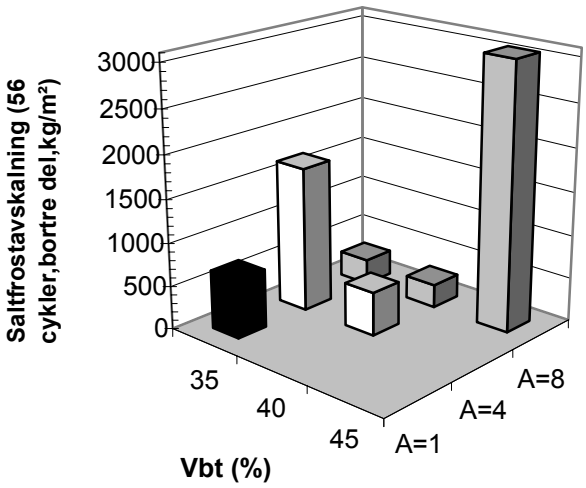

Figur 3 – Saltfrostavskalning i bortre delen av betongen efter 56 cykler vid varierande vbt och lufthalt, A (%).

Densitet, segregation och hållfasthet

Det observerades en klar effekt av lufthalten på hållfastheten hos betongen. Effekten av en densitetsskillnad var dock liten på hållfastheten i betongen. Segregation ägde rum i ytan av betongen nära pumpplatsen nästan oberoende av

betongens vbt. En del grövre ballast vaskade troligen ut från krönet närmast gjutplatsen och transporterades till nedre delen av provet, i den bortre delen av konstruktionen, vilket förfaller att vara logiskt. Trots effekten av segregationen på densiteten blev inverkan på betongens hållfasthet liten, ±4 MPa, figur 4.

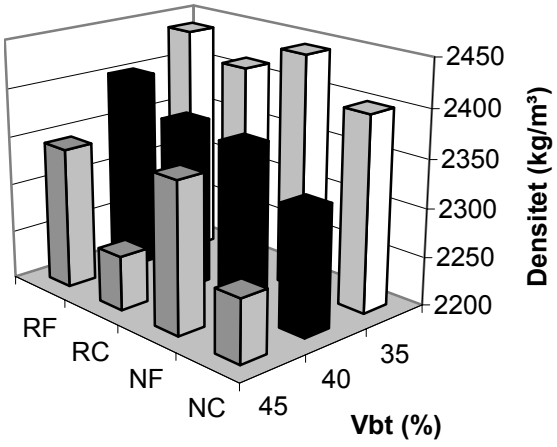

Figur 4 – Densitet som funktion av gjutplats och vbt. C = krön, F = botten av form, N = nära gjutplats, R = bortre del av betongen.

Rekommendationer

Baserat på resultat från tidigare försök, resultat från laboratorieförsök samt resultat från fältförsök uppfyllde SKB med vbt = 0.40 (7.5% silikastoft) och en lufthalt $\geq$ 4% kraven på inre frostbeständighet och saltfrostavskalning.

CONTENTS

SYMBOLS

a,b	denotes constants given in Table 2.1	
c/p	cement-powder ratio	
d	denotes the diameter of the specimen	(mm)
f_{cm0} =	10 MPa	
f_{cm}	denotes 28-day strength	(MPa)
t	denotes age	(days)
t_0	denotes age at loading	(days)
$t_{0,T}$	denotes age adjusted to 20 °C (all specimens were stored at 20 °C only)	
t_1	= 1 day	
$t_{1,T}$	= 1 day	
s	denotes constants given in Appendix 2.13	
w/b	water-binder ratio	
A	air content (%)	
AEA	air-entraining admixture	
B	increased amount of filler	
BTC	Concrete Technical Centre	
D	chloride migration coefficient	(m^2/s)
D	24% PFA and 9% SF	
DAA	deaerating admixture,	
D_f	durability factor	
E_{de}	denotes the elastic modulus, i.e. FRF, at the end of the testing.	
E_{d0}	denotes the elastic modulus, i.e. FRF, at the start of the testing.	
F	12% PFA and 5% SF	
FA	fly ash	
FRF	fundamental resonance frequency	
G =	15% GF and 5% SF	
GF	glass filler	
HPMC	hydroxypropyl methylcellose	
K	Limus 40 limestone filler	
KO28	limestone powder only	
N	new mixing order (filler at the last)	
N	nenotes number of cycles at the end of the test	
NC	normal concrete	
O	ordinary mixing order (filler at the first)	
P	denotes the value of the parameter	
PFA	fly ash	(%)
R	NC	
ROII28	normal concrete, ordinary mixing order, second, 28 days' start age	
S	specific surface of air voids	(1/mm)
S	Limus 15 limestone filler	
Sc	salt freezing and thawing scaling	(kg/m²)
SCC	Self-Compacting Concrete	
SF	silica fume	(%)
T =	CEMIII with 68% slag content	
T	5.5 m hydrostatic pouring pressure	
TSA	Thaumasite Sulphate Attack	
VMA	Viscosity-Modifying Admixtures	
α	= -1 for slowly hardening cement; = 0 otherwise.	
6	6% air content	
28	28 days' age at start of testing.	

1. INTRODUCTION, LIMITATIONS AND OBJECTIVE

1.1 Introduction

Self-Compacting Concrete, SCC, that does not require any energy for compacting in order to cover the reinforcement or fill out the mould has attracted a great deal of interest internationally and in Sweden. Nineteen full-scale bridges and other full-scale projects now exist from SCC [1]. The technique has also been introduced for dwelling houses, tunnels and office buildings [2-4]. SCC has been introduced for the production of poles, piles and pillars [5-12]. Regarding concrete under severe circumstances for construction of bridges, dams, tunnels and so forth, the requirements of durability are higher and a higher level of documentation is required than for concrete that is used for dwelling houses or office buildings. The primary durability properties are chloride ingress, fire resistance, internal freezing and thawing resistance, salt freezing and thawing scaling and sulphate resistance for concrete under severe situations. All mentioned properties of a typical construction concrete were studied at our department. Salt freezing and thawing scaling, internal freezing and thawing resistance and sulphate resistance did not differ much from the corresponding properties of normal concrete, NC. Chloride ingress was larger in SCC than in NC. It is known from the Great Bält railway tunnel and also from the Channel railway tunnel that large scale spalling of the concrete may occur during catastrophic fire especially in concrete at low water to cement ratio, w/c. Such scaling is avoided by including polypropylene fibre also in SCC or by avoiding large quantities of filler in SCC, i.e. by the use of a cement-powder ratio, c/p, high enough. w/b, high enough, was also important for avoiding fire spalling.

1.2 Limitations

Twelve SCC with w/c = 0.35, 0.40 or 0.45 and 12 NC with w/c varying between 0.45 and 0.70 were studied related to strength and freezing and thawing resistance. About 3 months age applied at the start of testing. The tests were carried out in fresh water (internal frost resistance) or in water with 3% of sodium chloride (salt frost scaling). The temperature during testing varied between +/- 20 °C, twice a day. The concrete was water-cured from casting until testing. All the specimens were core-drilled from a larger specimen of concrete. In this way the effects of bleeding, carbonation, concrete skin, crazing, segregation and so forth were avoided. The strength development was followed in parallel.

1.3 Objectives

The objectives were to investigate freezing and thawing resistance (internal frost resistance and salt frost scaling) of submerged cast SCC at different w/b and different air content for repair of concrete for water power plant dams and harbours in severe conditions. The objective was also to compare the result with the corresponding properties of normal submerged cast concrete, NC. Finally the objective was to give recommendations how to produce SCC for repair of water power plant dams and harbours durable to freezing and thawing attack.

2. PREVIOUS RESEARCH

2.1 Salt freezing and thawing resistance

2.1.1 General effects

An overview gave the effects of concrete constituents on the salt freezing and thawing scaling [13]. Effect of five parameters after 56 cycles were studied, Fig. 2.1, which gave an equation:

$$P = a \cdot \ln(Sc) + b \qquad (2.1)$$

a,b denotes constants given in Table 2.1
w/b water-binder ratio (x10)
A air content (%)
P denotes the value of the parameter
PFA fly ash (%)
S specific surface of air voids (1/mm)
Sc salt freezing and thawing scaling (kg/m²)
SF silica fume (%)

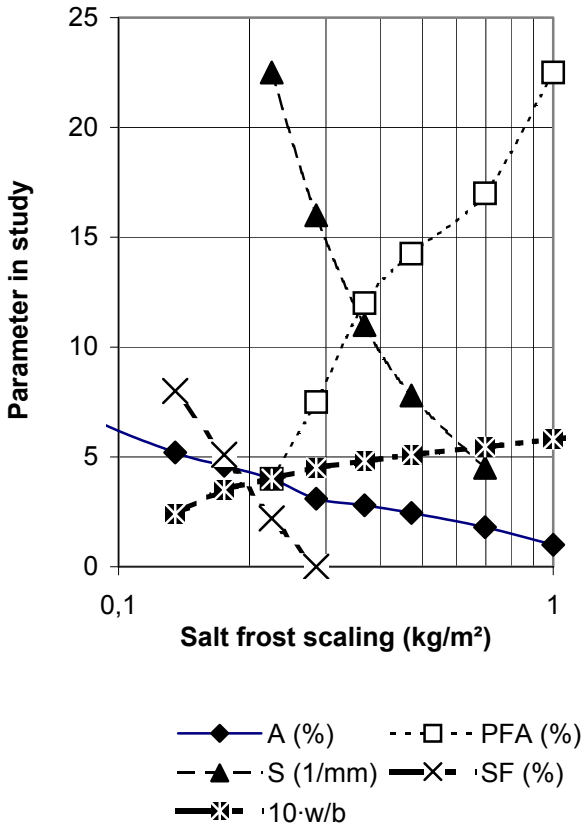

Fig. 2.1 - Effect of air content, A (%), fly ash, PFA (%), specific surface of air voids (1/mm), S, silica fume, SF (%) and water-binder ratio, w/b (x10) on salt freezing and thawing scaling of concrete.

Table 2.1 - Constants of equation (2.5)

P	A	PFA	S	SF	10·w/b
Sort	(%)	(%)	(1/mm)	(%)	-
a	-2.83	11.8	-15.6	-10.8	1.23
b	0.28	22.3	-2.8	-13.7	5.70

2.1.2 Influence of mineral additives

The salt freezing and thawing scaling increased with increasing amounts of fly ash and at higher w/b but decreased with all other parameters such as higher air content, higher silica fume content and with a larger specific surface of the air voids. The salt freezing and thawing scaling of concrete with pure Portland cement, OPC, and of concrete with additives was compared [14], Fig. 2.2. Concrete with OPC contained 4% air, concrete with 10% fly ash, PFA, and 5% silica fume, SF, 6.2% air and concrete with 40% fly ash and 5% SF 5.2% air. However, the increase of salt freezing and thawing scaling shown in Fig. 2.2 for concrete with additives may also be as a result of an increasing w/b. At about w/b = 0.38 the salt freezing and thawing scaling of concrete with 40% fly ash and 5% silica fume (5.2% air content) was 10 times that of concrete with pure Portland cement (4% air content) [14], which more or less confirms the results of [13], Fig. 2.1. In another study the effect of fly ash, ground blast furnace slag and silica fume on the salt freezing and thawing scaling was investigated [15]. Appendix 2.1 shows the mix proportions of the in this study and Fig. 2.3 the salt freezing and thawing scaling. The air content of all the studied concrete was close or equal to 6%. Salt freezing and thawing scaling increased in concrete with large amounts of slag compared with the corresponding scaling of Portland cement concrete, Fig. 2.3 [15]. The salt freezing and thawing scaling was acceptable at less than 0.5 kg/m³ scaling after 56 cycles [15].

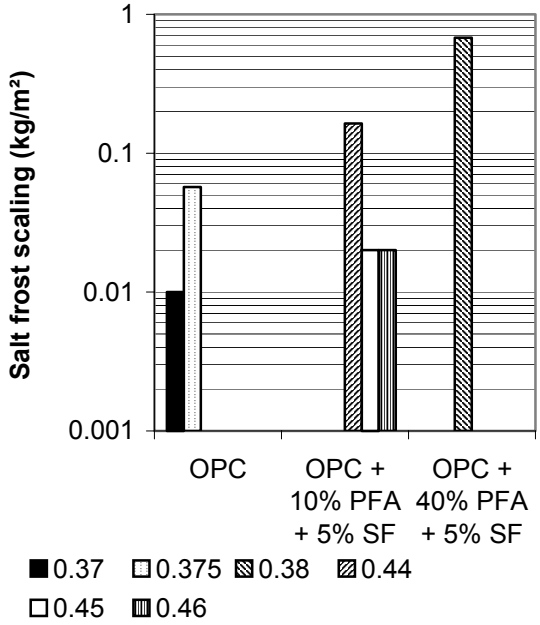

Fig. 2.2 - Salt freezing and thawing scaling of concrete with Portland cement and of concrete with additives. w/b is given (0.37 < w/b < 0.46).

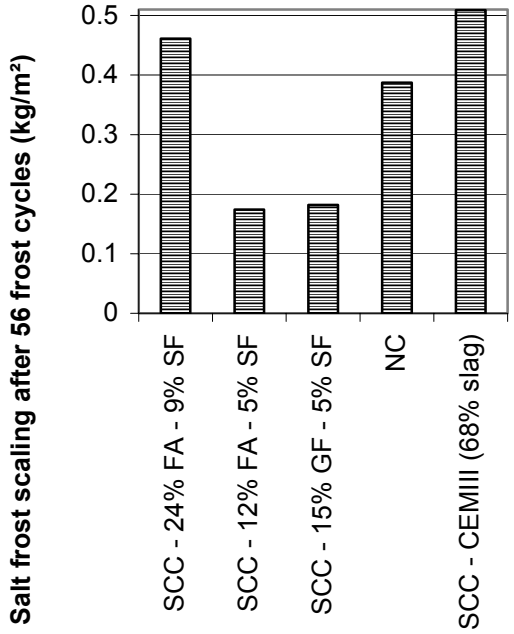

Fig. 2.3 - Salt freezing and thawing scaling of SCCs with additives. FA = fly ash, GF = glass filler, NC = normal concrete, SF = silica fume.

However, for concrete with 12% fly ash and 5% silica fume as calculated on the cement content, less salt freezing and thawing scaling was observed than for a normal concrete without these additives. For 24% fly ash and 9% silica fume larger salt freezing and thawing scaling was obtained than for the normal concrete, Fig. 2.3. The salt freezing and thawing scaling to a great degree also depends on the air void system created in the concrete. The salt freezing and thawing scaling is not only dependent on the type of binder.

2.1.3 Comparison between NC and SCC

Salt freezing and thawing scaling and internal freezing and thawing resistance of SCC and NC were studied by Rougeau, Maillard and Mary-Dippe [16]. Mix composition, properties, salt freezing and thawing scaling and FRF from this investigation is shown in Appendix 2.2. The FRF gives a measurement of dynamic elastic modulus, which in turn is a measurement of the internal damage. The following conclusions were drawn:

1. Salt freezing and thawing scaling and the loss of FRF were larger for NC than for SCC.
2. Salt freezing and thawing scaling increased with time for NC but remained constant for SCC at 0.9 kg/m², which was obtained after 28 cycles.
3. NC exhibited a total loss of the internal solidity after 150 freezing and thawing cycles while SCC lost only 7% of the cohesion.
4. After 300 freezing and thawing cycles the decline of the cohesion was 12% of SCC.

2.1.4 Effect of cement type

The salt freezing and thawing scaling of concrete with pure Portland cement (CEM I) and that of concrete with cement CEM II (14% limestone filler) was compared [17], Fig. 2.4. The w/b varied between w/b = 0.42 for concrete with pure Portland cement and w/b = 0.43 for concretes with limestone filler. The air content varied as follows:

1. Concrete with pure CEM I: 5.8% air
2. Concrete with CEM I + 13% PFA + 5% SF: 5.4 % air
3. Concrete with CEM II: 5.8% air
4. Concrete with CEM II +13% PFA + 5% SF: 7.2 % air

No significant effect of limestone filler in concrete on salt freezing and thawing scaling was observed (CEM I and CEM II) [17]. Concrete with CEM I, 13% PFA and 5% silica fume exhibited an increase of salt freezing and thawing scaling as compared to concrete with no additives. The effect of additives on the salt freezing and thawing scaling with CEM II could not be set since the air content was not constant.

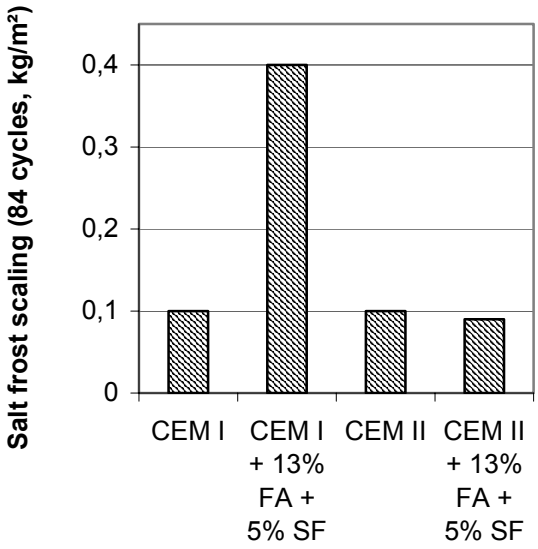

Fig. 2.4 - Salt freezing and thawing scaling with CEM and CEM II (14% limestone).

2.1.5 Effect of w/b, silica fume and slag

Salt freezing and thawing scaling after 56 freezing and thawing cycles at 28 days' starting age of concrete with 5% silica fume, SF, or with 30% blast furnace slag was compared with that of concrete without additives (OPC). All concrete had 4.6% air content [18]. Fig. 2.5 shows salt freezing and thawing scaling after 56 cycles versus w/b (1:1). The salt freezing and thawing scaling decreased with larger w/b, in contrary to what was demonstrated by [13], i.e. increase of salt freezing and thawing scaling with increase of w/b.

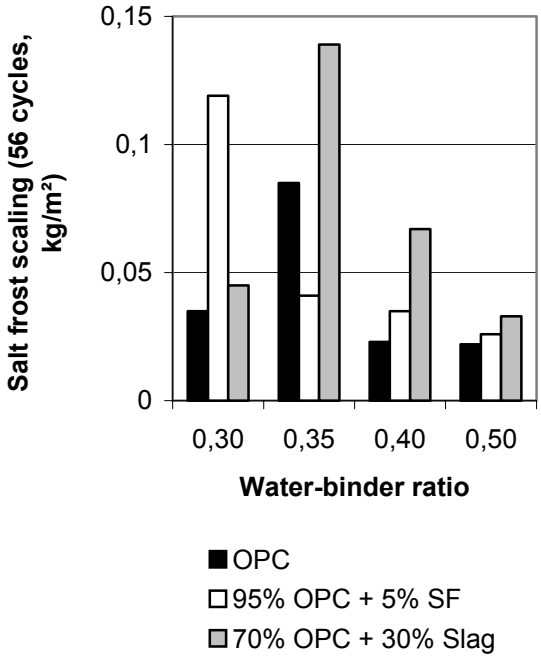

Fig. 2.5 - Salt freezing and thawing scaling after 56 cycles versus w/b with OPC, either 5% silica fume, SF, or 30% blast furnace slag (air content 4.6%).

At w/b = 0.35 the salt freezing and thawing scaling of concrete with OPC was about 4 times that of concrete with w/b = 0.50. At w/b = 0.35 the salt freezing and thawing scaling of concrete with 5% SF was about half that of concrete without silica fume, SF. Concrete without SF exhibited larger salt freezing and thawing scaling than concrete with OPC and 5% SF at w/b = 0.30, 0.40 and 0.50. On average concrete with 5% SF obtained about 35% larger salt freezing and thawing scaling than concrete with pure OPC (concrete with 30% slag obtained about 70% larger scaling on average than concrete with pure OPC). As related to strength the salt freezing and thawing scaling seemed to be increasing at higher strength (the air content was about 4.6%), Fig. 2.6. Concrete with 30% slag and 85 MPa strength (w/b = 0.35) obtained about three times as large freezing and thawing scaling as concrete with 30% slag and 90 MPa strength (w/b = 0.30), which may be an effect of self-desiccation. Self-desiccation is much more pronounced at low w/b. However, for concrete with 5% silica fume the opposite results were found: at w/b = 0.30 (100 MPa strength) the salt freezing and thawing scaling was about three times that of concrete with w/b = 0.35 and 90 MPa strength.

2.1.6 Effect of water absorption

Water absorption after capillary suction of 56 salt freezing and thawing tests, the loss of internal elastic modulus and the sulphate resistance of SCC with different amount of filler were studied [19]. The fillers in use were fly ash, PFA, or silica fume, SF or combinations of these two additives. No air-entrainment was used in the concrete (about 1.5% natural air content at higher water-binder ratio, w/b, and about 3% air content at low w/b). As expected, the water-absorption increased with larger w/b, Fig.s 2.7-8 [19]. However, with more additive of fly ash less absorption was observed. The structure then became more dense due to the interaction of OPC and fly ash.

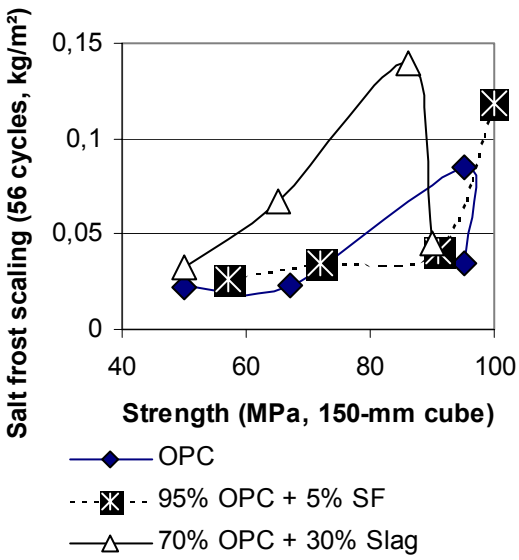

Fig. 2.6 - Salt freezing and thawing scaling after 56 cycles of concrete with pure OPC, 5% silica fume, SF, or 30% blast furnace slag (air content 4.6%).

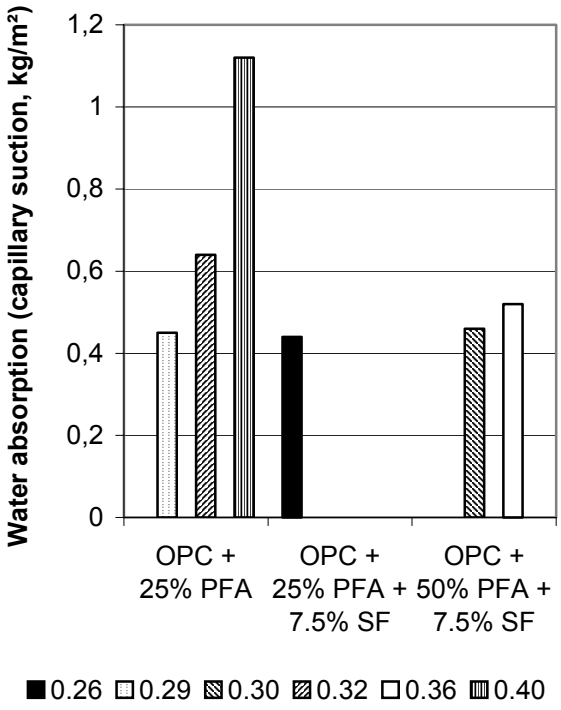

Fig. 2.7 - Capillary suction decreased with more fly ash, but increased with higher.

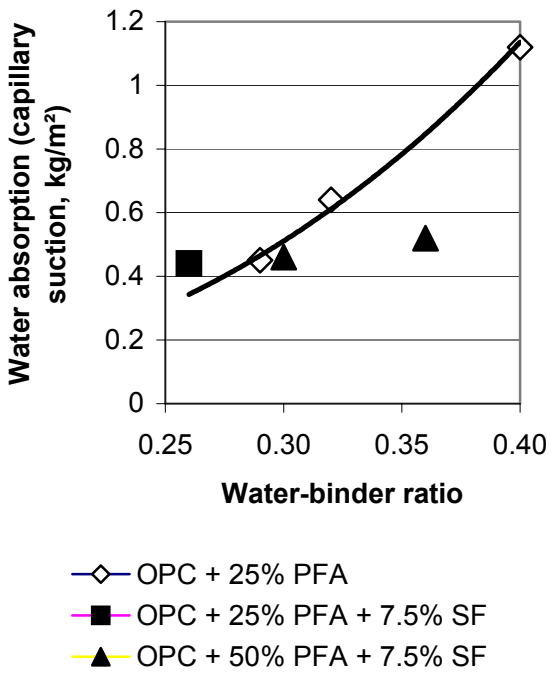

Fig. 2.8 - Water-absorption versus w/b.

Salt freezing and thawing tests were performed according to [20], Fig.s 2.9-10. Since no air-entrainment was used the denser structure with more fly ash (50% instead of 25%) caused larger expansion during the freezing and thawing cycles followed by larger water absorption [19]. The relative elastic modulus of concrete after 56 freezing and thawing cycles was also examined [19], Fig. 2.11-12. Large water absorption of concrete with 50% fly ash or with w/b = 0.40 caused internal destruction due to salt freezing and thawing attacks (the concrete did not contain air-entrainment). Concrete at w/b < 0.30 did not need air-entrainment to withstand 56 salt freezing and thawing cycles, Fig. 2.12, indicated by [21].

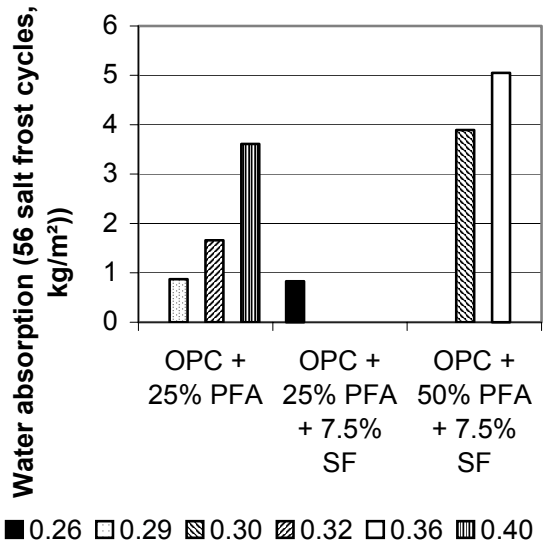

Fig. 2.9 - Water-absorption after 56 cycles increase with fly ash. w/b ratio is given.

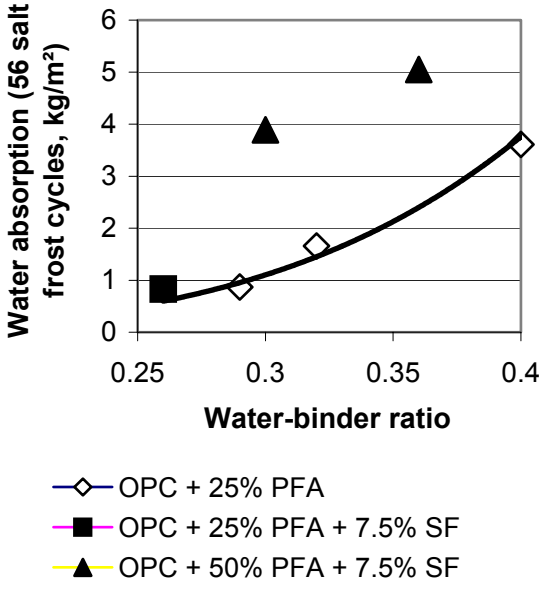

Fig. 2.10 - The water-absorption (after 56 salt freezing and thawing cycles) increased with the water binder ratio and with larger amount of fly ash.

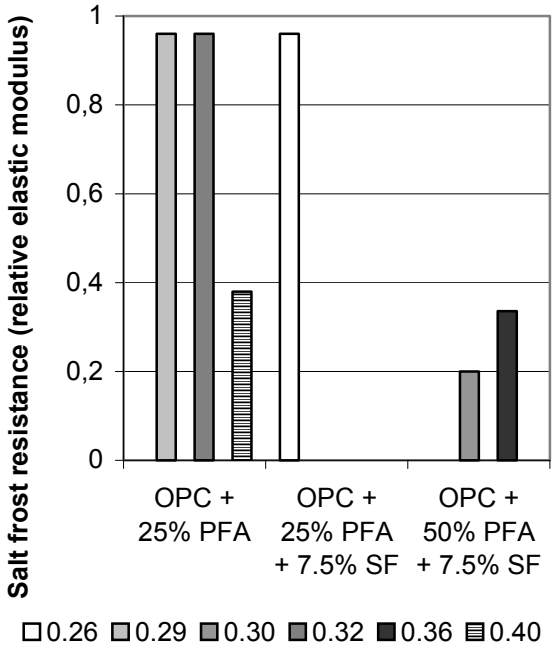

Fig. 2.11 - Relative elastic modulus after 56 freezing and thawing cycles. w/b ratio is given.

In this case self-desiccation of concrete prohibited internal expansion large enough to damage the concrete. On the other hand, the loss of elastic modulus was larger in concrete with 50% fly ash and 7.5% silica fume than with 25% fly ash despite a low w/b = 0.30, Fig. 2.11 [19].

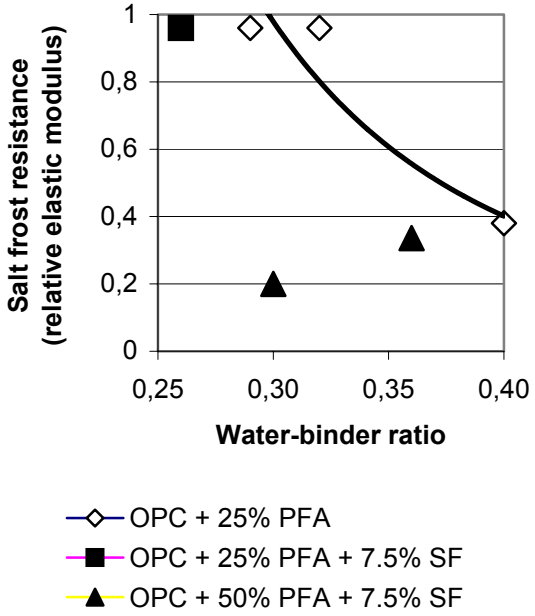

Fig. 2.12 - Relative elastic modulus of concrete after 56 freezing and thawing cycles versus w/b.

2.1.7 SCC

Concrete performs excellent with less than 0.20 kg/m² salt freezing and thawing scaling after 56 cycles, and good with less than 0.50 kg/m². Fig. 2.13 shows results of salt freezing and thawing scaling at 28, 56 and 112 freezing and thawing cycles of concrete shown in Appendix 2.3 [22-26]. Only comparison between the different concretes may be done. SCC obtained the same salt freezing and thawing scaling as NC did. The following conclusions were drawn at 112 cycles:

1. More filler did not increase the amount of salt freezing and thawing scaling.
2. At 28 days' start age salt freezing and thawing scaling was larger in SCC than in NC.
3. SCC with 5.5 m pouring pressure instead of 0.23 m did not obtain more salt frost scaling.
4. SCC with coarser limestone filler (Limus 40) obtained more salt frost scaling than SCC with finer limestone filler did (Limus 15).

2.2 Internal freezing and thawing resistance

2.2.1 Effect of mineral additives

Figs 2.14-16 show results on fundamental resonance frequency, FRF, length and mass change after 100 and 300 freezing and thawing cycles in distilled water [22-26]. Notations in Figs 2.14-16:

- D = 24% PFA and 9% SF
- F = 12% PFA and 5% SF
- G = 15% GF and 5% SF
- KO28 = limestone powder only
- ROII28 = normal concrete
- T = CEMIII with 68% slag content

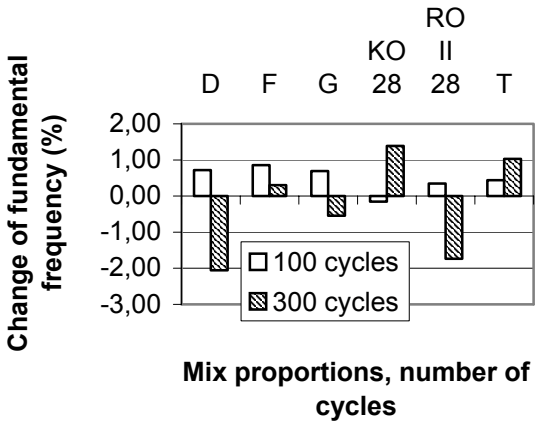

Fig.s 2.14 –FRF after 100 and 300 freezing and thawing cycles. Notations are given above.

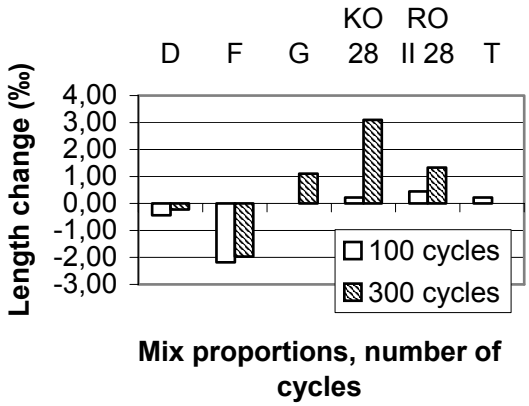

Fig.s 2.15 – Length after 100 and 300 freezing and thawing cycles (± 20 °C). Notations above.

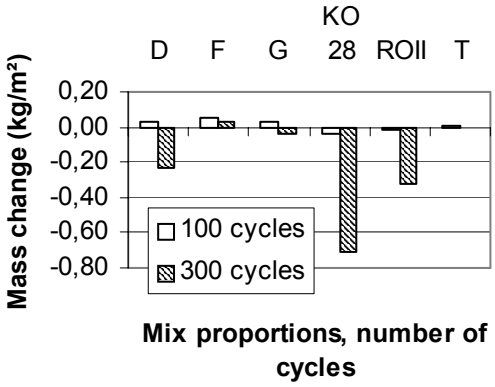

Fig.s 2.16 – Change of mass after 100 and 300 freezing and thawing cycles in distilled water.

For the mix proportions D and ROII the decrease of FRF after 300 freezing and thawing cycles coincided well with the loss of weight. For other mix proportions, F, G and T, small changes of the measured properties were observed, which indicates better performance to internal freezing and thawing resistance than concrete D and ROII did. After length changes the FRF increased in the SCC KO28 due to water absorption, Fig. 2.17.

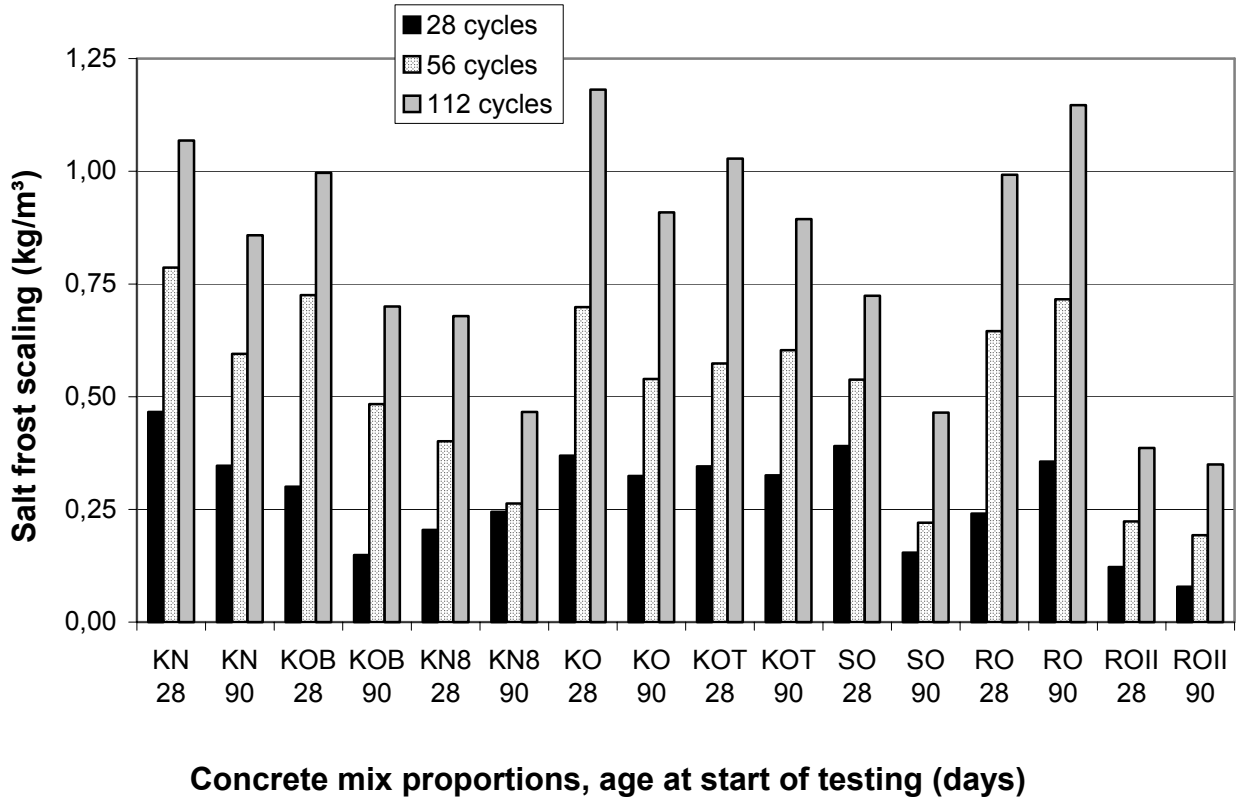

Fig. 2.13 – Salt freezing and thawing scaling at 28, 56 and 112 freezing and thawing cycles, Appendix 2.3. B = increased amount of filler; K = Limus 40 limestone filler; N = new way of mixing (filler last); O = ordinary way of mixing; R = NC; S = Limus 15 limestone filler; T = 5.5 m hydrostatic pouring pressure, II = second; 28 = 28 days' age at start of testing.

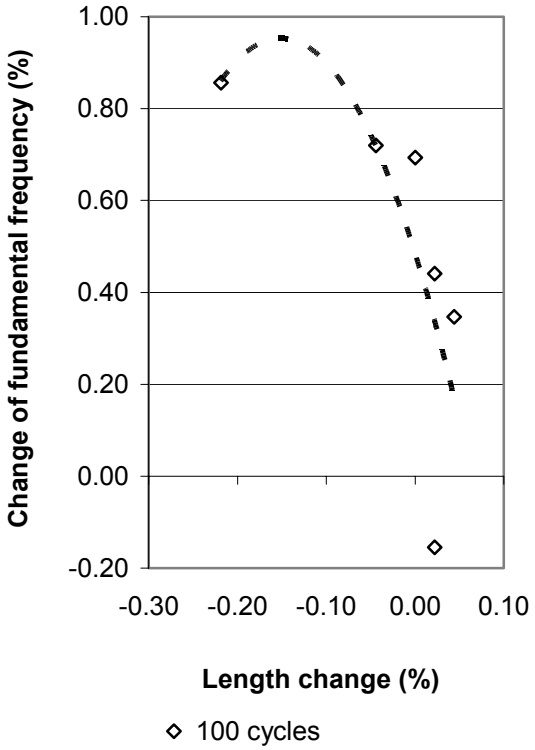

Fig. 2.17 – FRF versus length change.

2.2.2 SCC

Fig.s 2.18-20 show results on internal frost resistance on the FRF, length change and change of mass after 100 and 300 freezing and thawing cycles in distilled water (± 20 °C)of concrete in Appendix 2.3 with cement specifications given in Appendix 2.4. SCC in Appendix 2.3 exhibited much larger changes in FRF, length and mass than concrete in Appendix 2.1, which indicated the resistance to internal freezing and thawing to be of lower in SCC with limestone filler than in concretes with silica fume, fly ash, slag or glass filler. The first NC, RO, was almost destroyed after 300 freezing and thawing cycles (about 80% loss of FRF, about 1% increase in length and about 2,5 kg/m² loss of weight). The comparative Fig.s for NC named RO II were 2% loss of FRF, about 0.1% increase in length and about 0.3 kg/m³ loss of weight after 300 cycles. Fig. 2.21 shows FRF versus length change.

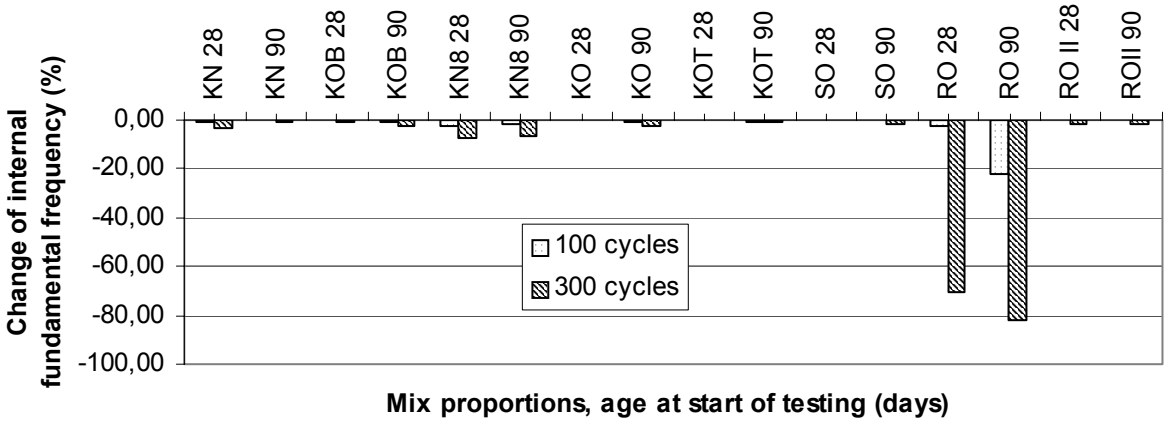

Fig. 2.18 – Change of FRF of concrete in Appendix 2.3 after 100 and 300 freezing and thawing cycles in distilled water (± 20 °C). B = increased amount of filler; K = Limus 40 limestone filler; N = new way of mixing (filler last); O = ordinary way of mixing (filler first); R = reference; S = Limus 15 limestone filler; T = 5.5 m hydrostatic pouring pressure instead of 0.23 m; II = second.

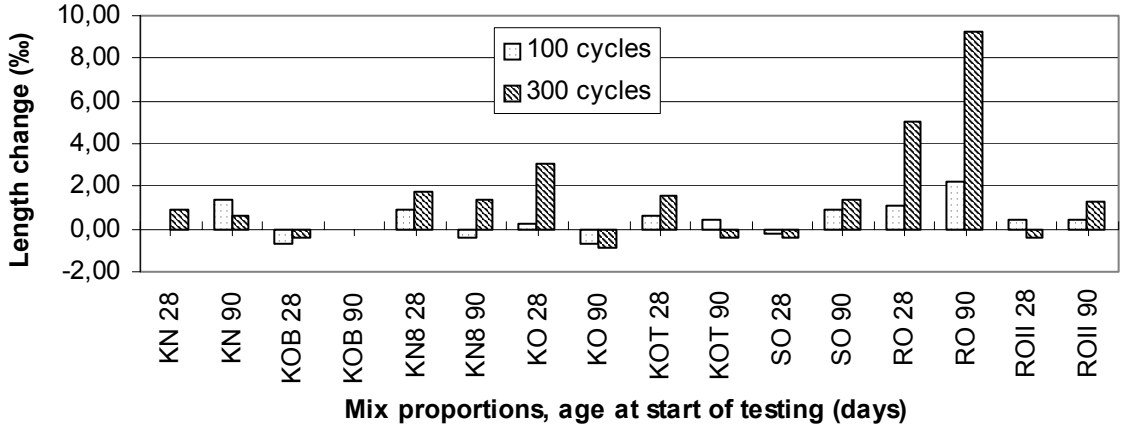

Fig. 2.19 – Length change of concrete after 100 and 300 freezing and thawing cycles in distilled water (± 20 °C).

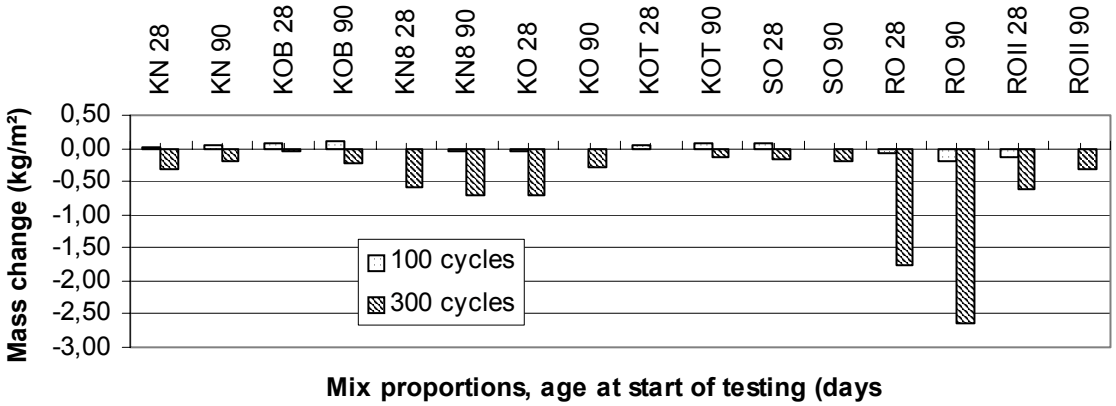

Fig. 2.20 – Change of mass of concrete after 100 and 300 freezing and thawing cycles in distilled water (± 20 °C).

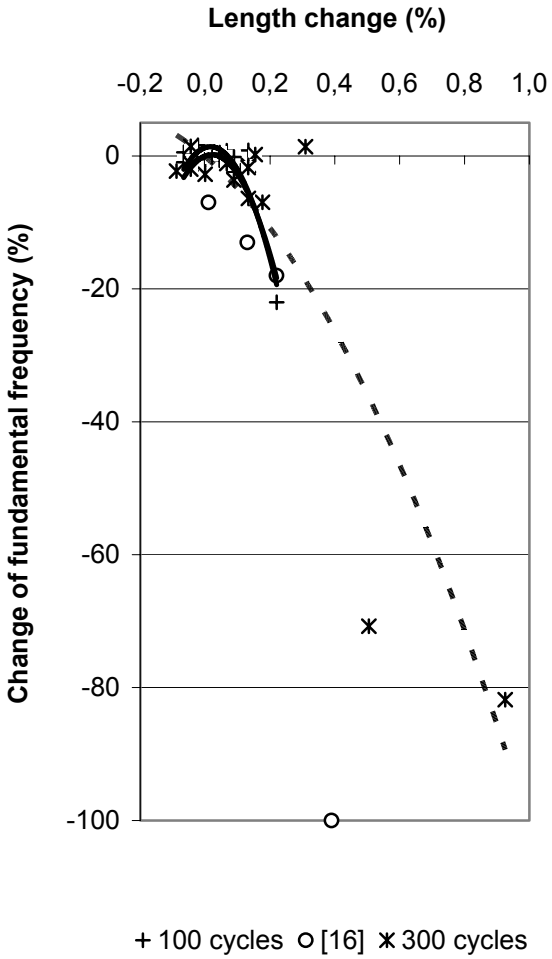

Fig. 2.21 –FRF versus the length change.

Fig. 2.22 shows a summary of change on average of FRF, Fig. 2.23 shows a summary of length change and Fig. 2.24 a summary of the loss of weight of SCC mix proportions with the same type of limestone filler (brand Limus 40) and 6% or 8% air content and of NC with 6% air content independent of the age at start of testing, Appendix 2.3-4. It may be observed that the SCC with 6% air content resisted internal freezing and thawing better than SCC with 8% air. Increased amount of air content is supposed to increase the internal freezing and thawing resistance as well. Therefore tests of the significance of the results on the effect of air-entrainment were performed on mix proportions KN and KN8 which show that the change of fundamental resonance frequency, FRF, and mass of concrete was significantly larger for SCC with 8% than for than for SCC with 6% air ($z > 2$; the difference in length change was not significant different since $z < 2$). Tests of significance of the results on the effect of compaction method were also performed on mix proportions KO, RO and RO II in Appendix 2.3. These tests show that the change of FRF and mass of concrete was significantly larger for NC than for both SCC mixes with 6% air ($z > 3$; difference in length change showed a significant different at 90 days' age at start of testing; $z = -5.7$).The conclusion is that it is not feasible to increase the air content too much in concrete that is supposed to obtain increased ability to resist internal freezing and thawing attack.

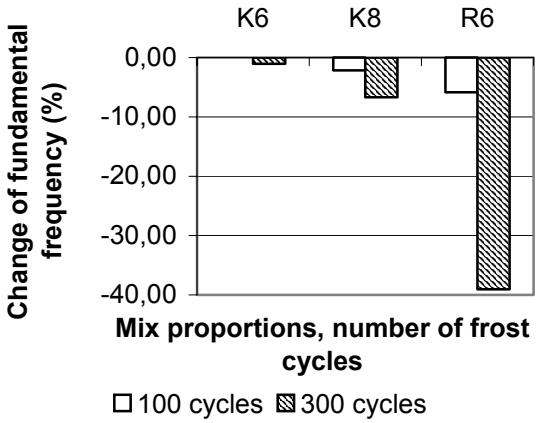

Fig. 2.22 – On average change of FRF of concrete in Appendix 2.3. K = SCC with limestone filler. R = NC; 6 = 6% air content.

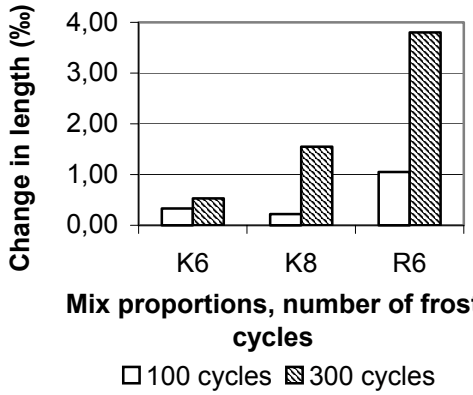

Fig. 2.23 – On average length change of concrete in Appendix 2.3. K = SCC with limestone filler. R = NC; 6 = 6% air content.

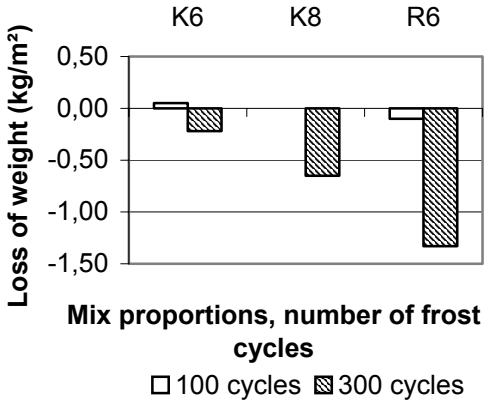

Fig. 2.24 –Loss of weight of concrete in Appendix 2.3. K = SCC with limestone filler. R = NC; 6 = 6% air content.

2.3 Thaumasite sulphate attack

Concrete shown in Appendix 2.3 (except for ROII) were tested for Thaumasite Sulphate Attack, TSA, in sodium sulphate 18 g/l (distilled water). TSA is of interest for concrete in harbours or concrete foundations when sulphates exist in the ground water. The sodium sulphate was replaced every month and slowly rotated by a propeller. The temperature was held at 5 °C. Fig. 2.25-2.26 show the change of fundamental resonance frequency, FRF, and the mass change over 900 days. The corresponding results for distilled water curing and seawater curing are also shown in the Fig. 2.25-2.26. Seawater from Barsebäck was used (1% sodium chloride). The following conclusions were drawn [27]:

1. No correlating was found between the water-powder ratio and the change of FRF with normal mixing order (filler first) nor the mass, i.e. the content of lime stone filler did not accept the properties, Fig. 2.27
2. With reversed mixing order (filler last) larger scaling of the surface of SCC was observed after 900 days of TSA (concrete KN 28 and KN 90), especially when combined with an increased amount of air content (KN8 28, KN8 90)
3. The damage of SCC with reversed mixing order was clearly visible
4. Distilled water curing or curing in seawater did not affect FRF nor the mass of SCC with reversed mixing order like curing in sodium sulphate did.
5. For NC with ordinary mixing order no large different was not observed of FRF nor the mass when the concrete was cured in distilled water or seawater.

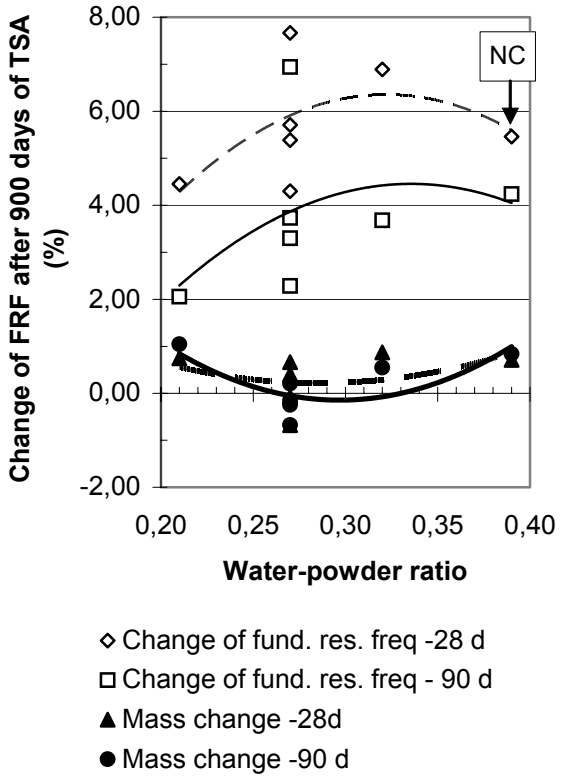

Fig. 2.27 – Change of FRF and the mass change over 900 days versus water-powder ratio, w/p, of TSA at w/c = 0.39. 28 = 28 days' age at start of testing.

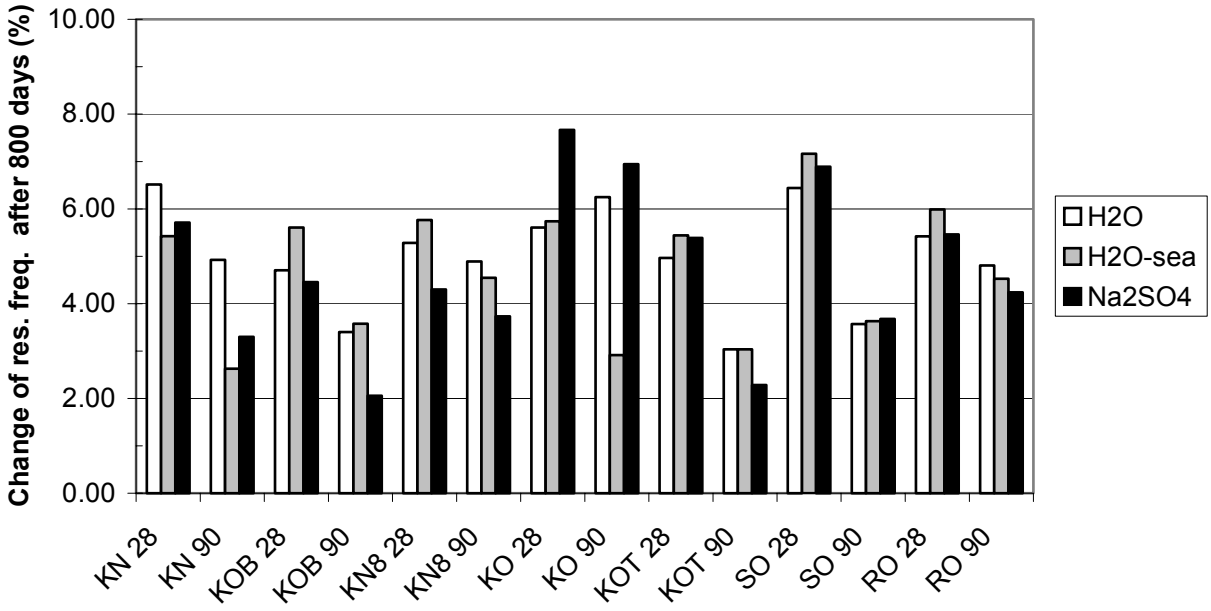

Fig. 2.25 - Change of FRF over 800 days of TSA.. B = increased amount of filler; K = Limus 40 limestone filler; N = new way of mixing (filler last); O = ordinary way of mixing; R = NC; S = Limus 15 limestone filler; T = 5.5 m hydrostatic pouring pressure, 28 = 28 days' age at start of testing.

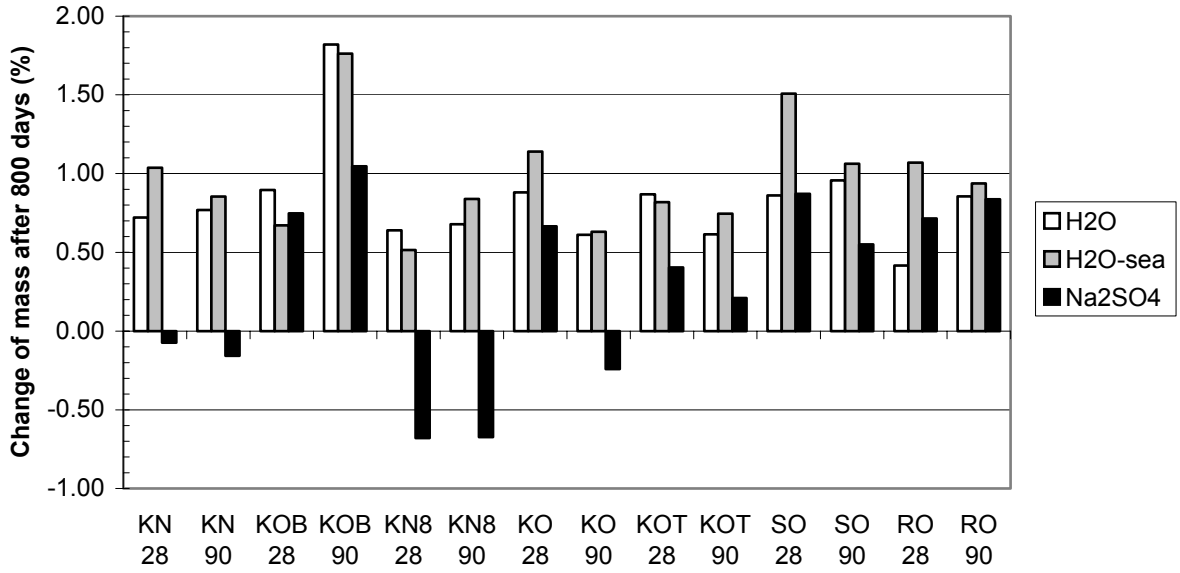

Fig. 2.26 - Change of mass change over 800 days of TSA. B = increased amount of filler; K = Limus 40 limestone filler; N = new way of mixing (filler last); O = ordinary way of mixing; R = NC; S = Limus 15 limestone filler; T = 5.5 m hydrostatic pouring pressure, II = second; 28 = 28 days' age at start of testing.

2.4 Chloride migration coefficient, D

2.4.1 Effect of w/c

It was important to achieve a submerged cast SCC that not only was resistant to frost but also to other aggressive factors in sea water such as chlorides. Fig. 2.28 shows D of 3-year old SCC with quartzite filler and of NC [22]. All concrete mixes contained Portland cement (CEMI42.5R Slite Std) except for concrete with w/c = 0.27, in which the low-alkali Portland cement (CEMI42.5BV/SR/LA Degerhamn) was used, Appendix 2.4 [22]. The mix proportion is given in Appendix 2.5. The measurement was performed with a rapid test method developed by Tang [28]. First of all w/c ought to be low in order to control D. For SCC with w/c = 39%, D = $13 \cdot 10^{-12}$ m^2/s was obtained. From Fig. 2.28 an expression for D at 3 years' age was obtained by linear regression (10^{-12} m^2/s, w/c in %) [22]:

$$D = (0.97 \cdot w/c - 25) \cdot 10^{-12}\ m^2/s \quad \{27\% < w/c < 80\%;\ R^2 = 0.96\} \qquad (2.1)$$

2.4.2 Effect of mineral additives

Another factor influencing on D is the content of mineral additives. D was studied for 3 Portland cement concretes and 1 silica fume, SF, concrete, Fig. 2.29 [29]. The mix proportions are found in Appendix 2.6 [29]. D decreased in concrete with silica fume compared with a pure Portland cement based concrete with the same w/c [29].

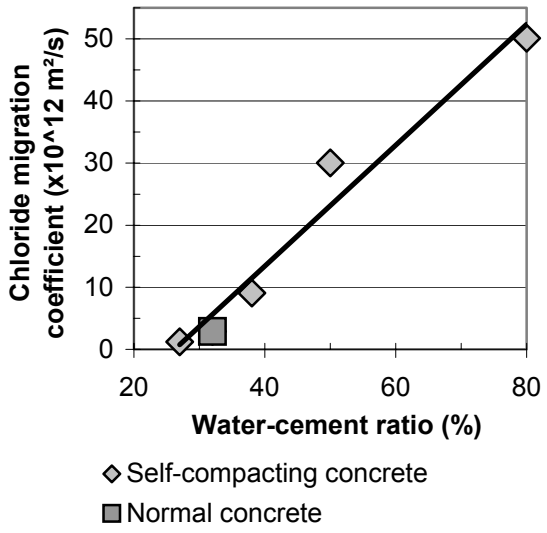

Fig. 2.28 - Chloride migration coefficient, D, of 3-year old SCC with quartzite filler and of NC.

The electrical conductivity was studied on concrete discs of NCs for the Great Belt Link, [30-32]. Especially in silica fume concrete the conductivity of NCs was reduced substantially. The effect of fly ash on the electrical conductivity in Portland cement concrete was insignificant [31]. Alteration of the amount of fly ash in NC did not affect D. In another project 4 types of SCCs and one NC for marine environment were studied, Fig. 2.30 [15]. The mix proportions of the concrete in the experiment are given in Appendix 2.1.

A decrease of D was observed when using slag cement or silica fume concrete. Also in this case the effect of fly ash on D in Portland cement concrete was found to be insignificant [32]. When using glass filler instead of fly ash D remained on the same level, Fig. 2.30. When using 68% slag of the slag cement a very low D was found, Fig. 2.30 [15].

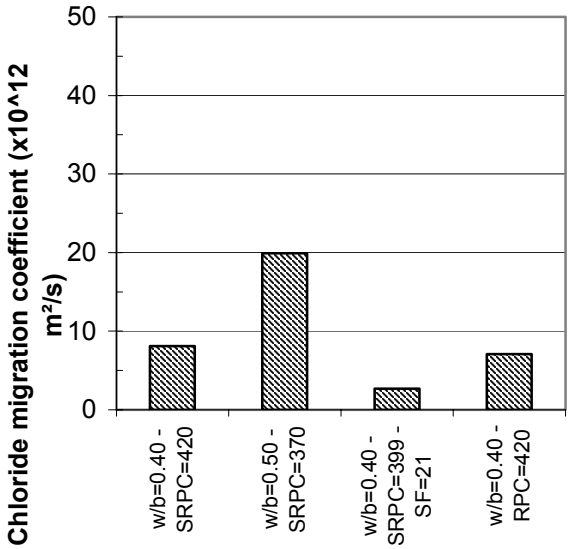

Fig. 2.29 - D of OPC and silica fume concrete.

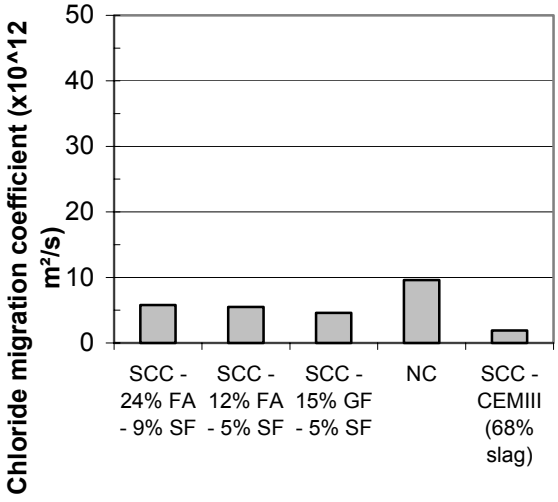

Fig. 2.30 – D was studied for SCC and NC. FA = fly ash, GF = glass filler, SF = silica fume.

2.4.3 Effect of self-desiccation

After water curing of concrete with low w/c, chlorides may be transported from the surface of the concrete to the depth of water front but no further since the pores are partly disconnected by air filled voids as a result of chemical shrinkage [33]. For concrete with low w/c < 0.40, this depth of water ingress varies from 2 cm up to 5 cm even after 7 years of exposure, Fig. 2.31 [34-36]. During 7 years D decreases substantially as compared to the initial D at young age.

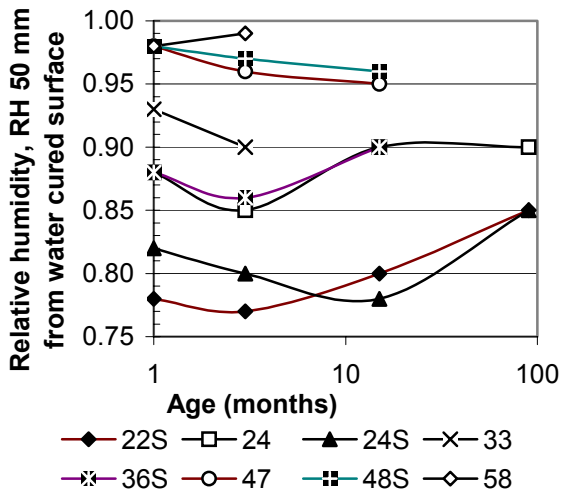

Fig. 2.31 - For concrete with low w/c < 0.40, the depth of water ingress varies from 2 cm up to 5 cm even after 7 years of exposure.

Hydration products will occupy all space in the concrete since the volume is limited for those to increase at low w/c [37]. The shortage of space in concrete with low w/c will actually stop both hydration and chloride migration with the effect of chemical shrinkage in a small distance from the surface of the concrete, i.e. within the surface cover layer of the reinforcement. The distance from the surface to the reinforcement normally exceeds 5 cm. Fig. 2.32 shows the relative humidity, RH, of submerged concrete with w/c = 0.40 (5% SF) [38].

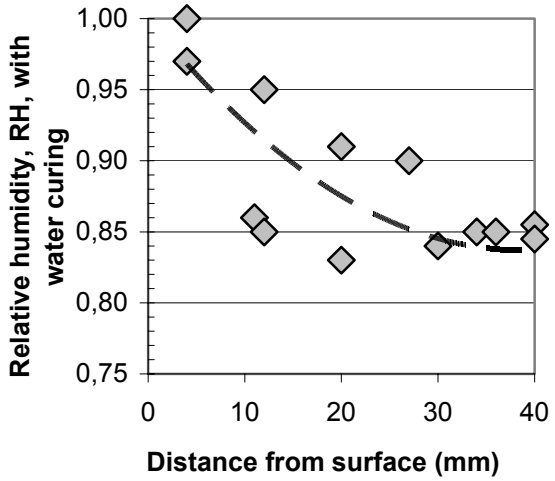

Fig. 2.32 - RH with w/c = 0.40 (5% SF).

In a homogenous system chemical shrinkage will cause self-desiccation [39]. At the internal part of a large concrete specimen with low w/c RH will coincide with RH obtained at self-desiccation. Reinforcement corrosion owing to chloride migration will normally be hindered by use of concrete with sufficiently low w/b ≤ 0.40, an adequate concrete cover provided that the surface is free from

cracks [39]. Formulae for estimating the chloride migration were introduced some 30 years ago for concrete in use at that time, i.e. with w/c > 0.40. These formulae do not account for self-desiccation since concrete with sufficiently low w/c was not in use at the time [40]. A great step in the understanding of D in NC with w/c > 0.40 was taken when the binding capacity related to the cement content was clarified [41]. Rapid tools for examining concrete were a great advantage for concrete optimising under severe conditions in sea [42]. Different models were put forward but still the effect of self-desiccation was not considered [43,44].

2.5 Long-term stability of silica fume concrete

2.5.1 General

One way of designing submerged cast SCC was to use silica fume for filler in order to avoid segregation and assure a good workability. Then it was of great importance to confirm the long-term stability of silica fume concrete which was done in a 13-year study [45-50]. Compressive strength, f_c, splitting tensile strength, f_{ct}, and hydration were studied on cores, 80 mm long and 40 mm in diameter, drilled out of large concrete specimens (250 kg each). Half of the specimens contained silica fume. All other material parameters were held constant. The concrete was poured in the shape of a disc, 1 m in diameter and 0.1 m thick. To simulate a long column, the flat sides of the disc were sealed by thick layers of epoxy resin; at least 2 mm. Also the circular rim of one third of the specimens was sealed by a minimum of 2 mm epoxy resin. The diffusion of moisture through the epoxy resin was negligible compared to the diffusion through the porous concrete. The rims of one third of the specimens were subjected to a climate with a temperature varying between 18°C and 24°C and an ambient relative humidity between 23% and 48% [51]. The circular rims of the remaining one third of the specimens were submerged and cured in water. A total of about 2400 measurements were carried out, Appendix 2.7.

2.5.2 Testing methods

At all ages except for 155 months cylindrical cores were taken in equal numbers at a distance of 50, 150 or 350 mm from the exposed surface in order to study strength and hydration. At 155 months' age cores were taken at about 100 mm distance from the exposed surface of the large concrete specimens. During the testing of strength inter-layers of hardboard were used. The width of the hardboard was 4.5 mm at the split tensile testing. The testing rate was 1 MPa/s (compressive strength) or minimum 30 s (split tensile strength). Cast-in plastic tubes were placed at different distances, 50, 150 and 350 mm, from the exposed circular surface of the column in order to measure the relative humidity, RH. Parallel to the cast-in items, thermocouples were placed in the concrete [52]. The measurement points of RH were protected by a cover made of expanded plastic insulation in order to minimize the effects of variations in the ambient climate in the laboratory. The measurement period of RH was 22 h. The probes were carefully calibrated [53]. At 155 months' age the RH measurement was performed on the drilled cores that were placed and sealed in double sealed 0.2-mm plastic bags. Three cylinders 40 mm in diameter and 80 mm long were submerged in 3% sodium chloride and frozen/thawed once a day between ± 20 °C. The weight of the cylinders was taken before and after the freezing, after 56, 112 and 300 cycles. Ignition tests were carried out to obtain the hydration of the specimens for strength [54]. The concrete was crushed into maximum 5 mm pieces and dried for 1 week at 105 °C before the ignition took place at 1050 °C for 16 h. Compensation was made for the ignition loss of cement and aggregate in the calculation of hydration losses [55].

2.5.3 Materials

Appendix 2.4 shows the chemical composition of the low-alkali cement CEM I 42.5 BV/SR/LA that was used [51]. Eight types of concrete were studied on 24 large concrete specimens. The aggregate consisted of crushed quartzite sandstone 8-12 mm (compressive strength: 333 MPa, splitting tensile strength: 15 MPa, Young's modulus: 60 GPa [56] and ignition losses: 0.25% [57]) together with natural gravel 0-8 mm (granite, ignition losses: 0.85% [57]. The silica fume was granulated powder (ignition losses: 2.25% [57], specific surface: 17.5 m^2/g). The superplasticizer (naphthalene sulphonate) was added 30 s after all the other materials during the mixing (mixing time: 240 s). In Appendix 2.8, the composition (kg/m^3 dry material) of the concretes, the properties in fresh state and the compressive strength are shown [58].

2.5.4 Compressive strength

Fig. 2.33 shows the development of strength in concrete with 10% silica fume and Fig. 2.34 without silica fume. Fig. 2.35 shows the efficiency factor of silica fume, i.e. the effect of 1 kg of silica fume in comparison with the effect of 1 kg of Portland cement on compressive strength. The strength was increasing continuously.

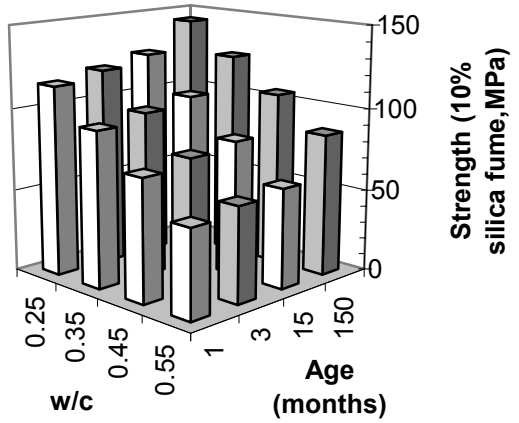

Fig. 2.33 – Compressive strength (10% silica fume,MPa).

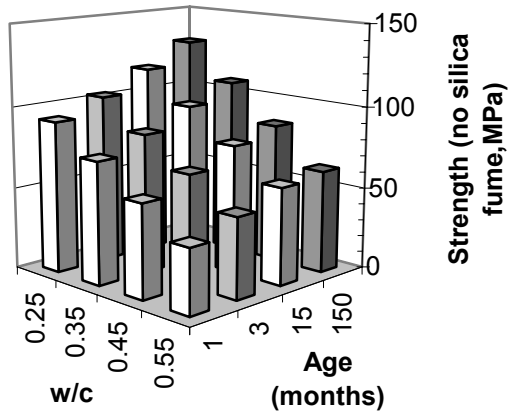

Fig. 2.34 –Strength (no silica fume,MPa).

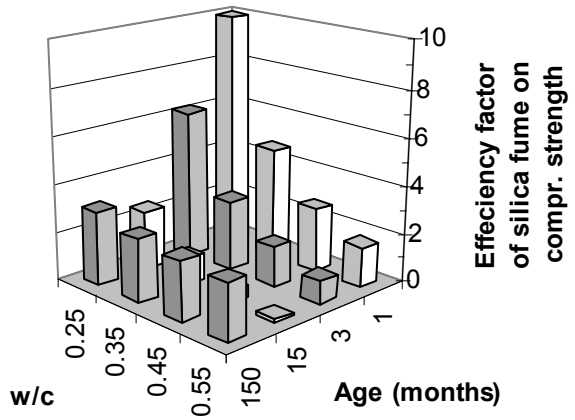

Fig. 2.35 - Efficiency factor of silica fume on compressive strength.

2.5.5 Split tensile strength

Fig. 2.36 shows the development of split tensile strength in concrete with 10% silica fume and Fig. 2.37 without silica fume. Fig. 2.38 shows the efficiency factor of silica fume, i.e. the effect of 1 kg of silica fume on split tensile strength in comparison with the effect of 1 kg of Portland cement. Fig. 2.39 shows the split tensile strength versus the compressive strength with 10% silica fume. Fig. 2.40 shows the split tensile strength versus the compressive strength without silica fume. Fig. 2.41, finally, shows split tensile strength versus compressive strength.

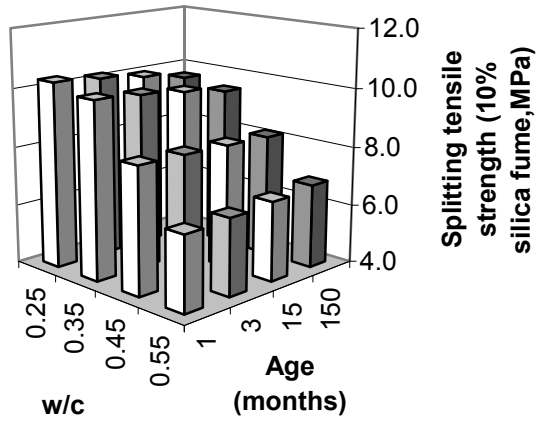

Fig. 2.36 – Split tensile strength (10% silica fume,MPa).

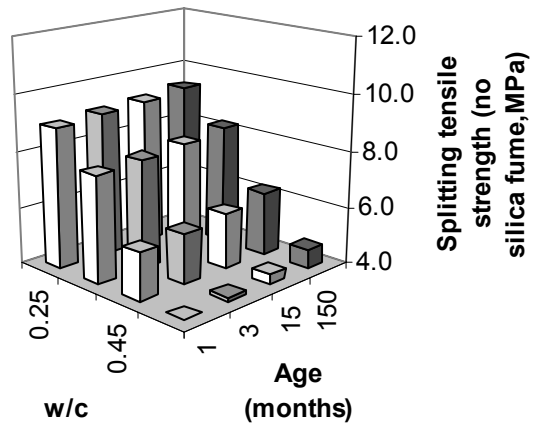

Fig. 2.37 – Split tensile strength (no silica fume,MPa).

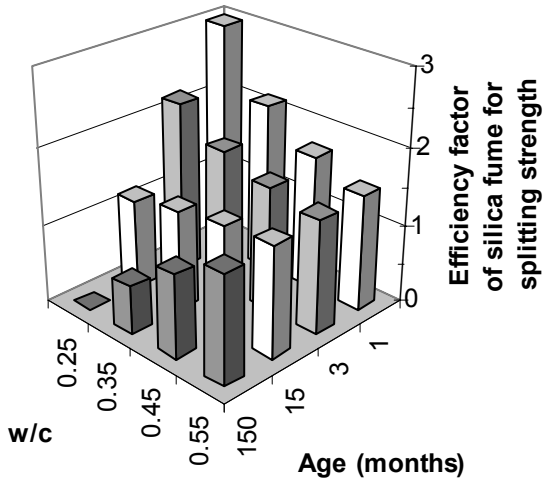

Fig. 2.38 - Efficiency factor of silica fume on split tensile strength.

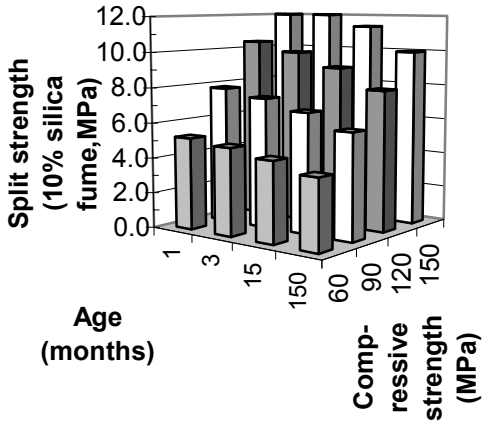

Fig. 2.39 - Split tensile strength versus the compressive strength with 10% silica fume.

2.5.6 Hydration

Fig. 2.42 shows hydration with 10% silica fume and Fig. 2.43 the hydration without silica fume. Fig. 2.44 shows efficiency factor of silica fume as related to hydration. Fig. 2.45 shows the compressive strength of concrete, with and without silica fume, versus the relative hydration.

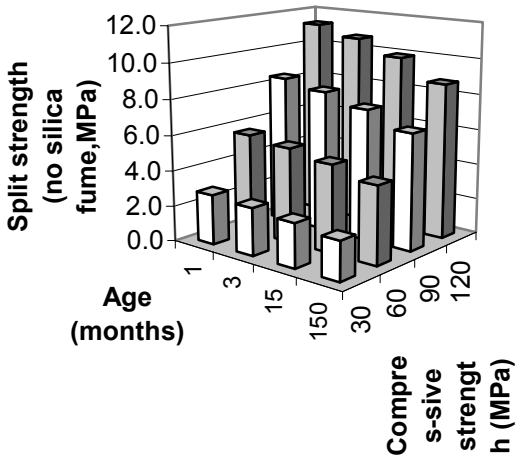

Fig. 2.40 - Split tensile strength versus the compressive strength without silica fume.

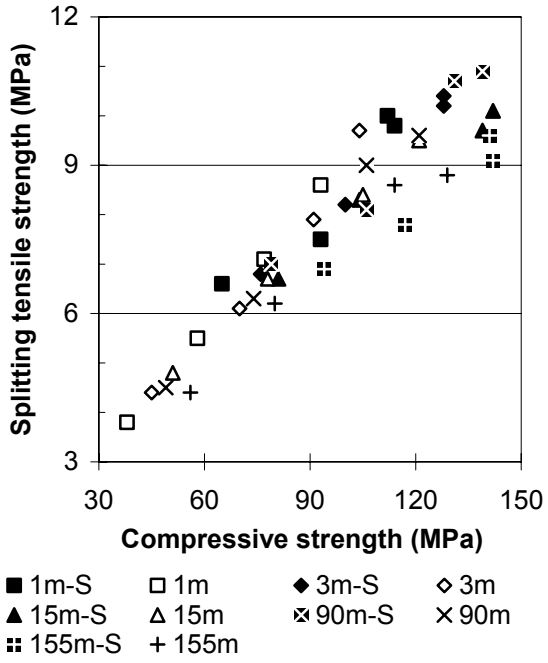

Fig. 2.41 - Split tensile strength versus compressive. m = months' age. S = 10% silica fume.

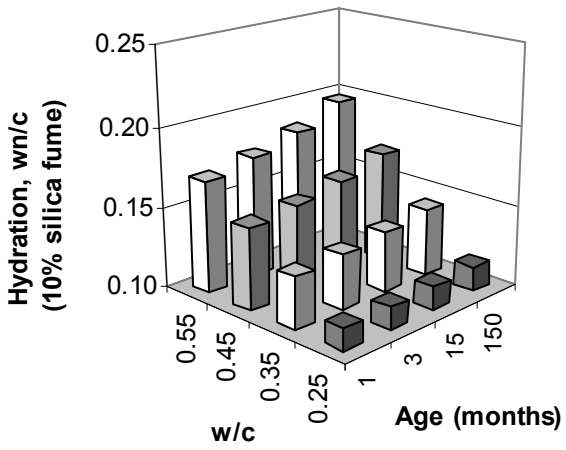

Fig. 2.42 - Hydration, w_n/c, (10% silica fume).

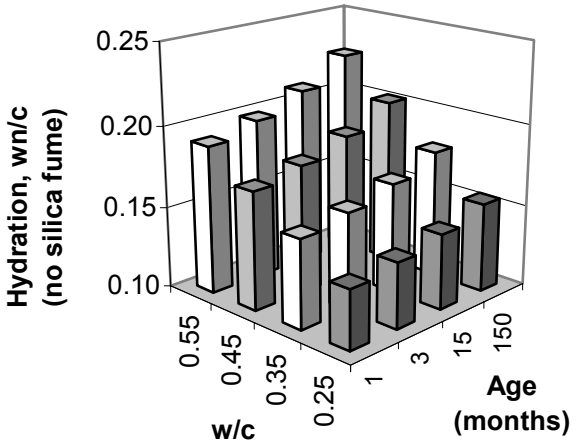

Fig. 2.43 - Hydration, w_n/c, (no silica fume).

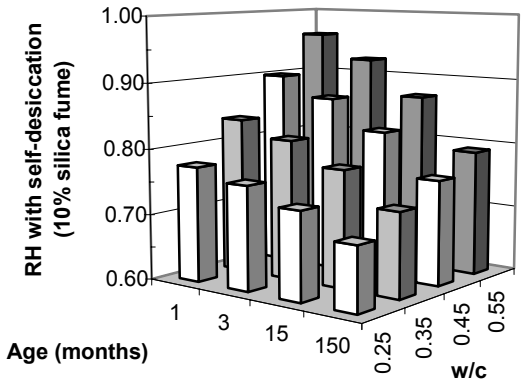

Fig. 2.46 – Self-desiccation (10% silica fume).

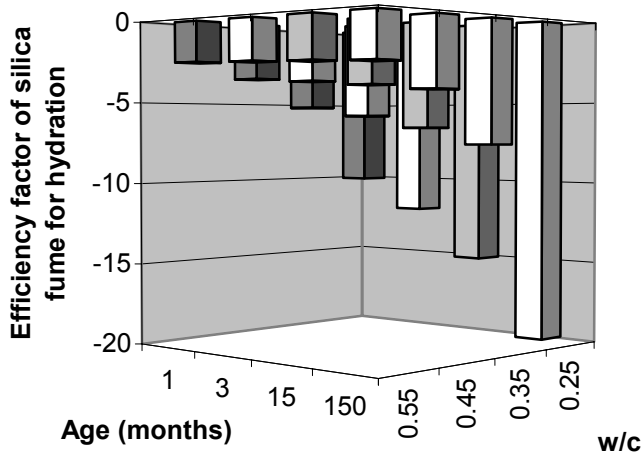

Fig. 2.44 - Efficiency factor related to hydration.

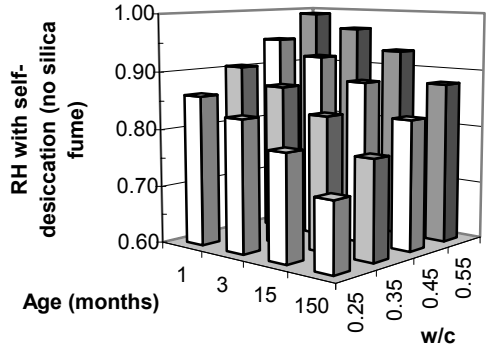

Fig. 2.47 – Self-desiccation (no silica fume).

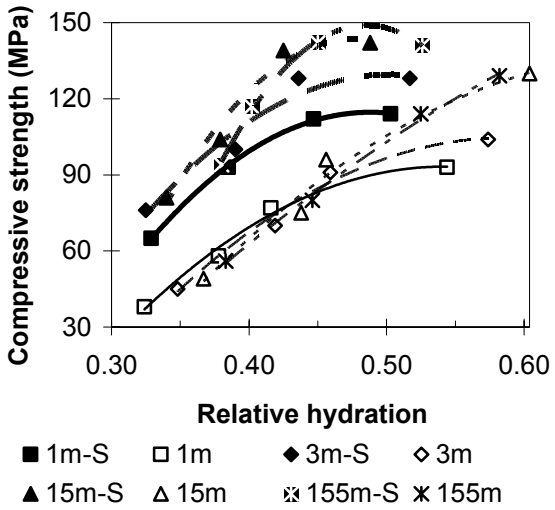

Fig. 2.45 - Compressive strength versus hydration.

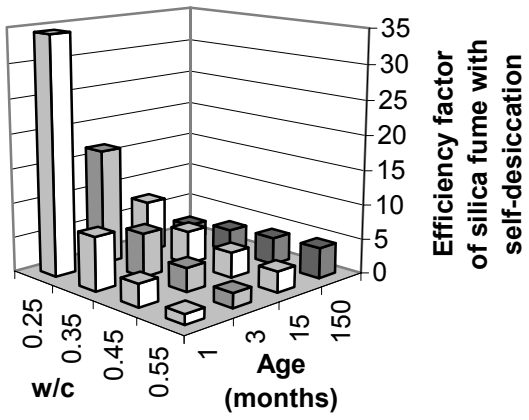

Fig. 2.48 - Efficiency factor of silica fume on self-desiccation.

2.5.7 Self-desiccation and salt frost resistance

Fig. 2.46 shows self-desiccation in concrete with 10% silica fume and Fig. 2.47 the self-desiccation without silica fume, Appendix 2.8. Fig. 2.48 shows efficiency factor of silica fume as related to self-desiccation. Fig. 2.49 shows the salt freezing and thawing scaling versus the w/c. An amount of 0.5 kg/m³ indicates good resistance.

Salt-frost scaling of SCC with and without silica fume (blended cement with 7.5% silica fume in all concrete, both NC and SCC, Appendix 2.9) was studied 224 cycles. w/b = 0.35 and w/b = 0.40 was used. Fig. 2.50 shows that the long-term salt-frost scaling performed well at least at 112 cycles.

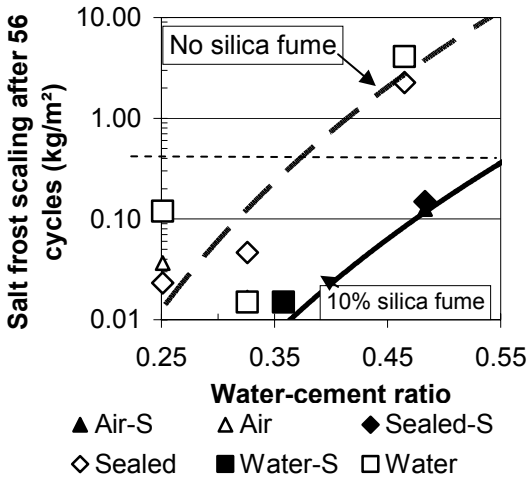

Fig. 2.49 - Salt freezing and thawing scaling vs w/c. Less than 0.5 kg/m³ gives good resistance.

The following conclusions were drawn:

- All concrete obtained excellent salt-frost resistance at 56 cycles, i.e. < 0.2 kg/m² scaling.
- Concrete SCC35 with w/b = 0.35 performed better than at SCC40 w/b = 0.40.
- Concrete NC35 with w/b = 0.35 without filler performed better than SCC35 and SCC35SF.
- The first concrete with w/b = 0.35 to break down, SCC35, contained limestone filler.
- SCC40 withstood 224 cycles acceptably.

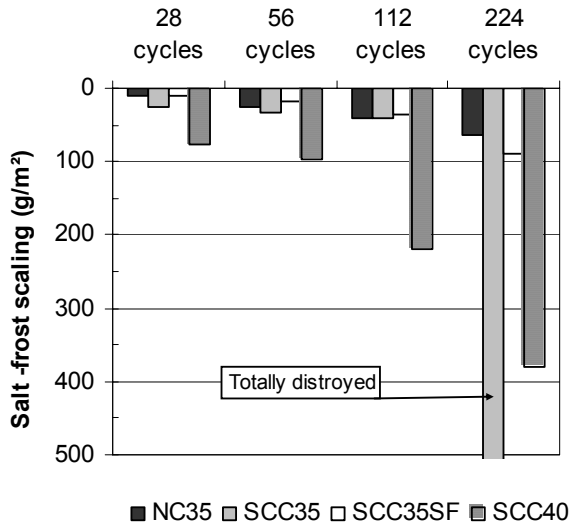

Fig. 2.50 - Results of long-term salt-frost scaling performed for 112 cycles. NC = normal concrete, SCC = Self-compacting Concrete with limestone filler, SF = silica fume filler only, 35 = w/b.

2.5.8 Conclusions of effect of silica fume in concrete

Mechanical characteristics are measured and their evolution interpreted as a function of the role of silica fume. Previous observations such as the decline of compressive strength in the long term or the influence of the hydration parameter have been found inconsistent. Large concrete specimens, containing 5000 kg of concrete in all, were used in long-term studies of the effect of silica fume on the properties of concrete related to strength, hydration and relative humidity. Half of the concrete contained 10% silica fume calculated in relation to the cement content. About 1000 cores were studied to determine their strength. About 2400 observations were carried out over 155 months. The following conclusions were drawn:

1) Silica fume had a positive effect on all the studied properties of concrete (compressive and splitting tensile strength and relative humidity) with the exception of degree of hydration. The effect was pronounced on concretes with low w/c. The silica fume had a larger effect on compressive and splitting tensile strength and relative humidity than cement did. The efficiency factor for silica fume compared with cement varied between 0 and 25 except for the effect on hydration which varied between - 3 and -20.
2) Due to the low degree of hydration of cement in concretes with low w/c< 0.43, silica fume still remained available for the pozzolanic interaction with the Portland cement, at least until 155 months' age. In concrete with higher w/c the pozzolanic effect stopped before 1 month's age due to insufficient silica fume in the mix proportions.
3) After a long time, 155 months, the efficiency factor of silica fume on the strength became about 2. Between 15 and 155 months' age the efficiency factor of silica fume related to compressive strength stabilized around 2 compared to cement. At w/c < 0.43 the efficiency factor of silica fume on splitting tensile strength decreased with time (= 0 at w/c = 0.25). This phenomenon was explained by the pronounced self-desiccation which consequently stopped the hydration in low w/c concretes. In concretes with higher w/c, no more silica fume remained for the pozzolanic interaction to continue after age 1 month.
4) The relationship between the degree of hydration and compressive strength developed differently in concretes with and without silica fume due to the pozzolanic interaction between Portland cement and silica fume. Hydration was an inconsistent parameter to describe properties with silica fume.
5) At 56 salt frost cycles with ± 20°C one period per 24 h a normal acceptable salt frost scaling was obtained with in concrete without air-entrainment and w/c < 0.55 combined with 10% silica fume in the mix design. For concrete without silica fume w/c < 0.35 was required to obtain frost resistance

without air-entrainment. The explanation was probably the ability of silica fume to prevent chloride ingress in the concrete. If no chlorides may enter the concrete no decrease of the freezing point of the water will take place and water will then not enter the concrete either. Behind the low chloride ingress lays the early self-desiccation of silica fume concrete which means that chlorides may not be transported in air-filled voids.

2.6 Deformations with silica fume concrete

2.6.1 General deformation requirements

When casting repair concrete around a previously damaged concrete it is essential to take into account the effect of shrinkage between the new concrete and the damaged one. For example the Öland Bridge was damaged to an extent of 50-100 mm of spalled concrete in the splash zone [61]. In this case a water-tight groove was built all around the damaged piers and 400 – 500 mm thick repair concrete cast dry surrounding the pier. Durability called for a concrete that was completely free of cracks. When the surrounding concrete cools then the concrete of the old piers or dam heat up and expand. This is when the dangerous and large tensile stresses occurs in the surrounding concrete with risk of through cracks. However, it is not possible to achieve crack-free concrete only by cooling since autogenous shrinkage also has to be taken into account (shrinkage that occurs in concrete with low water-cement ratio due to self-desiccation). At the Öland Bridge a sliding layer between the old pier and the new concrete solved the problem of obtaining crack-free concrete. Cooled concrete was only used for the purpose of limit the contraction during cooling. Normal practise is to cast concrete against a raw surface to obtain the best adhesion. It was the object of the deformation studies to obtain values of the autogenous shrinkage used in this project in order to judge the risk of long-term cracking. The studies were carried out in another project with exactly the same mix proportions as in this project [5-12].

2.6.2 Materials and methods

Materials for studies of the properties were delivered from Switzerland for optimization in Lund, Appendix 2.9. Fig. 2.51 shows the distribution of the particles of the materials in use. The materials were put in steel barrels in order to maintain a constant moisture level. The concrete was mixed in a 40-l compulsive mixer in the laboratory or in a 1000-l mixer of compulsive type in the field. The following mixing order was used: mixing with all dry material and water for ½ minute followed by mixing with all material including the superplasticiser for 2½ minutes. The materials were adjusted to an ideal grading curve using a computer program [62-66] to achieve optimal mix proportions. Cubes were cast from the mixes and stored sealed for one day in the mould followed by air curing. The tests and curing took place at 20 °C. For short-term tests of autogenous shrinkage before 1 day' age 3 horizontal boxes with a section of 100 x 100 mm and 400 mm long were used. One end of the box was free to move with the concrete that was placed in the box. The movement of the outside of the box was measured by 2 LVDTs that were placed at two level, 25 mm from the surface or 25 mm from the bottom of the box. The top surface of the box was insulated by two layers of aluminium foil. The boxes were either placed in an ambient RH of 60% or 95%. The concrete was cast in an ambient RH of 60% or 95%. For long-term tests after 1 day' age 3 + 3 cylinders, either 100 mm in diameter and 500 mm long or 55 mm in diameter and 300 mm long, 3 of each concrete type, were prepared in steel moulds. Air curing in relative humidity, RH = 60% after 1 day of sealed curing or sealed curing by double layers of aluminum foil took place. Cast-in items made of steel fixed measurement nuts on three sides of the specimen. Well-calibrated mechanical measurement devices were used. Of each concrete three creep cylinders of the two curing types were subjected to 30% of the ultimate strength in spring-loading devices starting at 14 days' age and run for up to 2 years.

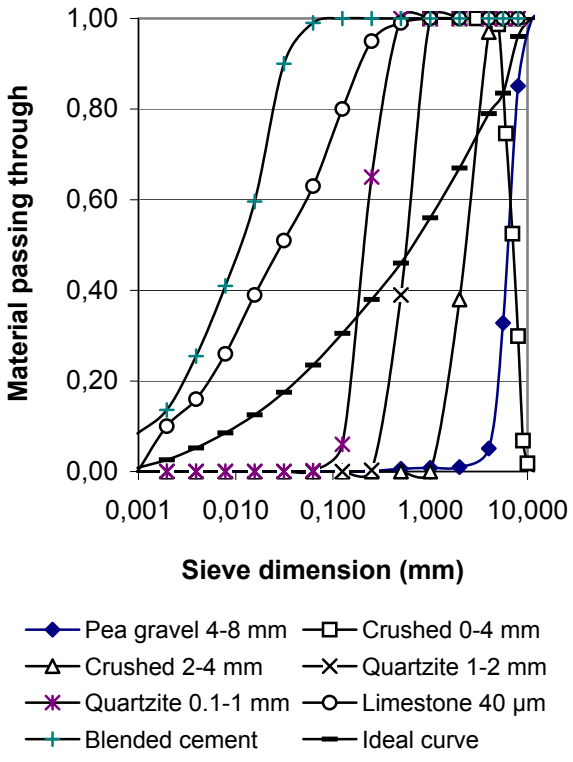

Fig. 2.51 – Particle distribution of material, Appendix 2.9.

2.6.3 Mix proportions and strength development

The mix proportions of the concrete for production of creep and shrinkage specimens are shown in Appendix 2.9 [67,68]. The distribution of the particles of the mix proportions is shown in Fig. 2.52. The mix proportion of NC shows gap-grading between 0.031 and 0.25 mm sieve dimension, which normally is cement-consuming. The SCC exhibited a more linear logarithmic distribution of particles in the fresh mix than the NC mix did. SCC performed almost perfectly with T_{50} between 5 and 10 s (time for a slump flow of 500 mm in diameter), with the L-box with the ratio of the height of SCC at front end to the height of SCC at vertical shaft varying between 0.75 and 1. Finally the ratio of the weight of aggregate of the upper part of segregation cylinder divided by the weight of aggregate of the lower part varied 0.96 and 1.01. The V-funnel results were 12 and 20 s, i.e. between 10 and 20 s like requested. The value of the V-funnel tests should not be too low since air then may be entrapped in the concrete (for NC entrapped air is avoided by vibrating tools). Fig. 2.53 shows a rapid strength development of the mixes in Appendix 2.9 [66,67].

2.6.4 Shrinkage and creep

The shrinkage of moisture insulated specimens of concrete was investigated for either w/b = 0.35 or w/b = 0.40, Appendix 2.9. The specimens were cast and placed in an ambient RH of 60% or 95% RH. After 1 days the shrinkage became about 210 millionths in an ambient RH of 60% and about 80 millionths in an ambient RH of 95%.

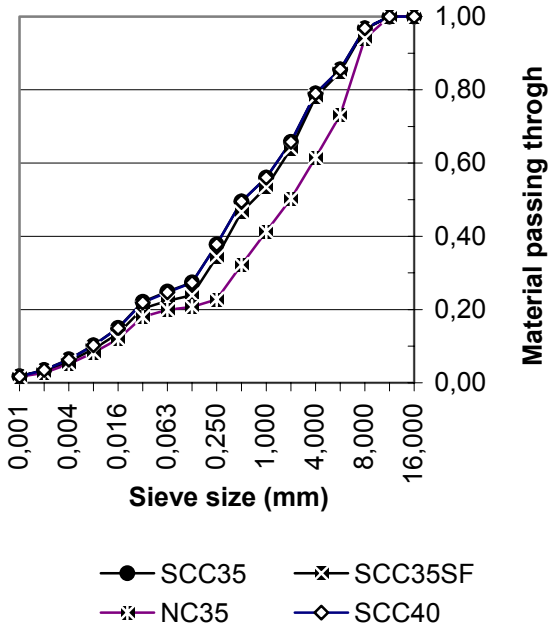

Fig. 2.52 - Particle distribution of fresh concrete, Appendix 2.10. SF = silica fume. 35 = w/b (%).

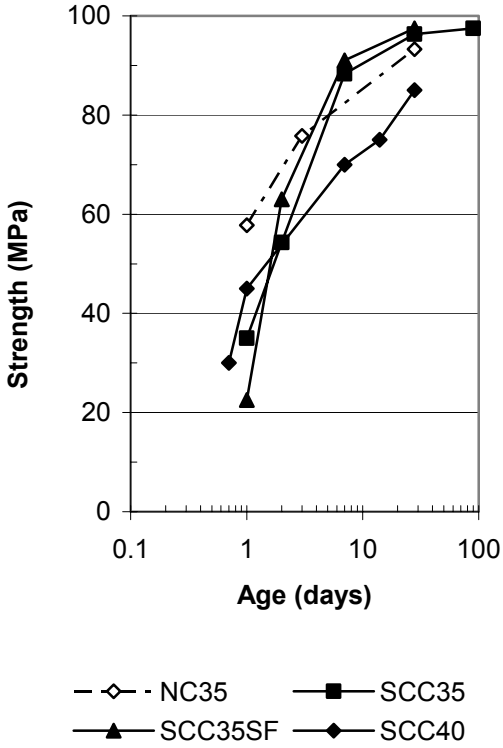

Fig. 2.53 – Strength development.

The self-desiccation will cause a decrease of RH in concrete with w/b = 0.35 of less than 5% which cause RH > 95% in the concrete. About 80 millionths of autogenous shrinkage then should be added to the values shown below. Fig. 2.54 shows 1-day shrinkage of concrete with w/b = 0.35 at RH = 60%. Fig. 2.55 shows 1-day shrinkage of concrete with w/b = 0.35 at RH = 95%. Fig. 2.56 shows 1-day shrinkage of concrete with w/b = 0.40 at RH = 60%. Fig. 2.57, finally, shows 1-day shrinkage of concrete with w/b = 0.40 at RH = 95%. The difference between 1-day shrinkage in RH = 60% and RH = 95% environment was due to leakage of moisture during the preparation of specimens or due to leakage of moisture from the specimen after preparation. If the preparation took place at RH = 95% the leakage became smaller. Fig. 2.58 shows that shrinkage of SCC was about 20% larger than in NC probably due to the lower aggregate content of SCC than of NC [69-71]. Fig. 2.59 shows the creep compliance of concrete 100-mm cylinders.

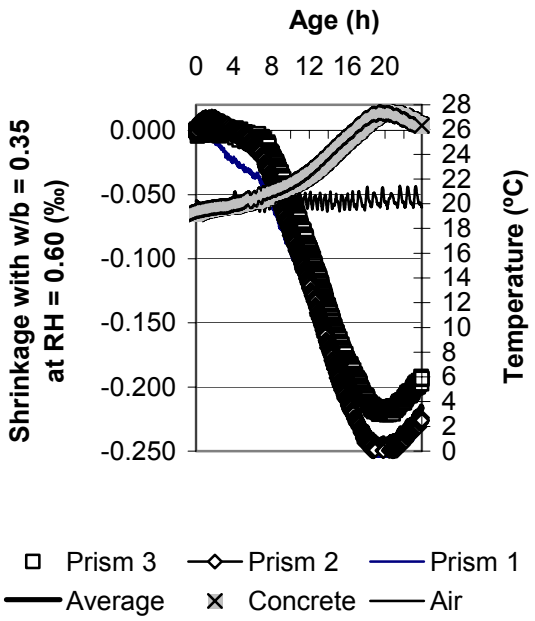

Fig. 2.54 - One-day shrinkage of concrete with w/b = 0.35 at RH = 60%.

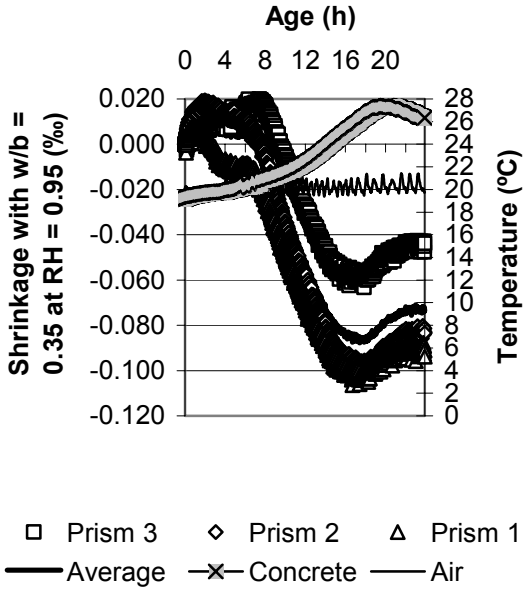

Fig. 2.55 - One-day shrinkage of concrete with w/b = 0.35 at RH = 95%.

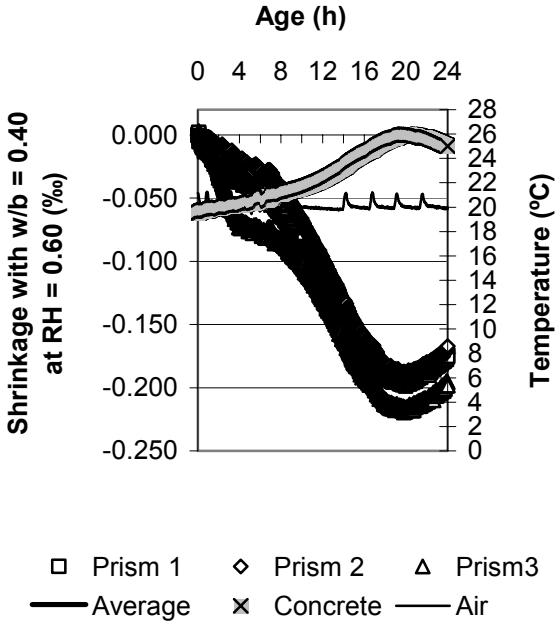

Fig. 2.56 - One-day shrinkage of concrete with w/b = 0.40 at RH = 60%.

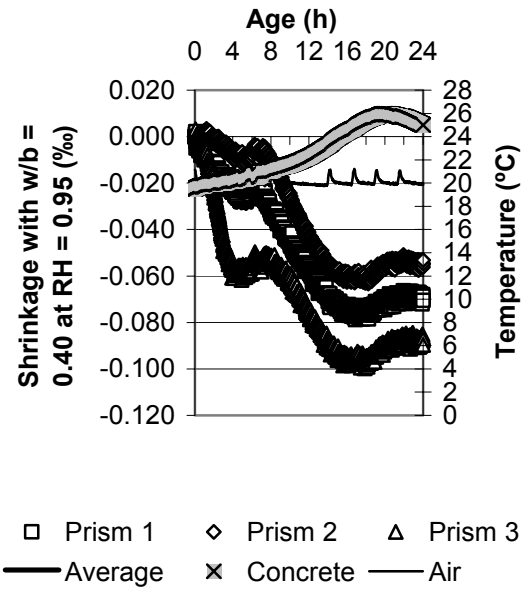

Fig. 2.57 - One-day shrinkage of concrete with w/b = 0.40 at RH = 95%.

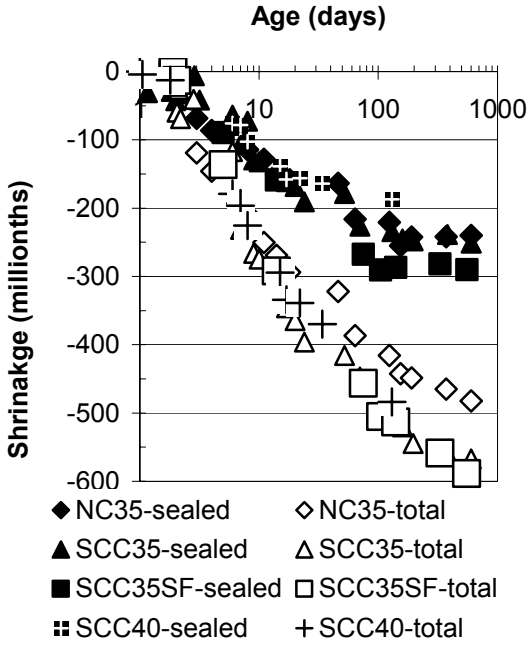

Fig. 2.58 – Shrinkage of 100-mm cylinders.

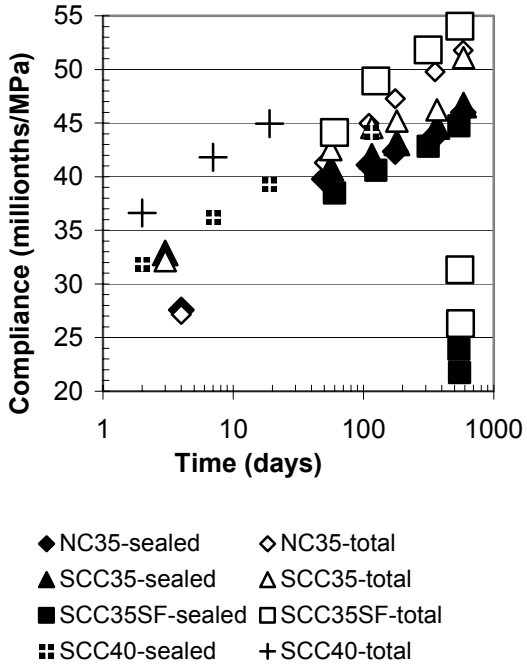

Fig. 2.59 – Creep compliance of 100-mm cylinder

One concrete was unloaded (SCC35SF) which gave the deformation directly after unloading and also after 1 week of recovery. Since the elastic modulus was lower at unloading than at loading the creep coefficient after unloading became somewhat larger, Appendix 2.10 [59]. After 1 week of recovery the effect of the increase of the elastic modulus was more or less compensated for, Appendix 2.10. No significant difference between creep of NC and that of SCC was observed. Some size effect on total shrinkage was observed in Fig. 2.60, due to more rapid drying of cylinders 55 mm in diameter than that of 100-mm cylinders.

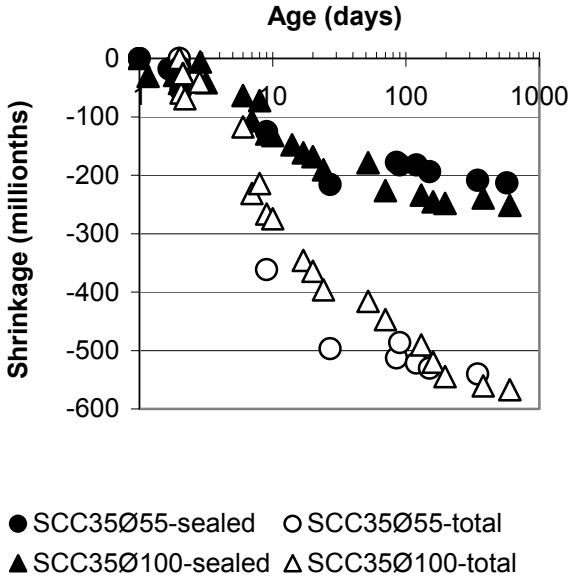

Fig. 2.60 – Shrinkage of 55-mm and 100-mm concrete cylinders, Appendix 2.9.

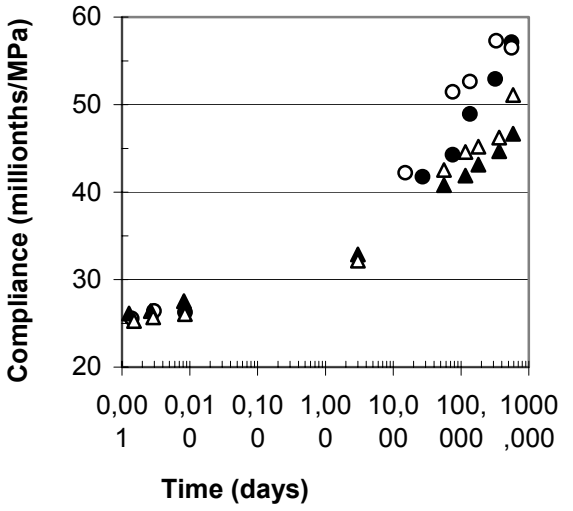

Fig. 2.61 – Creep compliance of 55-mm and 100-mm concrete cylinders, Appendix 2.9.

However, after 1 year the shrinkage of concrete cylinders did not differ due to specimen diameter, which confirmed previous knowledge, Fig. 2.60. Some small size effect was also observed for the creep of the concrete, somewhat larger creep compliance for 55-mm cylinders than for cylinders 100 mm in diameter, independent of the type of compacting, Fig. 2.61. Fig. 2.62 shows small creep coefficient. Fig. 2.63 shows the elastic modulus 100 s after the start of loading of the creep specimens. Even though strength of NC was smaller than that of SCC, the elastic modulus was larger due to larger aggregate content of NC (0.75) compared with that of SCC (0.72-0.73).

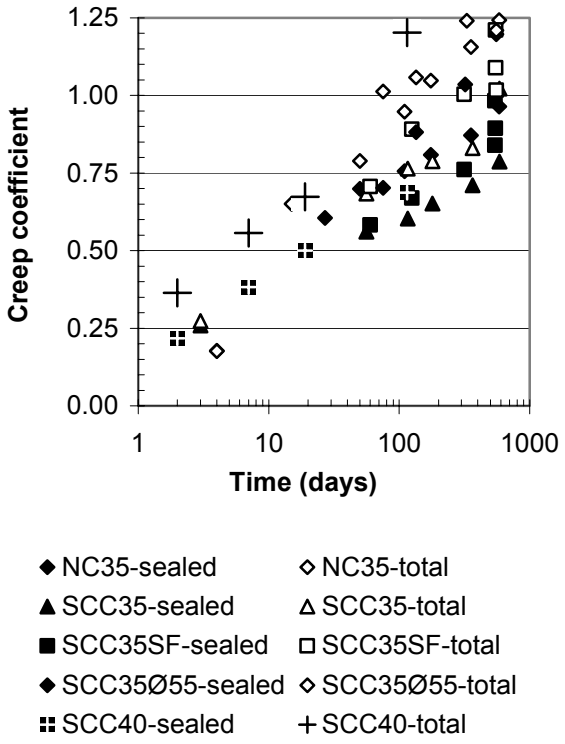

Fig. 2.62 – Creep coefficient versus time. SF = silica fume. 35 = w/b (%).

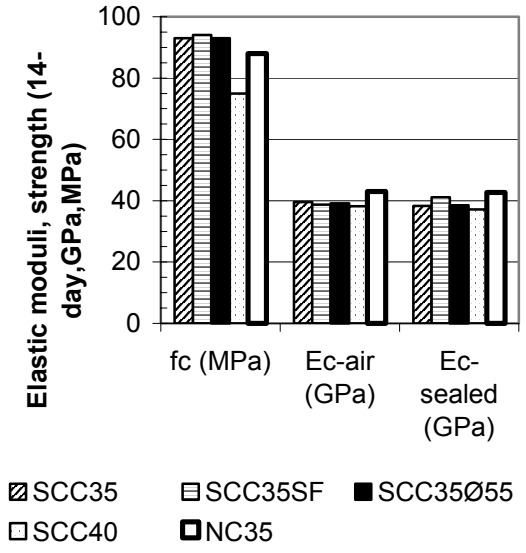

Fig. 2.63 – Elastic moduli and strength of creep specimens. SF = silica fume, 35 = w/b (%), Ø55 = 55-mm diameter.

2.6.5 Comparison with fib 2000 Model for creep and shrinkage

Comparisons were made between results of the fib Model 2000 for creep and shrinkage and these results [72-83]. The elastic modulus was derived according to the following formula [72-77]:

$$E_c(t) = 21.5\cdot(f_{cm}/f_{cm0})^{1/3}\cdot\exp(1-(28/t/t_t)^{0.5}\cdot s/2) \quad (2.2)$$

where
f_{cm0} = 10 MPa
f_{cm} denotes 28-day strength (MPa)
t denotes age (days)
t_1 = 1 day
s denotes constants given in Appendix 2.11.

The creep compliance of concrete was derived according to the following formulae [72-77]:

$$J(t,t_0) = 1/E_c[n(t_0) + \varphi(t,t_0)] \quad (2.3)$$

$$n(t_0) = E_c/E_c(t_0) \quad (2.4)$$

$$\varphi(t,t_0)=\alpha_2 [1+\alpha_1 (1-RH/100)/(0.1\cdot d/200)^{1/3}]\cdot 5.3/(f_{cm}/f_{cm0})^{0.5}\cdot 1/(1+t_0^{0.2})\cdot[(t-t_0)/(\beta_H+t-t_0)]^{0.3} \quad (2.5)$$

$$t_0=t_{0,T}\cdot[9/(2+(t_{0,T}/t_{1,T})^{1.2})+1]^{\alpha} \quad (2.6)$$

$$\beta_H=150\cdot[1+(1.2\cdot RH/100)^{18}]\cdot d/200+250\cdot(3.5\cdot f_{cm0}/f_{cm})^{0.5} \quad (2.7)$$

$$\alpha_1=(3.5\cdot f_{cm0}/f_{cm})^{0.7} \quad (2.8)$$
$$\alpha_2=(3.5\cdot f_{cm0}/f_{cm})^{0.2} \quad (2.9)$$

where
d denotes the diameter of the specimen (mm)
f_{cm} denotes 28-day strength (MPa); f_{cm0} = 10 MPa
t denotes the age (days)
t_0 denotes age at loading (days)
$t_{0,T}$ denotes age adjusted to 20 °C (all specimens were stored at 20 °C only)
$t_{1,T}$ = 1 day
α = -1 for slowly hardening cement; = 0 otherwise.

Total shrinkage was derived as the sum of an autogenous part and a drying part according to the following formulae stated below [72-77]. The fib Model includes the cylinder strength of the concrete, $f_{cc,cyl}$, which was calculated by multiplication of the strength, $f_{cc,cube}$ [71] (MPa).

$$\varepsilon_{cas}(t)=(1-\exp(-0.2\cdot(t)^{0.5}))\cdot\alpha_{as}\cdot(f_{cm}/f_{cm0})/(6+f_{cm}/f_{cm0}))^{2.5} \quad (2.10)$$

$$\varepsilon_{cds}(t,t_s)=110\cdot(2+\alpha_{ds1})\cdot\exp(-\alpha_{ds2}\cdot f_{cm}/f_{cm0})\cdot 1{,}55\cdot(1-(RH/100)^3)\cdot((t-t_s)/(350\cdot(d/200)^2+(t-t_s)))^{0.5} \quad (2.11)$$

$$f_{cc,cyl} = 0.71\cdot f_{cc,cube} \quad (2.12)$$

where
d denotes diameter of cylinder (mm)
f_{cm0} = 10 MPa
f_{cm} denotes strength at 28 days' age (MPa)
t denotes time (days)
t_s denotes age at start of drying (days)
α denotes constant given in Appendix 2.12.

From the estimation it was clear that the fib Model underestimated autogenous shrinkage, Fig. 2.64. Only about 40% of the measured autogenous shrinkage was estimated [10]. The aggregate content in SCC compared with that of NC would affect in the same order the total shrinkage estimations, which performed well with the fib Model [78-84]. The creep estimation with the fib Model performed well except for NC, where a small overestimation took place. Even though Fig. 2.62 indicates larger creep coefficient of NC than of SCC, the deformation at the same stress may be smaller in NC than in SCC since the elastic modulus of NC is larger than that of SCC, Fig. 2.61.

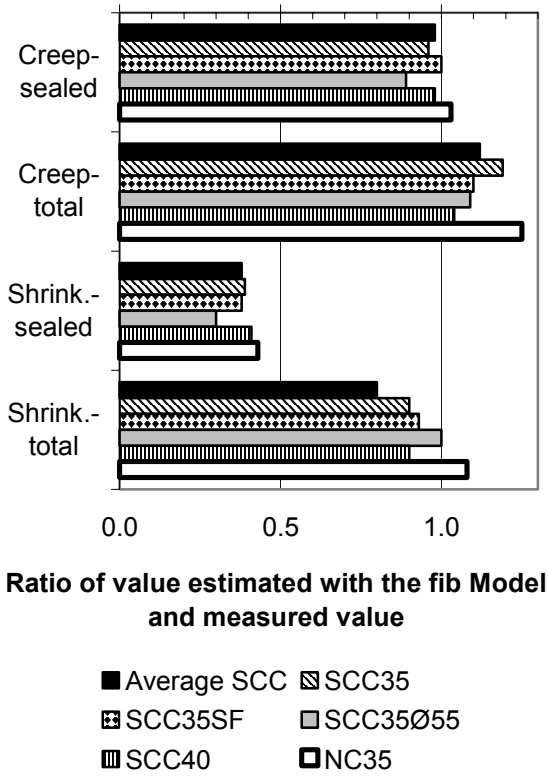

Fig. 2.64 - Ratio of shrinkage and creep estimated with the fib Model to the measured value.

2.6.6 Consequences of autogenous shrinkage

About 0.25‰ of autogenous shrinkage will occur after 1 day's age since the early 1-day shrinkage probably will be compensated by early creep. The surface of the old, repaired concrete will supply the new concrete with moisture about 25 mm from the surface which also will be the case for the surface of the new concrete. In these parts of the submerged concrete no autogenous shrinkage will occur. In the resisting part autogenous shrinkage will occur, partly restrained by the surface of the submerged cast concrete but also by the repaired concrete. It is thus essential that the adhesion between the repaired concrete and the new one does not exceed the tensile strength of the old concrete at any time. The surface of the new concrete may crack dependent on the thickness of the repair layer. In order to distribute the tensile stress and to diminish the crack width it is important to use a suitable reinforcement net in the new concrete and also to connect the repair layer to the existing concrete by core drilled anchors. Provided that the distance of the reinforcement bars is 200 mm the crack with will be limited to maximum 0.05 mm.

2.7 Submerged cast concrete

2.7.1 General

The advantage by use of submerged cast concrete compared with normal concrete is to avoid a dry keeping barrier around the construction during the production at site [61]. Submerged cast concrete is used by the Road Administration primary for foundation of bridges in rivers and at repair of these constructions [85]. Substantial damages have been observed at the upstream side of uninsulated dams of concrete water power plant. In this positions repair is necessary. In order to resist penetration of water in the fresh state anti-washing out compound are necessary to add to a concrete that is cast submerged by a pump hose. In Sweden cellulose based anti-washing out compound is used but abroad mostly polymer based anti-washing out compounds (branch mark: Wellan gum). When using these compounds it seems to result in low frost resistance. Both the Road Administration and the water power plants require a repair concrete to be durable to frost. To be cast submerged the process and the level of the concrete is checked by divers and afterwards by visual inspection and by strength tests of drilled cores. In advance of the pumping the slump (flow) of the concrete is tested. Pre-testing of the concrete also may take place of frost resistance and strength as for a construction concrete. The w/c of a normal concrete for foundation of bridges in rivers and at dams of concrete water power plants normally is high (around w/c = 0.50) which is an disadvantage as concerns frost resistance. Even though the repair concrete will be frost resistant the existing construction may deteriorate when subjected to further frost attack. In order to prevent frost water power dams may be insulated but bridge foundations not. All damaged concrete at bridge foundation must be carefully cleaned and the lose part and parts damaged by frost removed before casting a new face of the structure. Probably the repair concrete may not be used in sea or brackish water since chlorides then may be mixed into the fresh concrete.

2.7.2 Requirements at construction

According to the requirement of the Swedish Road Administration pre-casting of submerged cast concrete has to be performed in two moulds with a prescribed concrete with a settled grading curve of the material in the fresh mix proportion [85-87]. The two types of moulds have the following two purposes [85-87]:

- Ability of filling and covering reinforcement
- Self-levelling without compaction

For these purposes the following sizes of moulds 2 x 1 x 1 m and 4 x 0.5 x 1 m are used (length x width x height). Mix proportions of the concrete are to be documented and tested until 90 days' age. The remaining requirements are as follows:

- Design values for concrete strength class C20/25 are to be used
- The concrete thickness is to be minimum 1 m
- The foundation slab is to be without cracks
- Horizontal joints are not allowed
- Agitator is to be used at delivery of ready mix
- The lowest concrete strength class is C28/35
- Minimum 350 kg/m³ cement is to be used
- Filler content (< 0.25 mm) is to be > 8%
- Concrete without anti-washout powder is to have slump > 120 mm
- Retarding agent is to be included in the mix proportions and the setting checked
- Non-frost resistant concrete may be used
- Anti-washout powder is to be used when statically reinforcement is included

2.7.3 Requirement at repair

Few literature references exist as to describe the routines at repair. The following requirements seem to exist [85,88]:

- Cleaning with chisel cutting, shot pealing or blasting
- Repair extent
- Repair methods
- Material

For repair of mainly minor faults the follwing is described [85,88]:

- Methods how to reach the place of repair, caisson, dry or wet groove
- Methods to remove and prepare concrete
- Mix proportions of concrete repair material
- Techniques for repair
- Strengthening and pre-stressed reinforcement

2.7.4 Testing methods

Several methods used for normal concrete may not be used for material meant for underwater contreting where much more viscous material is used [85,89]. The stream test was developed in Belgium. It consists of a 2 m long and 0.10-0.15 m wide 20-° sloping channel with the concrete placed in the middle, Fig. 2.65. The amount of washout material is not quantified only judged visually.

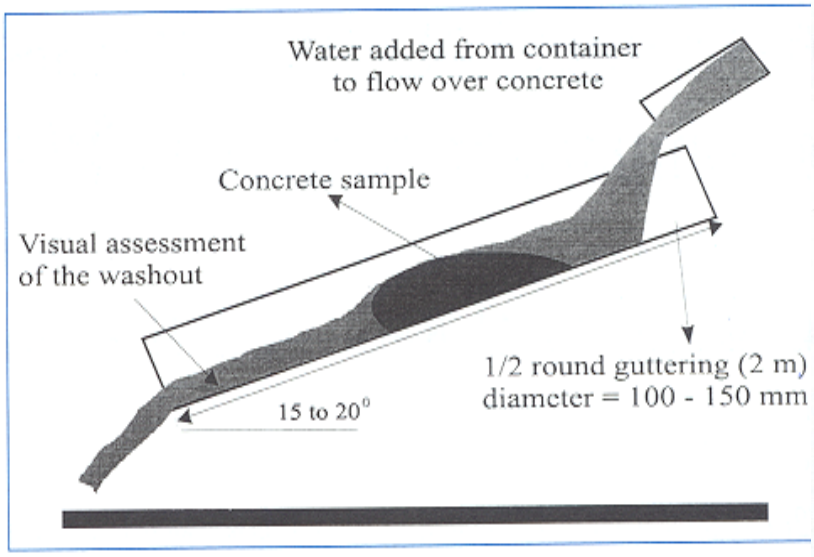

Fig. 1 – Stream test.

Fig. 2.65 – Stream test [85,89].

Fig. 2 – Plunge test (CRD C61).

Fig. 2.66 – The Plunge test [85,91].

The drop test consists of a scoop that is placed in water. By visual judgement of the muddiness of the water the tendency of washout is determined [85,90]. A pH factor test was suggested in Japan to determine the risk of washout of a concrete sample. The Plunge tests was also developed in Belgium and is used at the University of Ghent [85,91], Fig. 2.66. The cage contains holes with 3-mm diameter. The weight of the cage with concrete is taken before and after it has been sank three times underwater in a larger pipe, Fig. 2.66. The spray tests apparatus is shown in Fig. 2.67 [85,91]. A mould within the apparatus is filled with about 1 kg concrete and sprayed with constant water pressure for 4 min. The loss of material is weighed. Fig. 2.68 shows the Orimet test apparatus which is a flow ability test also used for SCC [85,92]. The time to empty the Orimeter is measured in the test. A L-box was designed [85,88]. The modified L-box apparatus is shown in Fig. 2.69 with normal concrete K40 [88], in Fig 2.70 with underwater concrete without anti-washout additive [85], in Fig. 2.71 with underwater concrete with anti-washout additive and finally in Fig. 2.72 with SCC (slump flow 570 mm only).

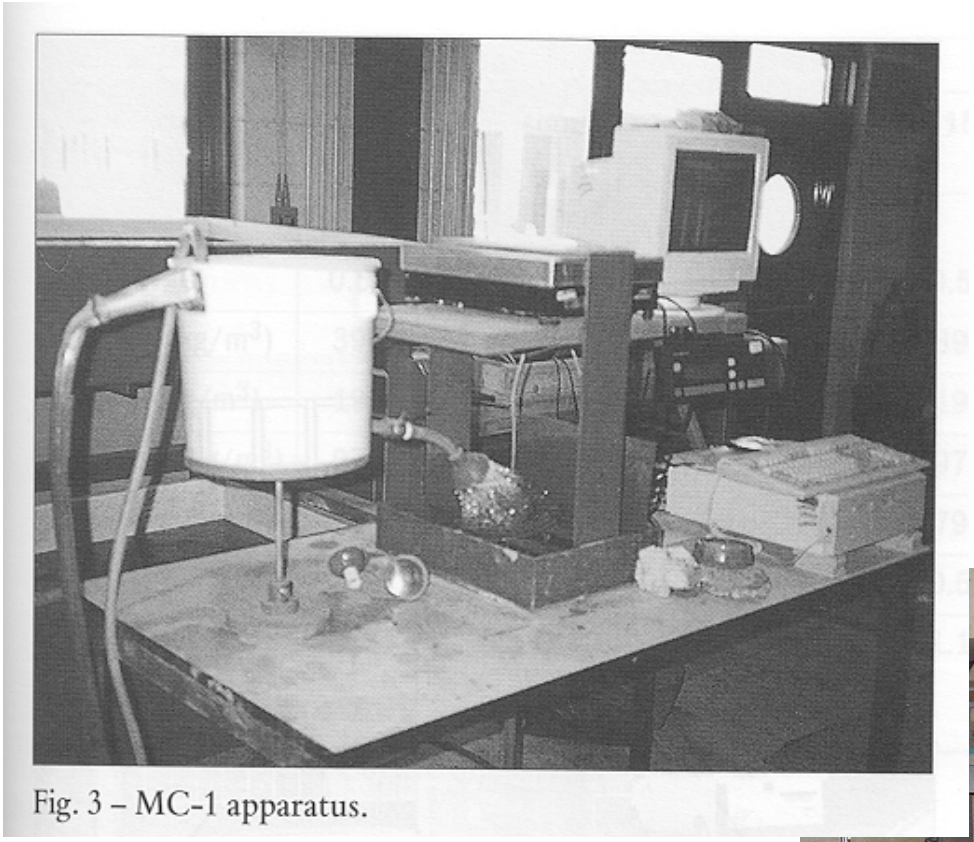

Fig. 3 – MC-1 apparatus.

Fig. 2.67 – Spray test [91].

Fig. 2.68 - Orimet test apparatus - a flow ability test also used for SCC [85,92].

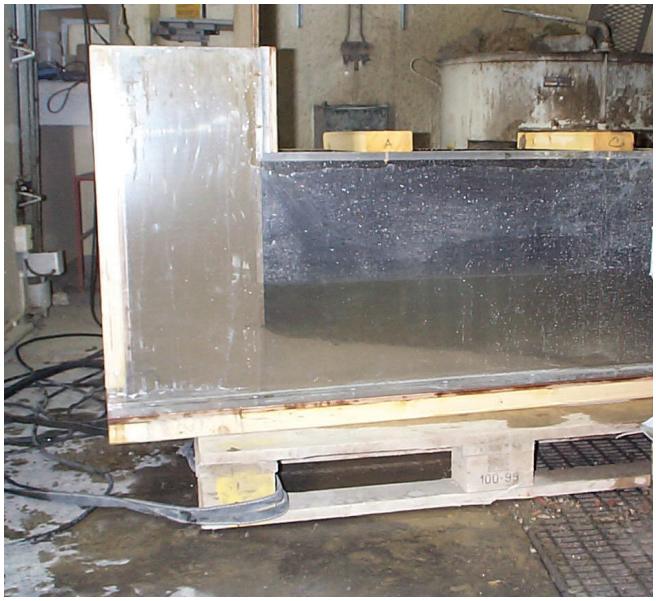

Figs. 2.69 - Modified L-box apparatus with normal concrete K40 [85].

Fig 2.70 - Modified L-box apparatus with underwater concrete without anti-washout additive [85].

Fig. 2.71 - Modified L-box with underwater concrete with anti-washout additive [85].

Fig. 2.72 - Modified L-box with SCC (slump flow 570 mm 570 mm only) [85].

2.7.5 Frost resistance

Frost resistance for concrete with Viscosity-Modifying Admixtures, VMA, was studied for w/c = 0.32, w/c = 0.40 and w/c = 0.45 [93]. The mix proportions are given in Appendix 2.13. Two types of VMA were used: a natural polymer, welan gum, G, and semisynthetic polymer, hydroxypropyl methylcellose, HPMC. The test results indicate that the air-entraining admixture, AEA, was most effectively added after VMA and the superplasticiser, which was a different mixing order to that normally is used, i.e. AEA entered in the beginning of the mixing together with the water [93]. First of all the spacing factor vs the air content was settled at w/c = 0.47, Fig. 2.73.

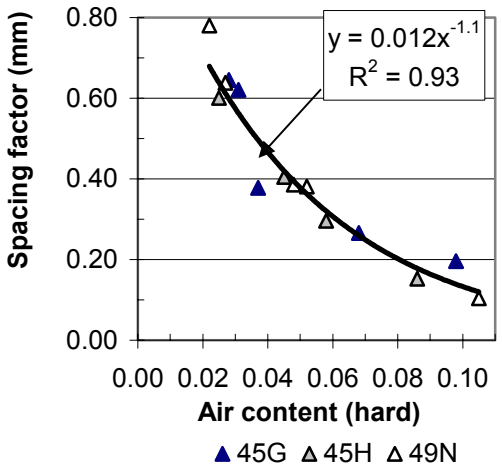

Fig. 2.73- Spacing factor vs air content (w/c=0.47).

The following equation was obtained (w/c= 0.47):

$$L_{w/c=0.47} = 0.012 \cdot A^{-1.1} \quad (2.12)$$

A denotes the air content
L denotes the spacing factor (mm)

Once when the AEA was sufficiently well entered into the concrete it seemed as if the spacing factor became sufficiently low [93]. About A = 8% coincided with L = 0.20 mm which is a normally required spacing factor in order to obtain salt-frost resistance of concrete. Fig. 2.74 shows the spacing factor versus the hardened air content [93]. It was clear that the spacing factor depended both on w/c and the air content. The following equation was found based on Fig. 2.74, Fig. 2.75:

$$L = 0.05 \cdot (w/c - 0.26) \cdot A^{2 \cdot (w/c - 1)} \quad (2.13)$$

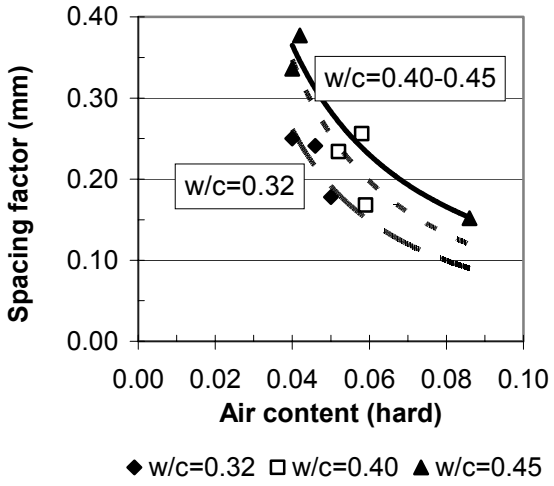

Fig. 2.74 - Spacing factor vs hardened air content.

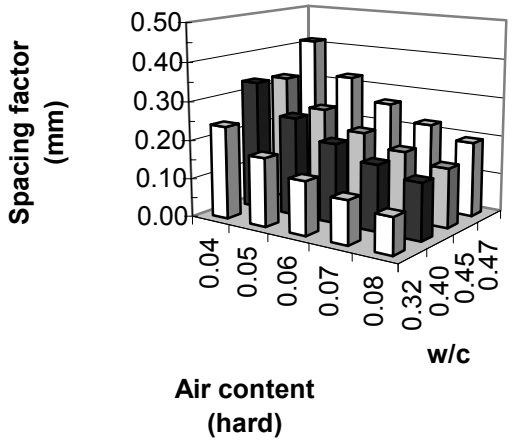

Fig. 2.75 – Spacing factor with equations (2.12) and (2.13) versus w/c and hardened air content.

Fig. 2.76 shows the spacing factor versus the hardened air content for different types of VMA, natural (gum) or synthetic (HPMC) and for normal concrete. What ought to be observed is the large increases of AEA needed especially for concrete with HPMC in order to obtain sufficient air in the concrete, even deaerating admixture, DAA, was required which makes the concrete sensitive during transport and so forth. No influence of the types of VMA on the spacing factor was observed at constant air content, Fig. 2.76. The elongation of the concrete after 309 frost cycles in fresh water was measured both versus the fresh and the hardened air content [93,94] (concrete with w/c = 0.45 did not withstand 309 cycles), Figs. 2.77-2.80. No difference of the elongation was observed related to w/c or types of VMA or between concrete with and without VMA (normal concrete) as related to the elongation. However, some increase of the elongation was observed at higher air content which may be an effect of lower strength at higher air content [93]. Normally AEA is used in concrete in order to prevent internal damages and thereby large elongation. However, for concrete with w/c = 0.32 and w/c = 0.40 no change of the internal resonance frequency was observed and therefore no internal damage [93].

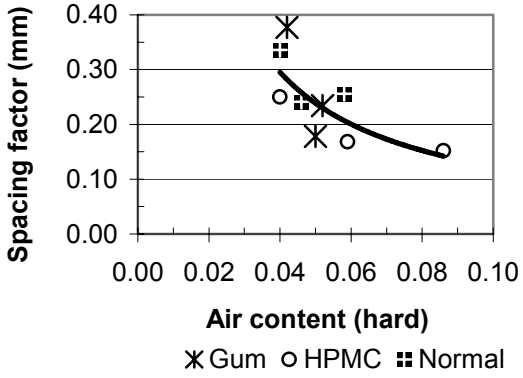

Fig. 2.76 - Spacing factor vs hardened air content, natural VMA (gum), synthetic (HPMC), normal.

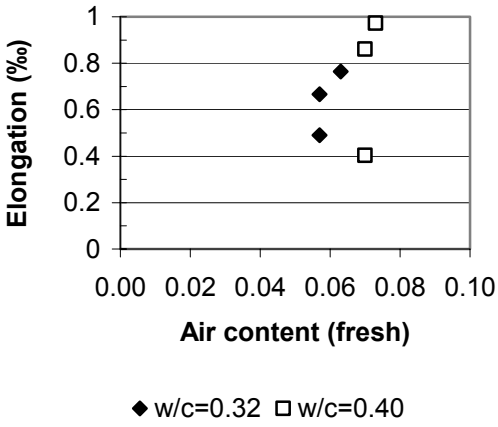

Fig. 2.77 - Elongation after 309 frost cycles in fresh water versus the fresh air content.

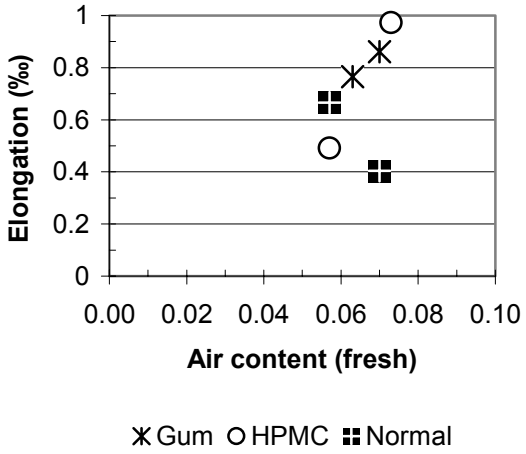

Fig. 2.78 - Elongation after 309 frost cycles in fresh water versus the fresh air content.

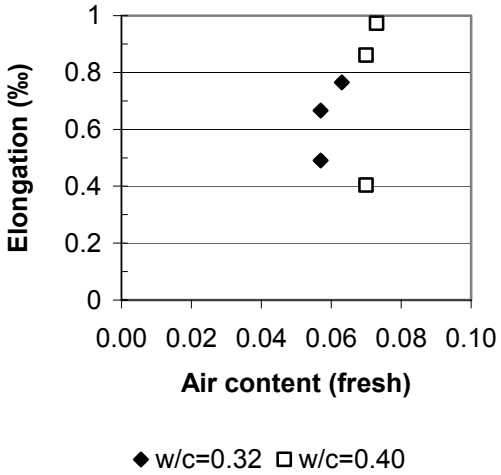

Fig. 2.79 - Elongation after 309 frost cycles in fresh water versus hardened air content.

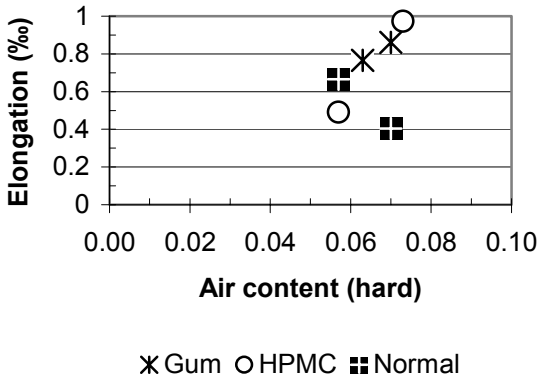

Fig. 2.80 - Elongation after 309 frost cycles in fresh water versus hardened air content.

Scaling resistance was studied on slabs, 280 x 230 x 75 mm [93,95]. The top of the surface was ponded with 3% NaCl after 14 days of wet curing followed by 14 days of air curing. The slabs were frozen 50 cycles and the cumulated mass loss was measured [93,95], Figs. 2.81-2.84. Salt-frost scaling was correlated with hardened air content, Fig. 2.83. No influence of the VMA was observed.

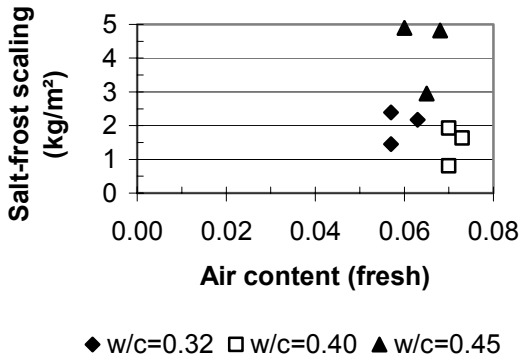

Fig. 2.81 – Salt-frost scaling vs fresh air content.

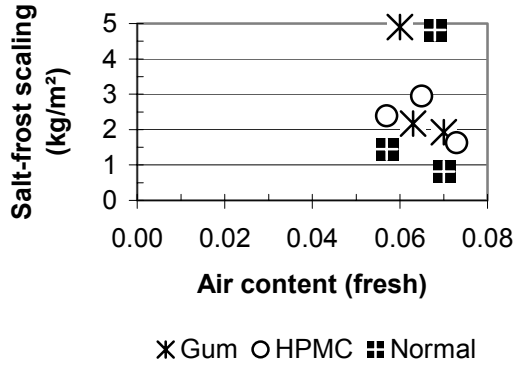

Fig. 2.82 – Salt-frost scaling vs fresh air content.

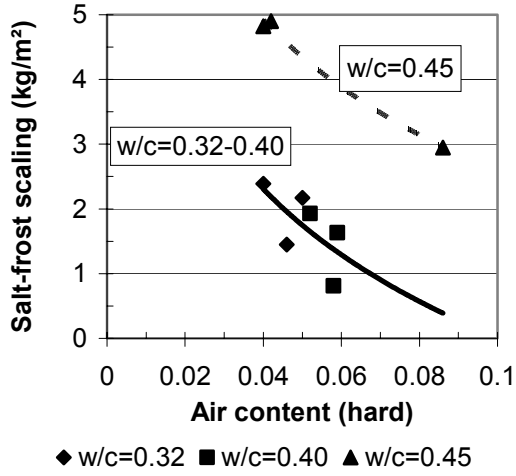

Fig. 2.83 – Salt-frost scaling vs hardened air content.

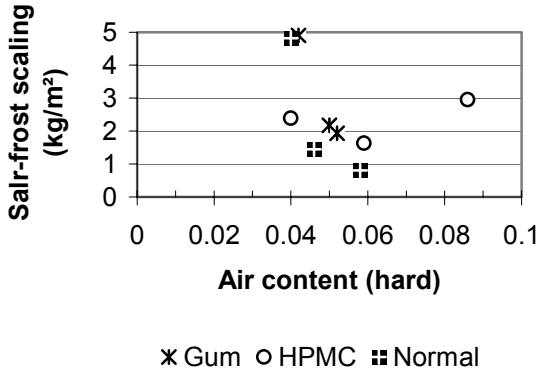

Fig. 2.84 – Salt-frost scaling vs hardened air content.

Result were also correlated with the specific surface, S, of the air void content [93]. Fig. 2.85 shows the specific surface versus the hardened air content. A more or less linear relationship was obtained (VMA of synthetic type, H, gave a more rapid increase with the air content than VMA of natural type, G, gave):

$$S_{w/c=0.47} = 1.54 \cdot A + 7.50 \quad (2.14)$$

A denotes the hardened air concrete (%)
S denotes specific surface of air voids (1/mm)

At lower w/c the specific surface, S, rose more with the air content than at w/c = 0.47, Fig. 2.86 [93]. The following relationship was found between the specific surface, S (1/mm) and the hardened air content, A (%), also shown in Fig. 2.87:

$$S = 41 \cdot (A \cdot (0.5 - w/c) + \ln(w/c) + 1) \quad (2.15)$$

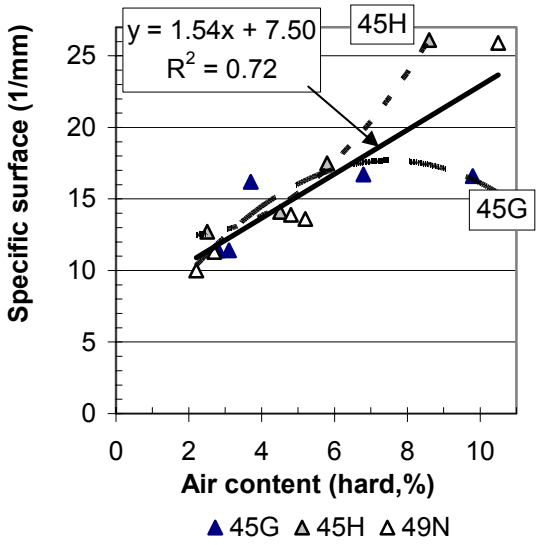

Fig. 2.85 – Specific surface versus the hardened air content at w/c = 0.45 – 0.47.

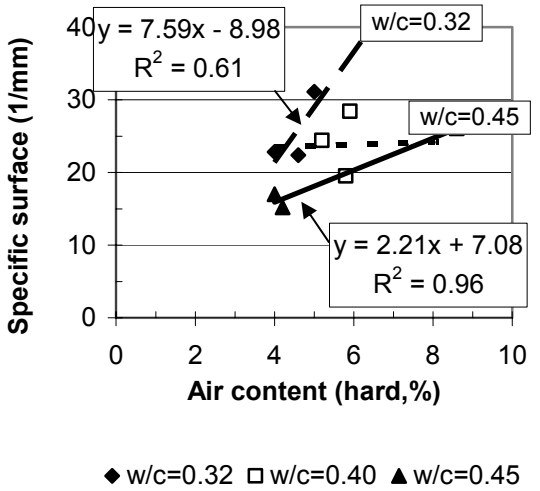

Fig. 2.86 – Specific surface versus the hardened air content at w/c = 0.32 – 0.45.

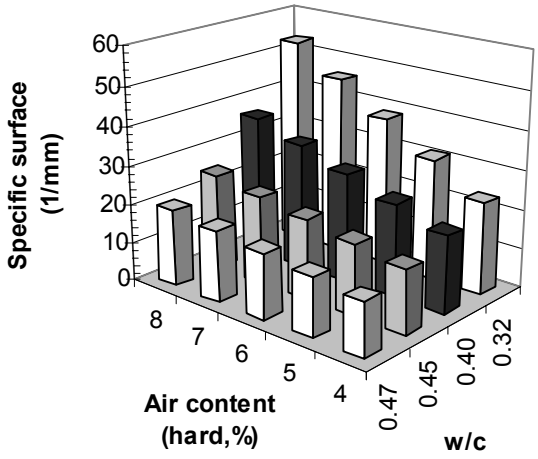

Fig. 2.87 – Specific surface of air voids (1/mm) versus hardened air content (%), eqs. (2.14) - (2.15).

At low w/c the specific air content was more influenced by the air content which was an effect of the pore structure, much finer at low w/c than at higher. Fig. 2.88 shows that no effect of the type of VMA was observed on the specific surface. As related to the elongation of concrete after 309 cycles of freezing and thawing in fresh water no effect of the type of VMA was observed, Fig. 2.89. However, the elongation became larger at higher specific surface which was unexpected and may be an effect of the air concrete being larger at higher specific surface as well, fig. 2.90. the following relationship was obtained:

$$\varepsilon = 0.0046 \cdot S^{1.56}$$

S denotes specific surface of air voids (1/mm)
ε denotes elongation after 309 cycles (‰)

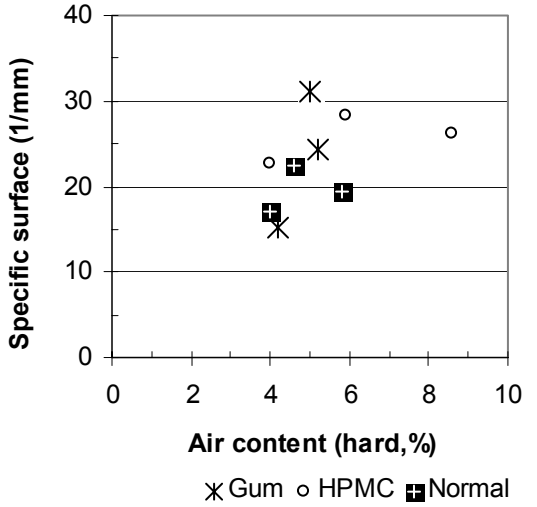

Fig. 2.88 - No effect of the type of VMA was observed on the specific surface.

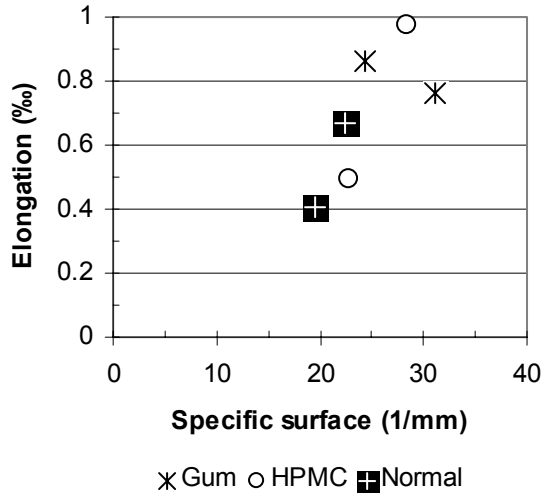

Fig. 2.89 - Effect of the type of VMA on the specific surface and the elongation after 309 cycles.

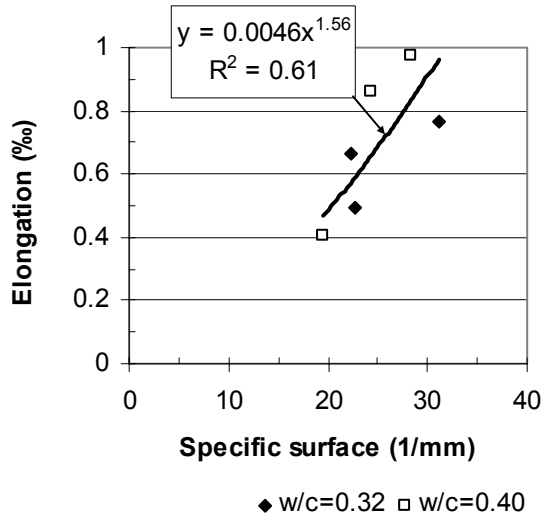

Fig. 2.90 – Effect of specific surface on elongation of concrete after 309 cycles.

Normally there is a clear effect of the specific surface on the salt frost scaling, Fig. 2.91. Fig. 2.91 shows that a higher specific surface was required to obtain the same salt frost scaling for concrete with VMA as for normal concrete. For concrete with w/c = 0.45 a relationship existed between salt frost scaling and the specific surface but not for concrete with lower w/c, Fig. 2.92 [93]. This in turn was most probably an effect of self-desiccation, i.e. at low w/c a great part of the air voids were formed due to the chemical shrinkage of water during hydration [35,96]. Still, the salt frost scaling reported seemed to be very high [93].

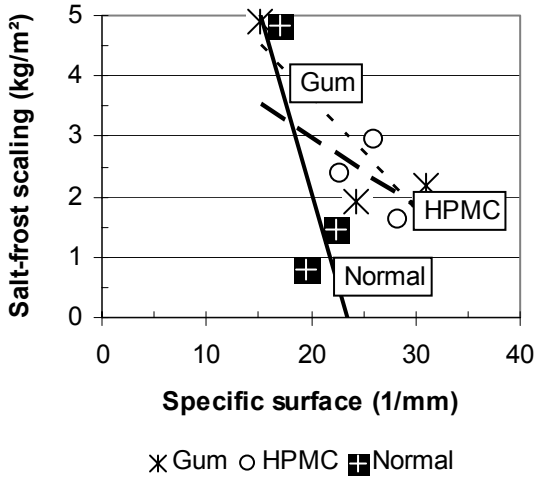

Fig. 2.91 - Higher specific surface was required to obtain the same salt frost scaling for concrete with VMA as for normal concrete.

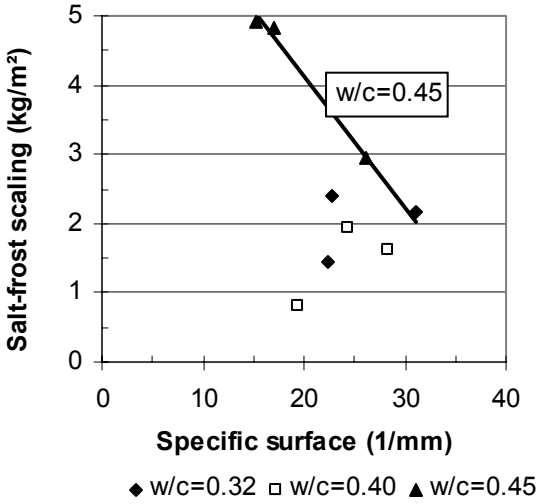

Fig. 2.92 - Concrete with w/c = 0.45 had a relationship between salt frost scaling and specific surface but not the other concrete with lower w/c.

3. MATERIALS, MANUFACTURE AND METHODS

3.1 Material

Crushed gneiss (E-modulus 61 GPa and strength 230 MPa), pea gravel, crushed sand, natural sand, limestone filler (brand Limus 40), Fortico blended cement (CEM II/A-D-52,5, 7.5% silica fume), granulated silica fume (brand Elkem Micropoz) and Degerhamn cement (CEM I42.5BV/SR/LA) were used in the mix compositions, Fig. 3.1-4, Appendices 2.4 and 3.1-2 [97]. Melamine-based superplasticiser was used for NC (brand Flyt 97M), polycarboxyl ether for SCC (brand Glenium 51) and air-entertainment agent based on fir oil and fatty acids (brand Microair). The materials were put in steel barrels in order to maintain a constant moisture level. The concrete was mixed in a 40-l or 1000-l compulsive mixer in the laboratory or at ready mixer at BTC. The following mixing order was used:

1. Mixing dry material, air-entrainment and water ½ min.
2. Mixing with superplasticiser 2½ min.

3.2 Manufacture of specimen

3.2.1 Vattenfall

One third of the specimen was cast or core drilled by Vattenfall at different locations [85].

3.2.2 LTH

One third of the specimen were cast at LTH in water in a L-box, in the following way, Fig. 3.3-4:

1. Casting and curing in water and core drilling either at the near (N) or at the remote (R) end (in the shaft) of the L-box.
2. Internal frost thaw resistance in distilled water or fresh water: 3 cylinders 50 mm in diameter and 150 mm in height.
3. Salt frost thaw scaling with 3% sodium chloride: 3 discs 94 mm in diameter and 40 mm in height [98].

3.2.3 BTC

The field test at BTC was carried out with submerged cast concrete in a full-scale beam, 0.25 x 1 x 6 m. At the field test one side of mould consisted of a prefabricated concrete element and the other side of wood or transparent glass fibre [97]. The mould was filled with water before the casting took place. The cores, 50 x 150 mm, for test of internal frost resistance, were taken by core drilling. Of each concrete 3 specimens were used from each corner of the beam, i.e. a total of 36 cores. The age of the concrete at the start of the testing at LTH and at BTC was 90 days.

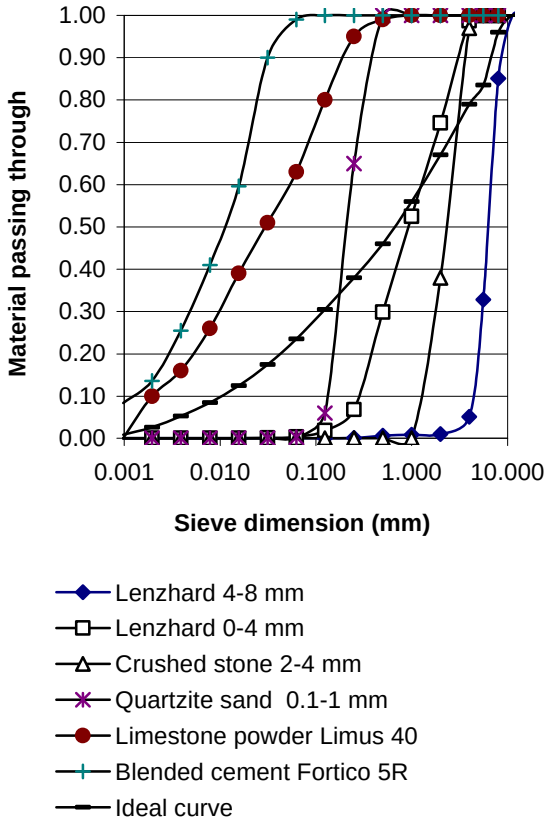

Fig. 3.1 – Grading curves of materials at LTH.

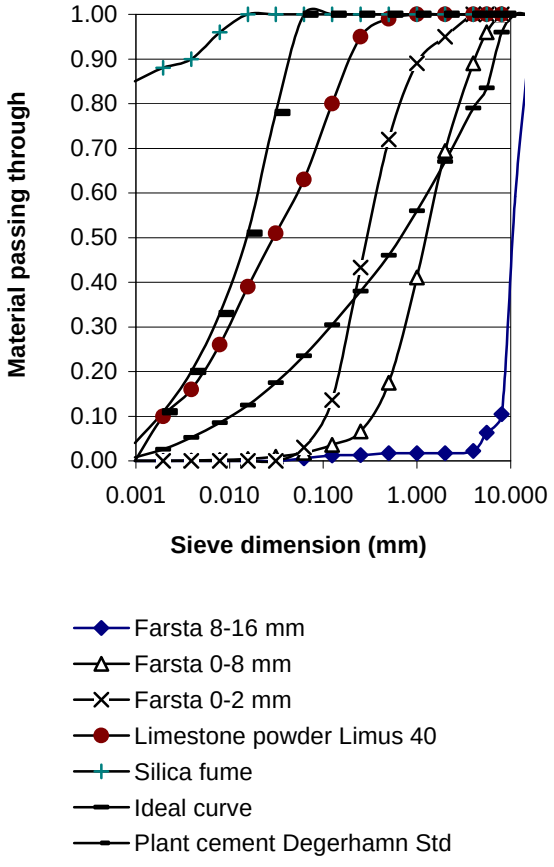

Fig. 3.2 – Grading curves of materials at BTC.

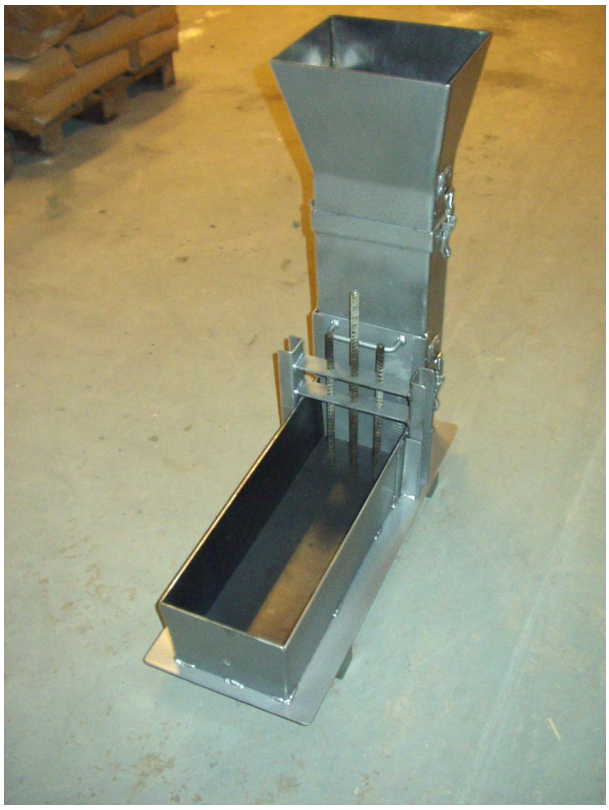

Fig. 3.3 – Bottom of L-box filled with water before a sliding gate was opened at the end of the box in order to cast concrete in the vertical shaft submerged in the box and to cure it there.

Fig. 3.4 – Bottom of L-box filled with water before a sliding gate was opened at the end of the box in order to cast concrete in the vertical shaft submerged in the box and to cure it there.

Fig. 3.5 – Field test at BTC with one side of mould consisting of a prefabricated concrete element and the other of wood or transparent glass fibre. Photo: Iad Saleh.

Fig. 3.6 – Field test at BTC with one side of mould consisting of a prefabricated concrete element and the other of wood or transparent glass fibre. Photo: Iad Saleh.

3.3 Methods

3.3.1 Internal frost resistance

The adequacy of resistance of a given concrete to frost attack was determined by freezing and thawing tests described by ASTM 666-92. The tests continued until 300 cycles or until the dynamic elastic modulus was reduced to 60% of its original value [94]. The damage was assessed after 100 and 300 of frost cycles between +20 °C and – 20 °C of freezing and thawing in distilled water with two full cycles per day. The conditions of ASTM 666-92 are more severe than those occurring in practice since the prescribed heating and cooling cycle is between + 4 °C and – 18 °C at a rate of cooling of 14 °C/h. In most part of the world, a rate of 3 °C/h is rarely exceeded [84]. The tests were started at about 90 days' age. For tests of internal freezing and thawing resistance cylinders 50 mm in diameter and 150 mm long were placed in distilled water solution after 14 days of pre-storage in water saturated with lime. The specimen was placed in a rubber container, fully immersed in distilled water, Fig. 3.7. The frost thaw cycle varied between – 20 °C and 20 °C, twice a day, Fig. 3.8. Cooling rate of specimen at internal freezing was around 12 °C and the heating rate varied between 10 °C/h and 20 °C, Fig. 3.9. The dotted line indicates the air temperature. Compared with ASTM 666-92 the cooling rate was slightly lower but still much more severe than that in practice. The weight and the fundamental resonance frequency, FRF, of the specimen were observed after 100 and 300 cycles. The durability factor, D_f, is given by the following expression:

$$D_f = n/3 \cdot E_{de}/E_{d0} \qquad (3.1)$$

n nenotes number of cycles at the end of the test

E_{de} denotes the elastic modulus, i.e. FRF, at the end of the testing.

E_{d0} denotes the elastic modulus, i.e. FRF, at the start of the testing.

The decrease of the elastic modulus due to internal damages was obtained by measurement of the FRF in a Grindosonic apparatus. D_f is of interest primarily in a comparison of different concrete, preferably when only one variable is changed. Generally, a value smaller than 40 means that the concrete is probably unsatisfactory, values between 40 and 60 are regarded as doubtful while values over 60 indicate that the concrete is probably satisfactory [84]. More than 60% loss of elastic modulus, i.e. more the 60% loss of FRF, at 300 cycles is unsatisfactory for the internal frost resistance.

Fig. 3.7 - Specimen in rubber container, immersed in distilled water (internal frost resistance tests).

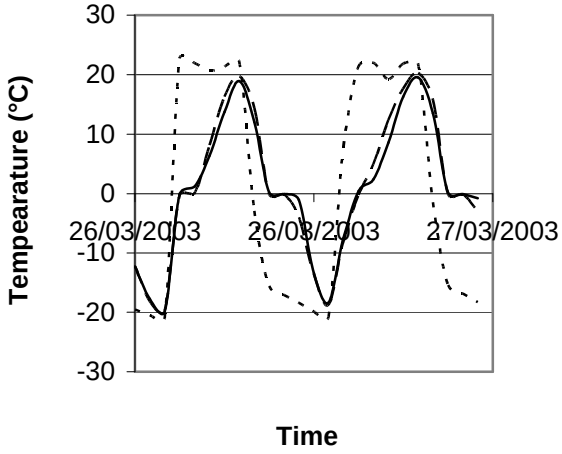

Fig. 3.8 – Temperature of specimen at internal freezing and thawing resistance tests.

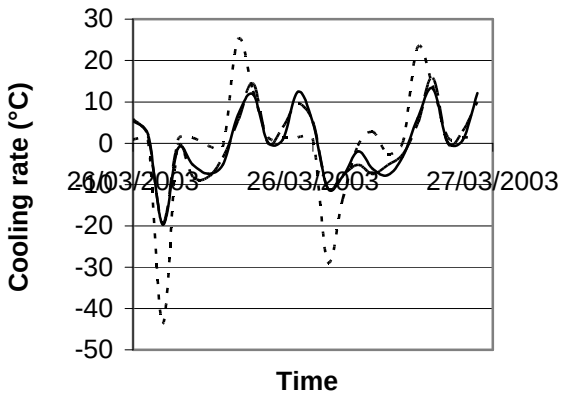

Fig. 3.9 – Cooling rate of specimen at internal freezing and thawing resistance tests.

3.3.2 Salt freezing and thawing resistance

Salt freezing and thawing resistance was studied by a method previously used by Lindmark [98] which is similar to the CDF-method [20]. For tests of salt frost thaw scaling cylinders 100 mm in diameter and 40 mm long were placed in 3% sodium distilled water solution after 14 days of prestorage in water saturated with lime. The specimen was placed in a plastic container, fully immersed, Fig. 3.10. The frost thaw cycle varied between – 20 °C and 20 °C, twice a day, Fig. 3.11. The maximum temperature was slightly lower than in tests with internal frost resistance but also lower the temperature. A minimum temperature less than 18 °C is of great importance for damages to occur. At these tests the minimum temperature well was below 20 °C, Fig. 3.11. The air temperature is shown with a dotted line. The cooling rate of the specimen is shown in Fig. 3.12. The cooling rate varied between 12 °C/h and 14 °C/h the air temperature cooling rate being shown with a dotted line. The scaling of the specimen was observed after 28, 56 and 112 cycles. Good salt freezing and thawing resistance is supposed with a one-side scaling less than 0.5 kg/m² and very good salt freezing and thawing resistance at less than 0.2 kg/m². This method consist of a all-side freezing which is supposed to be more severe the one-side testing procedure.

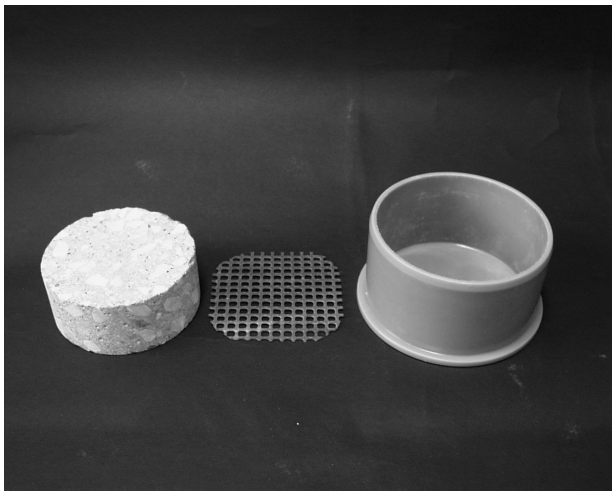

Fig. 3.10 - Specimen for tests of salt freezing and thawing scaling in 3% sodium distilled water.

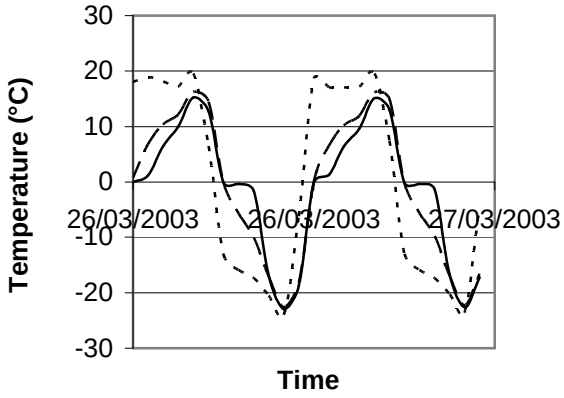

Fig. 3.11 – Temperature of specimen for salt freezing and thawing scaling tests.

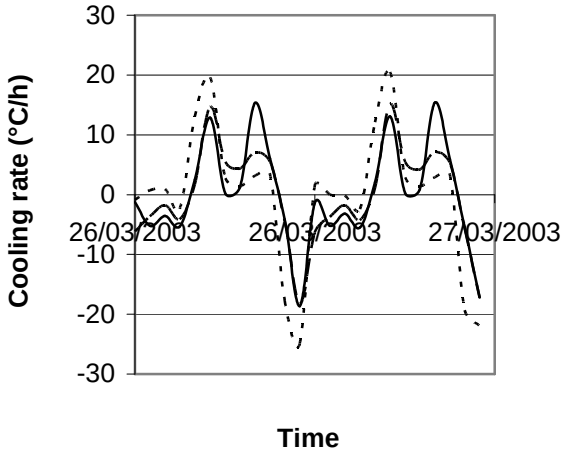

Fig. 3.12 – Cooling rate of specimen for salt freezing and thawing scaling tests.

3.3.3 Strength

A water-cured cube, 100-mm, was tested for strength at a rate of 1 MPa/s in a Seidner testing machine. The testing machine was calibrated. The accurate strength would be 1 MPa higher. An eccentricity in placing the cube or the cylinder may have affected the test result. The fault of eccentricity was less than 1 mm. The hourglass shape of fragments after testing the cube indicated a highly centric placing. At high strength a circular conical part of the cube remained after testing. From the field beams Ø100 x 100 mm cylinders cored were tested after grinding of the ends.

4. RESULTS

4.1 Grading curves of the fresh concrete

4.1.1 Laboratory concrete cast at LTH

The grading curve was calculated for sieves between 0.063 mm and 11.2 mm:

$$s = 0.54 \cdot d^{0.28} \quad (4.1)$$

d denotes sieve diameter (mm)
s denotes material passing through

4.1.2 Field concrete cast at BTC

The grading curve was defined by slightly larger average particle size and a lower slope [97]:

$$s = 0.53 \cdot d^{0.26} \quad (4.2)$$

4.2 Strength

4.2.1 Concrete delivered by Vattenfall

Strength results at 28 days' age are shown in Fig. 4.1 and Appendix 3.1 [85].

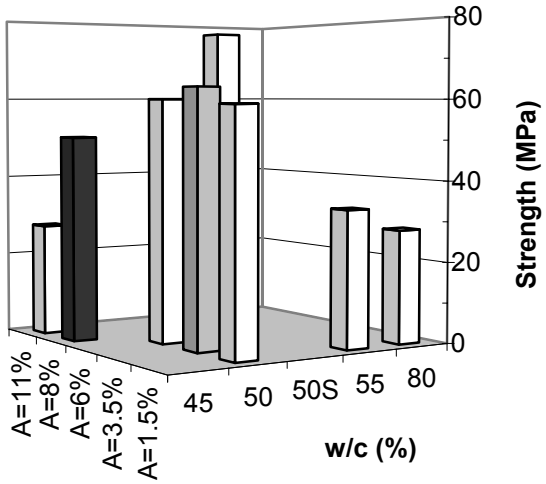

Fig. 4.1 – Concrete strength at 28 days' age delivered by Vattenfall. A = air content (%). S = SCC.

4.2.2 Concrete cast at LTH

Appendix 3.2 and Fig. 4.2 show on average 28-day strength. Fig. 4.3 shows on average strength development after 90 days.

4.2.3 Field concrete cast by BTC

Fig. 4.4 and Fig. 4.5 show on average 28-day strength results dependent on the position of the wall cores [97]. Fig. 4.6 shows the standard deviation of strength of concrete cast in the field. C = crest; F = foot; N = near pump; R = remote. Fig. 4.7 shows the variance of the 28-day strength [97].

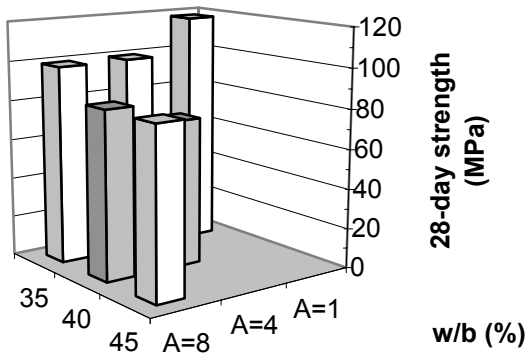

Fig. 4.2 - On average strength of concrete cast at LTH. A = air content (%).

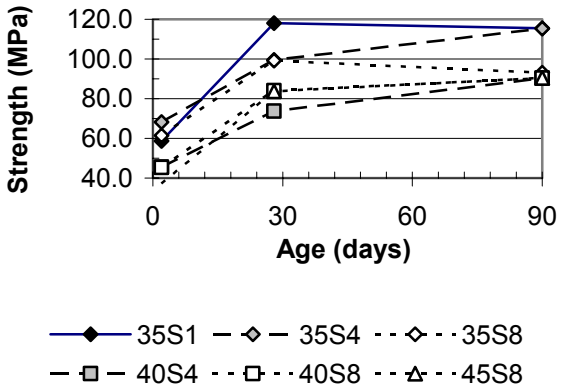

Fig. 4.3 - Strength on average at LTH. 1 = air content (%); 35 = w/b; A = air content (%).

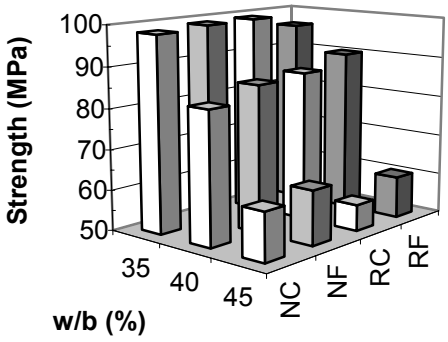

Fig. 4.4 – Strength of concrete cast in the field. C = crest; F = foot; N = near pump; R = remote.

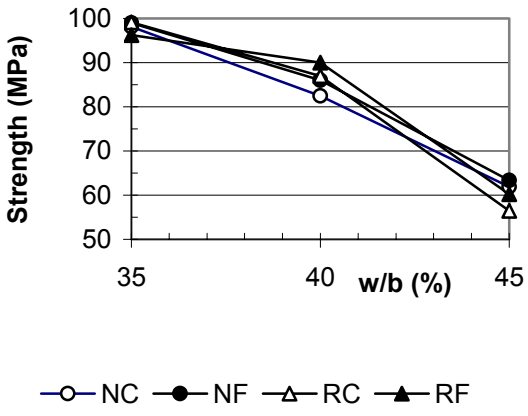

Fig. 4.5 – Strength of concrete cast in the field. C = crest; F = foot; N = near pump; R = remote.

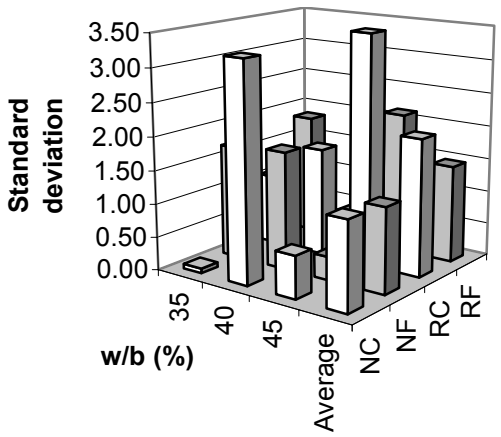

Fig. 4.6 – Standard deviation of strength of concrete cast at BTC. C = crest; F = foot; N = near pump; R = remote.

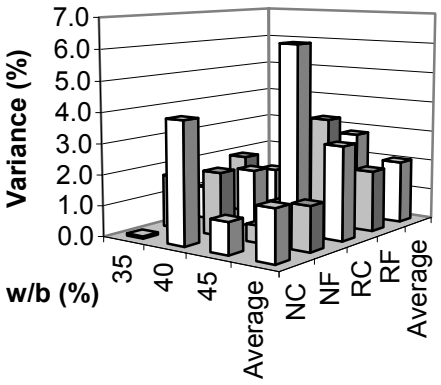

Fig. 4.7 – Variance of strength of field concrete. C = crest; F = foot; N = near pump; R = remote.

4.3 Internal freezing and thawing resistance

4.3.1 Concrete delivered by Vattenfall

Figs 4.8-9 and Appendix 4.1 show that all concrete except for one concrete with w/b = 0.45 and 11% air content and one SCC with w/b = 0.48, did not fulfil the ASTM 666 requirements as concerns internal loss of FRF, i.e. elastic modulus to be larger than 40% after 300 cycles. Eight of 12 concrete were totally destroyed even before 100 frost cycles. Concrete with anti-wash out powder was not durable to internal freezing and thawing even through 8% air content was studied at w/b = 0.45. Concrete with anti-wash out powder was durable to internal freezing and thawing when 11% air content was studied at w/b = 0.46. However, at high air content the strength became too low. SCC with w/b = 0.48 and 6% air content exhibited a high grade of internal freezing and thawing resistance. Only 4.5% loss of FRF and 0.9% loss of weight after 300 frost cycles was observed. These results confirm the previous studies that SCC generally is more resistant to internal freezing and thawing attack than normal concrete is [22,23].

4.3.2 Concrete cast at LTH

Figs 4.10-11 and Appendix 4.2 show the performance of internal frost resistance of concrete cast at LTH. Concrete with w/b = 0.35 and w/b = 0.40 showed good internal frost resistance both related to FRF (less than 15% losses after 300 cycles) and scaling (no loss of weight). Small losses of FRF were observed of concrete cast at the remote end of the L-box. At w/b = 0.45 too large scaling was obtained at the remote end of casting in the L-box.

4.3.3 Concrete cast at BTC

Figs 4.12-13 and Appendix 4.3 show internal frost resistance of concrete that were cast by BTC [97], i.e. large loss of FRF in concrete with w/b = 0.35.

4.4 Salt freezing and thawing resistance

4.4.1 Concrete tested at LTH

Fig. 4.14 and Appendix 4.4 show large salt frost scaling for all normal concrete delivered by Vattenfall except for concrete with as much as 11% air content (46U11: 0.5 kg/m³ after 56 cycles). Concrete with anti-wash out powder was not durable to salt freezing and thawing scaling even through as much as 8 % air content was studied at w/b = 0.45. SCC, with w/b varying between 0.35 and 0.40 exhibited an excellent salt freezing and thawing resistance at the near end of the L-box at casting. At the remote end of the L-box air probably was washed out which reduced the freezing and thawing resistance. Eight percent of air content was required in order to fulfil freezing and thawing resistance at the remote end of the L-box at casting submerged SCC except for w/c =0.45. For w/c = 0.45 not even 8% air content was enough to fulfil a salt freezing and thawing scaling of less than 0.5 kg/m², Fig. 4.14.

4.4.2 Comparison between LTH and Vattenfall

The tests performed by Vattenfall [85] only showed a fifth of the salt frost scaling after 56 cycles compared with the test performed by LTH, Fig. 4.15. The difference between the two methods was large – the LTH methods exhibited on average 5 times as large salt frost scaling compared with the Borås method (concrete 49U3T was not taken into account since it was totally broken before 56 cycles with the LTH method). In practise this means that concrete that was supposed to be salt frost resistance according to the Borås method (45U8 and 46 U11) were not resistant to freezing and thawing according the LTH method provided that the maximum salt frost scaling was set at 0.5 kg/m² for both the methods. The reason for the difference was the rapid freezing at LTH, according to ASTM 666-92, 12 °C/h [94].

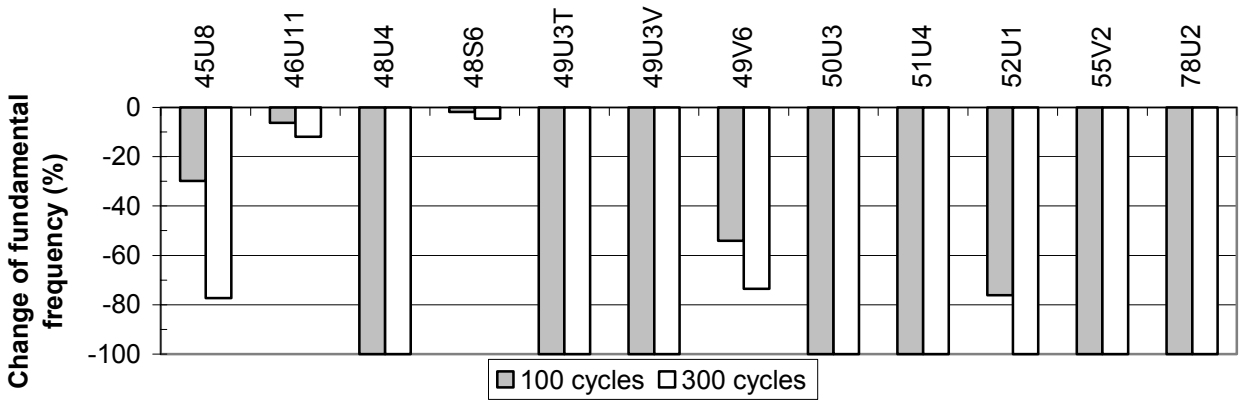

Fig. 4.8 - Internal freezing and thawing resistance, FRF, after 100 and 300 cycles of concrete delivered by Vattenfall. S = SCC; U=submerged concrete; 2 = air content (%); 45 = w/b (%).

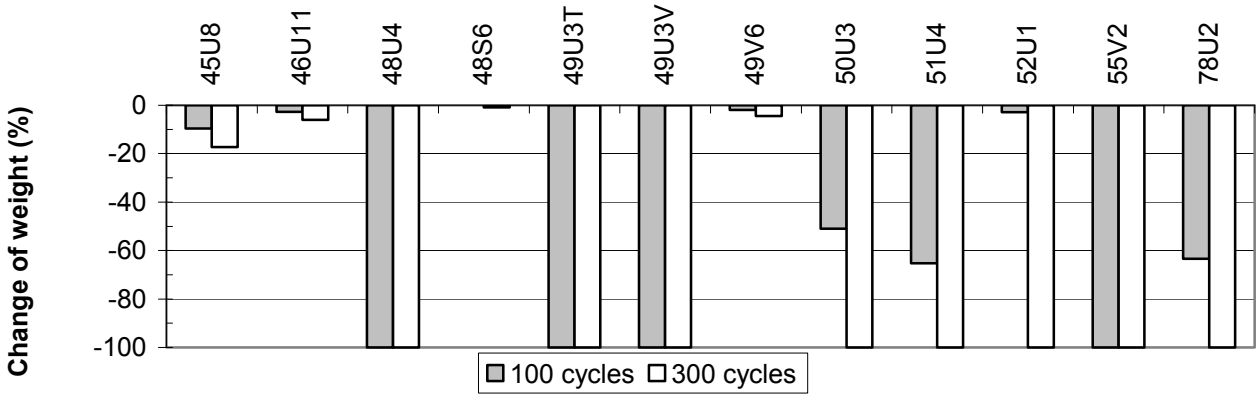

Fig. 4.9 - Internal freezing and thawing resistance, loss of weight, after 100 and 300 cycles of concrete delivered by Vattenfall. S = SCC; U=submerged concrete; 2 = air content (%); 45 = w/b (%).

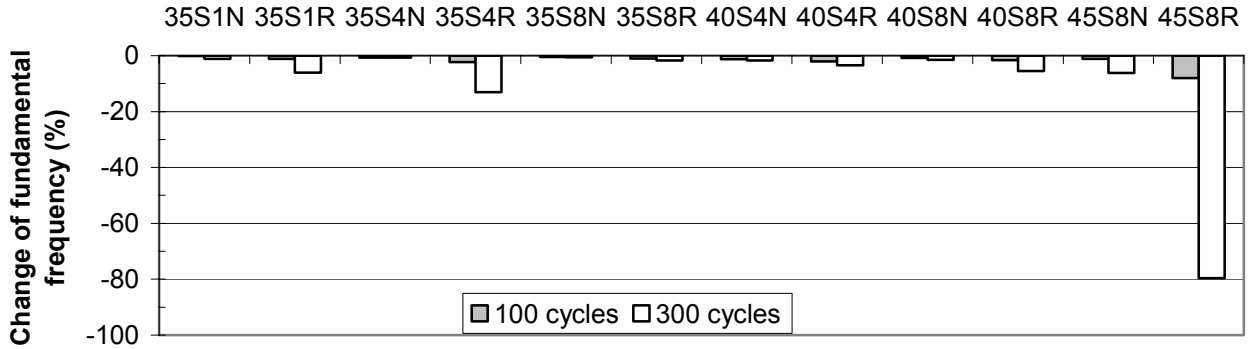

Fig. 4.10 - Internal freezing and thawing resistance, FRF, after 100 and 300 cycles of concrete cast at LTH. 35 = w/b (%); N = near end of casting; R = remote; S = 7.5% silica fume; 4 = air content (%).

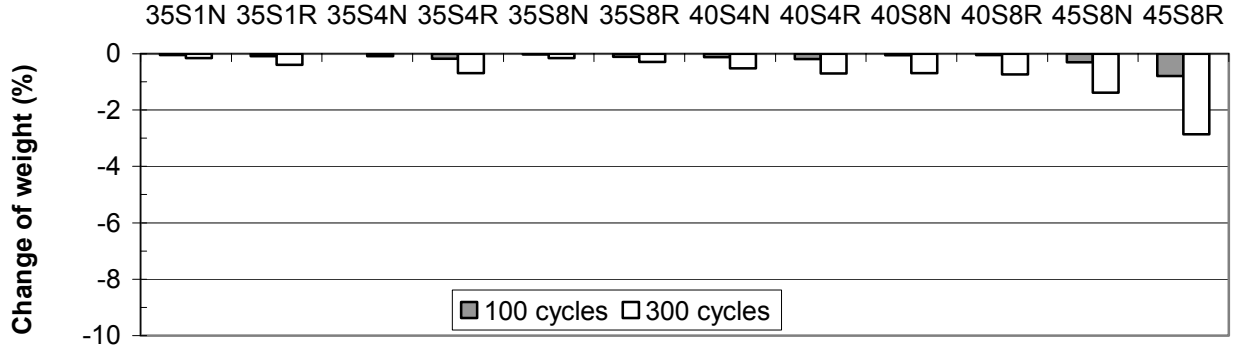

Fig. 4.11 - Internal freezing and thawing resistance, loss of weight, after 100 and 300 cycles of concrete cast at LTH. 35 = w/b (%); N = near end of casting; R = remote; S = 7.5% silica fume; 4 = air content (%).

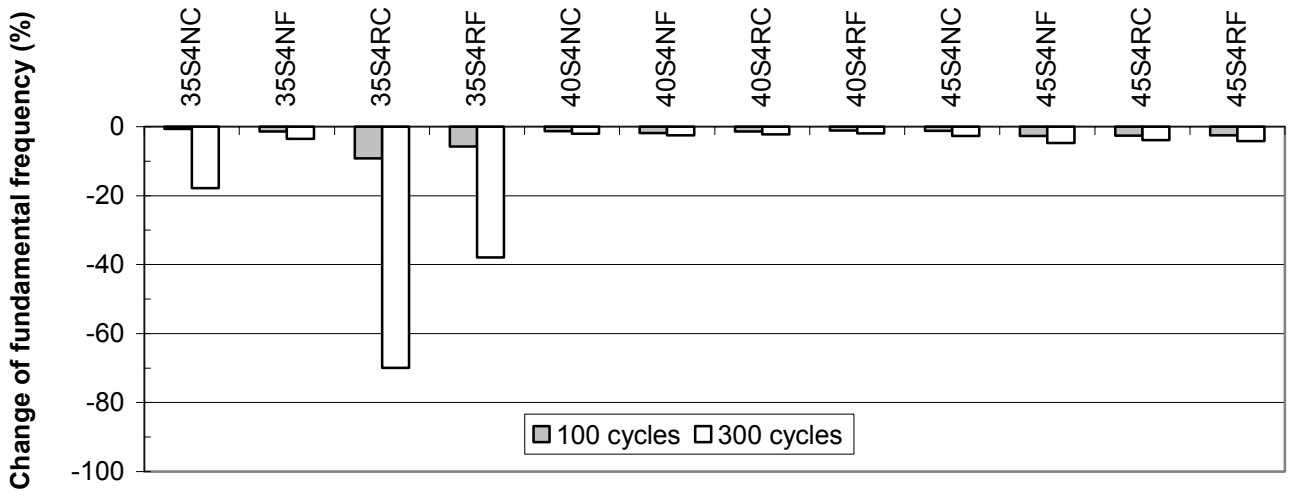

Fig. 4.12 - Internal freezing and thawing resistance, FRF, after 100 and 300 cycles of concrete cast at Farsta. 35 = w/b (%); S = 7.5% silica fume; 4 = air content (%); C = crest; F = foot; N = near the; R = remote.

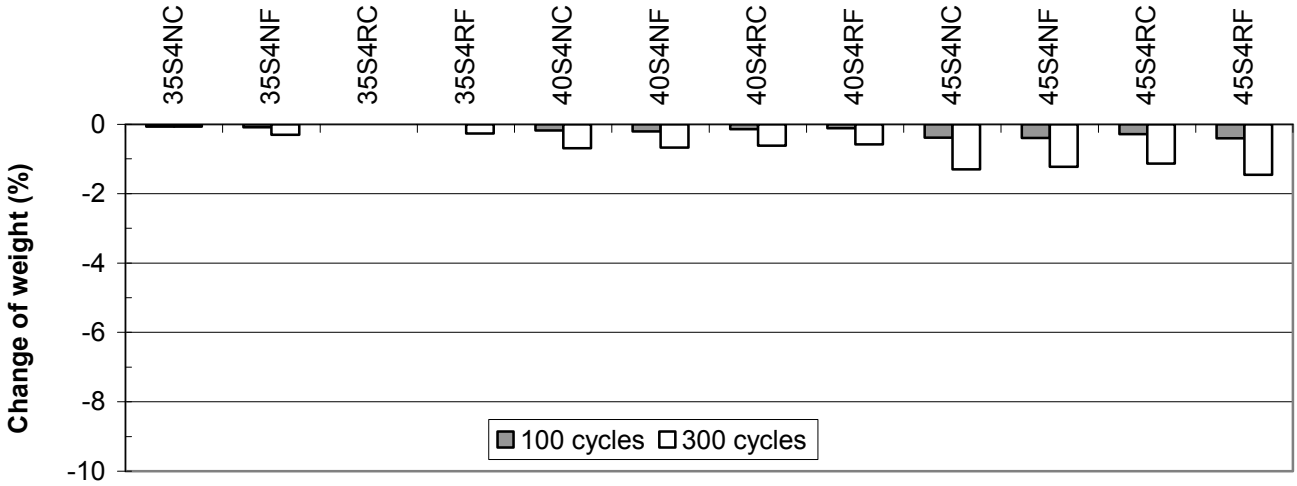

Fig. 4.13 - Internal freezing and thawing resistance, FRF, after 100 and 300 cycles of concrete cast at Farsta. 35 = w/b (%); S = 7.5% silica fume; 4 = air content (%); C = crest; F = foot; N = near the; R = remote.

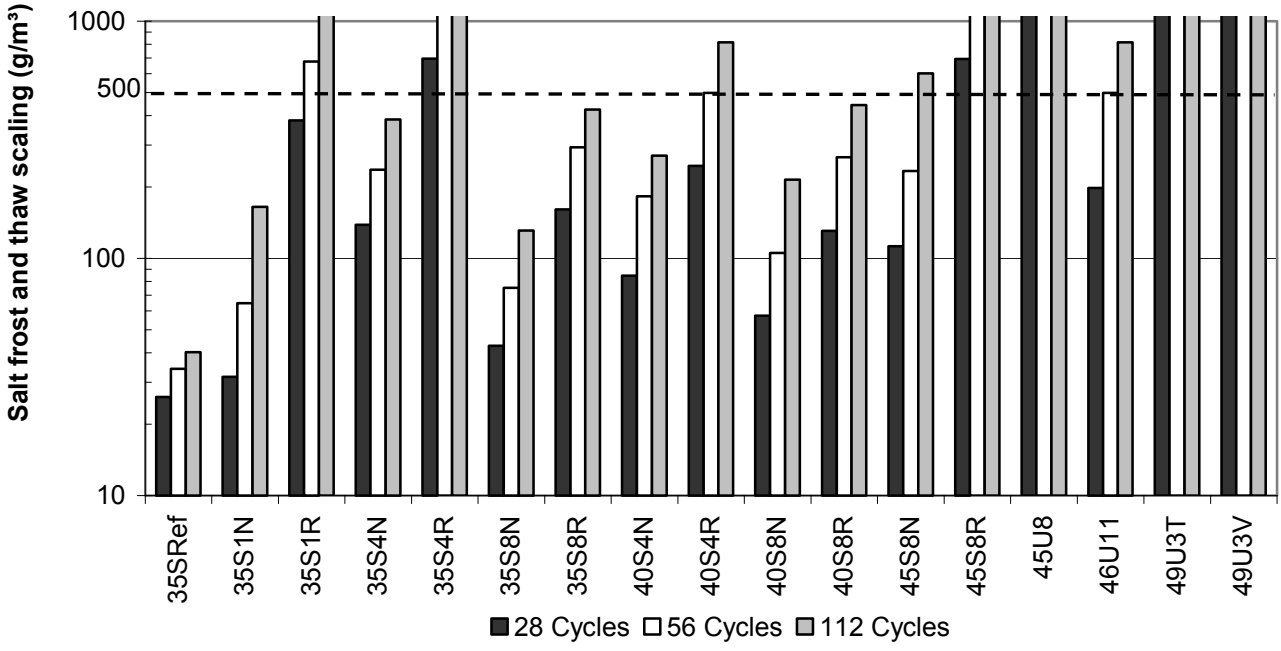

Fig. 4.14 – Salt freezing and thawing resistance of concrete. N = near the casting place; R = remote; Reference cast above water; S = 7.5% silica fume; U=submerged concrete; 2 = air content (%); 45 = w/b (%).

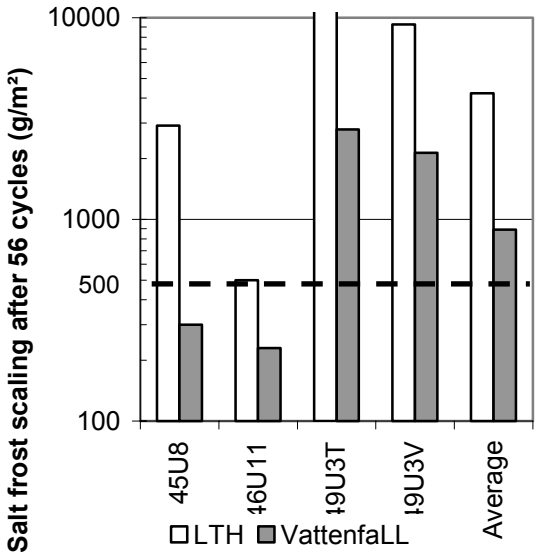

Fig. 4.15 – Salt frost scaling on the same concrete by LTH and Vattenfall. 45 = w/b (%); U = anti-washing-out powder; 3 = air content (%); T = specimen cured dry; V = specimen cured wet.

4.5 Density

4.5.1 Concrete cast at LTH

One indirect way of determine the effect of difference in air content may be to observe the density. The diameter and the length of all specimens were established before the freezing tests were carried out. Fig. 4.16 shows that position of the specimen slightly affected the density versus air content.

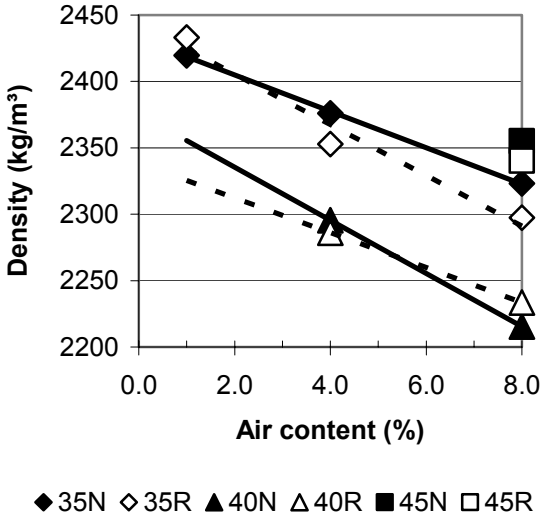

Fig. 4.16 - The position of the specimen did not affect the density versus air content. 35 = w/b (%); N = near the casting place; R = remote position.

However, for concrete with w/b = 0.45 the results were inconsistent. This was observed for the strength with w/b = 0.45, i.e. too large strength in comparison to the air content (probably only 1%).

4.5.2 Concrete cast at BTC

Table 4.1 and Figs. 4.17-18 show large differences between the density of concrete with w/b = 0.40 and w/b = 0.45 at crest and foot of the casting probably due to segregation of aggregate [97].

Table 4.1 - Density at crest and foot dependent on the position of the casting versus w/b (kg/m³). C = crest; F = foot; N = near the; R = remote.

w/b (%)	35	40	45	Average
NC	2401	2326	2264	2330
NF	2443	2367	2354	2388
RC	2414	2371	2256	2347
RF	2438	2402	2345	2395
Average	2424	2366	2305	2365

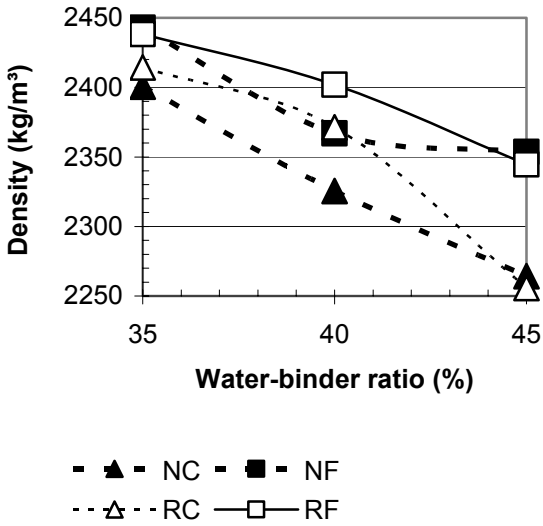

Fig. 4.17 - Density at crest and foot dependent on the position of the casting versus w/b. C = crest; F = foot; N = near the; R = remote. 35 = w/b (%).

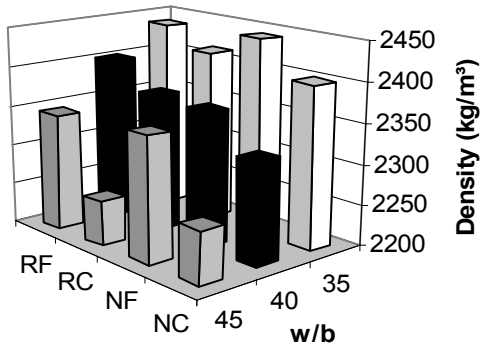

Fig. 4.18 - Density at crest and foot dependent on the position of the casting versus w/b. C = crest; F = foot; N = near the; R = remote. 35 = w/b (%).

5. ANALYSIS AND DISCUSSION

5.1 Grading curves of the fresh concrete

5.1.1 Comparison with normal concrete, NC.

Analyses were performed on the differences of particle grading in fresh concrete of the different mixes. The following particle grading of fresh NC was foreseen, Figure 5.1 [62]:

$$s = a \cdot d^b \quad \{0.125 < d < 0.7 \cdot d_{max}\} \qquad (5.1)$$

s denotes particle passing through
a 38%
b constant according to Table 5.1
d particle diameter (0.1 < d < 10 mm)
K cube strength of concrete (MPa)

Table 5.1 - Constant b in equation (5.1)

K	25	60	90	120	150
b	0.32	0.24	0.20	0.18	0.16

NC follows more or less the grading foreseen in Figure 5.1, i.e. much less fines than in SCC. For NC and sieves varying between 0.063 mm and 16 mm a = 37% and b varying between b = 0.24 (corresponds to K60) and b = 0.35 (K30) were obtained. For sieves varying between 0.063 mm and 16 mm and SCC without fibres a = 47% was obtained with b varying between b = 0.24 (K60) and b = 0.27 (more inclined, correspond to K30).

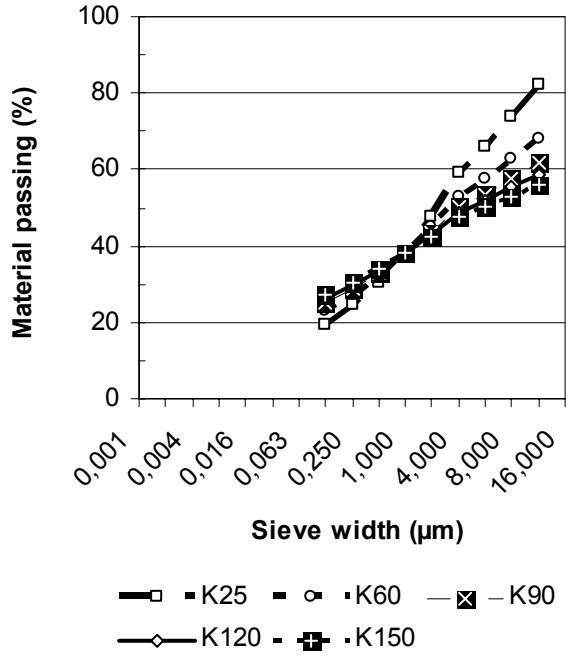

Figure 5.1 – Ideal particle grading of fresh NC.

5.1.2 Comparison with other SCC

The following consideration should be taken when constructing a grading curve for fresh SCC as described by equation (5.1), Fig. 5.2 [99]:

- a = 47%
- b = 0.27 (K30)
- b = 0.24 (K60)

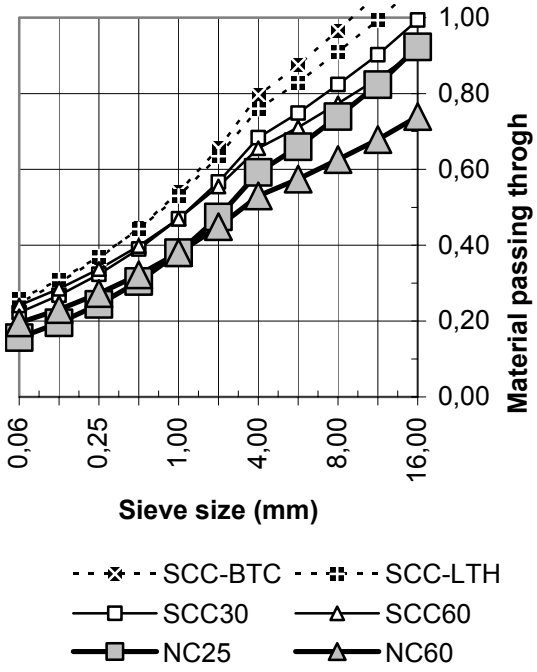

Figure 5.2 – Grading curves of fresh concrete. NC = normal concrete; SCC = Self-Compacting Concrete; 25 = cube strength (MPa).

With field concrete the following constants in equation (5.1) were obtained:

- a = 53%
- b = 0.26

With concrete cast at LTH the following constants in equation (5.1) were obtained:

- a = 54%
- b = 0.28

Little cement + filler in SCC gave a risk of segregation. i.e. low a-value in equation (5.1); too flat grading gave a risk of blocking for concrete with 4% fibres, i.e. too low b-value in equation (5.1). It is clearly seen from Fig. 5.2 that more fine are required in submerged cast SCC than in normal cast SCC. In turn also more fines are required in SCC than in NC in order to avoid segregation, also required by the Road Administration. When SCC is cast submerged there is a great risk of water ingress in the concrete during the casting.

5.2 Strength

5.2.1 Concrete delivered by Vattenfall

It was clear that large content of air in the concrete in order to avoid frost damages on submerged cast concrete affected the strength results substantially, Fig. 4.1 and Appendix 3.1 [85]. Increase of air content as a method to avoid frost damages was not a feasible, Fig. 5.3, as strength became unacceptably low. Fig. 5.4 shows the strength of concrete with w/c = 0.45-0.50. The following relationship was obtained [85]:

$$f_c = (20\text{-}A)\cdot(w/c)^{-1.28} \qquad (5.2)$$

f_c denotes compressive strength (MPa)
w/c denotes water-cement ratio {0.45 < w/c < 0.80}
A denotes air content {1 < A < 11%}

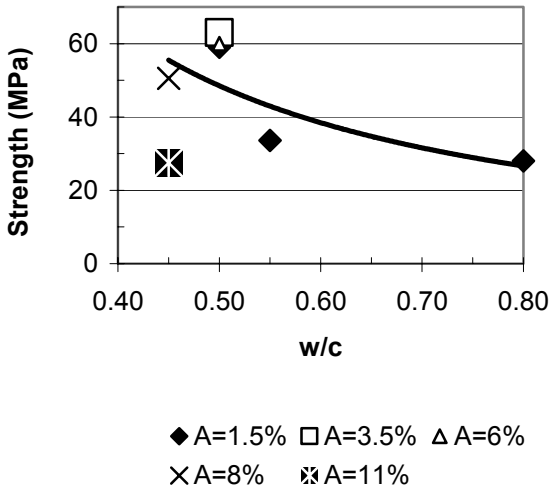

Figure 5.3 – Strength results of submerged cast concrete obtained by Vattenfall.

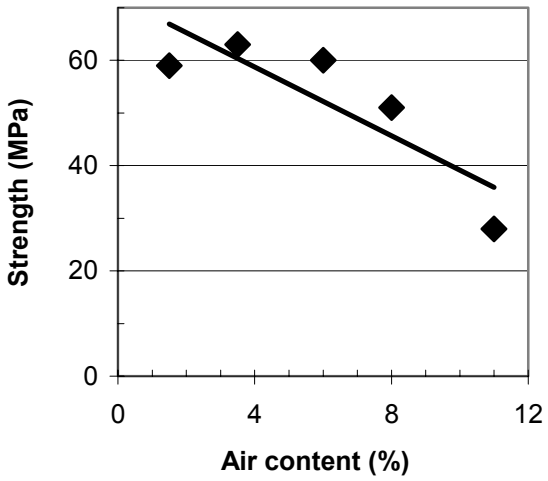

Fig. 5.4 - Strength with w/c = 0.45 - 0.50.

5.2.2 Concrete cast at LTH

Appendix 3.2, Figs. 4.2 and 4.3 show some inconsistent in the strength development, especially at w/b = 0.45 as combined with 8% air content. The explanation for this development was shown in Fig. 4.16, i.e. increasing density with increasing air content in concrete with w/b = 0.45. Probably some air was lost between mixing and casting of the concrete. Fig. 5.5 shows the strength of the SCC cast at LTH with different air content and w/b varying between 0.35 and 0.45.

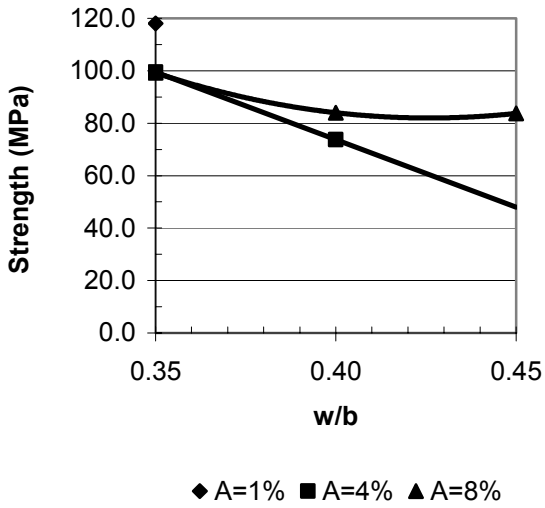

Fig. 5.5 - Strength of SCC cast at LTH with different air content, A, at w/b = 0.35 and = 0.40.

From Fig. 5.5 the following formula was obtained for the compressive strength (MPa):

$$f_c = 40\cdot w/b\cdot(A\text{-}12)\text{-}18\cdot A+250 \qquad (5.3)$$

w/b water-binder ratio {0.35 < w/b < 0.40}
A denotes air content {1 < A < 8%}

5.2.3 Field concrete cast at BTC

Figs. 4.4 and 4.5 show that on average 28-day strength results was dependent on the position of the wall cores [97]. In concrete with w/b = 0.40 and = 0.45 the strength at the foot was about 2 MPa higher than at the crest at the near end of the pumping. With w/b = 0.40 and = 0.45 the strength at the foot was about 4 MPa higher than at the crest at the remote end of the pumping. At w/b = 0.35 the strength was independent of the position of the casting. Both results indicate that segregation took place at w/b = 0.40 and = 0.45 but not at w/b = 0.35. The standard deviation of strength, Fig. 4.6, the variance, Fig. 4.7, confirm the above-mentioned results and also shows larger values at the crest of the casting than at the foot except for SCC with w/b = 0.35. The following relationship was obtained for the 28-day strength with 4% air content, f_{c4} Fig. 5.6 (MPa):

$$f_{c4} = 0.283\cdot[-(w/b)^2 + 66.6\cdot(w/b) - 760] \qquad (5.4)$$

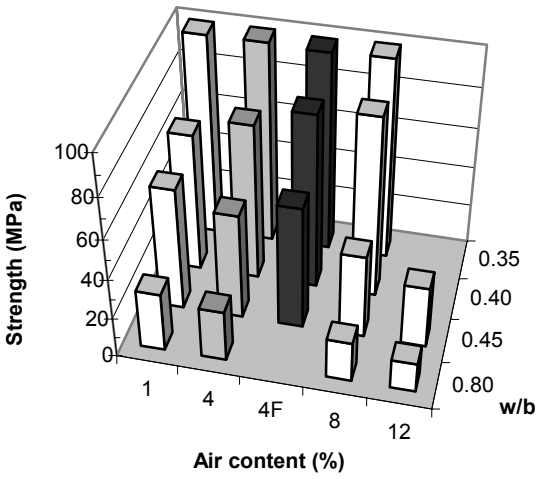

Fig. 5.6 – 28-day strength with varying air content and w/b with equations (5.2) – (5.4). F = field.

5.3 Freezing rate of concrete

Figs 5.7-10 show the freezing rate in the specimen cast at BTC (Figs. 5.7-8 – internal frost resistance) and at LTH (Fig. 5.9 – internal and salt frost resistance). As seen in Fig. 5.7 the freezing rate varied between 6 and 9 °C/h and between 7 and 9 °C/h in Fig. 5.8. Fig. 5.9 shows freezing rates varying between 8 and 11 °C/h. The freezing rate exceeding 3 °C, which is the fastest recorded, but did not fulfil the ASTM 666-92, 14 °C/h [84].

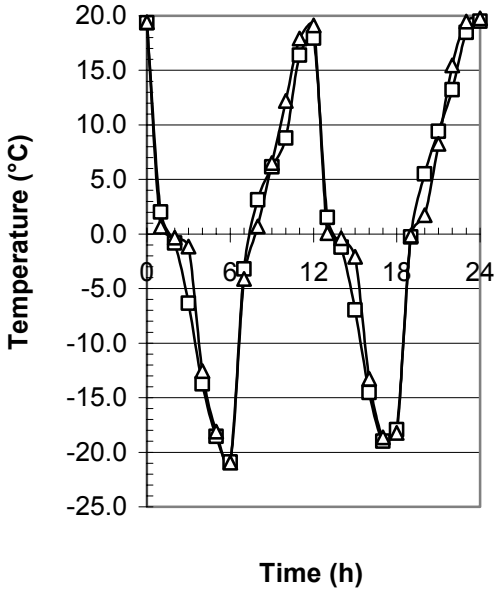

Fig. 5.7 - Freezing rate varied between 6 and 9 °C/h (specimen cast at BTC – internal frost resistance).

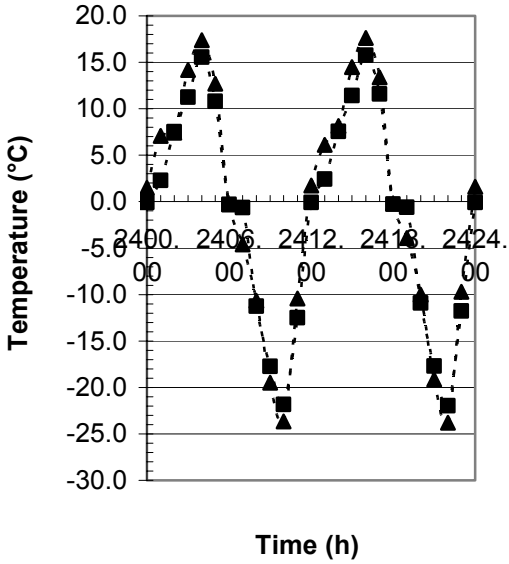

Fig. 5.8 – Freezing rates varied between 7 and 9 °C/h (specimen cast at BTC – internal frost resistance).

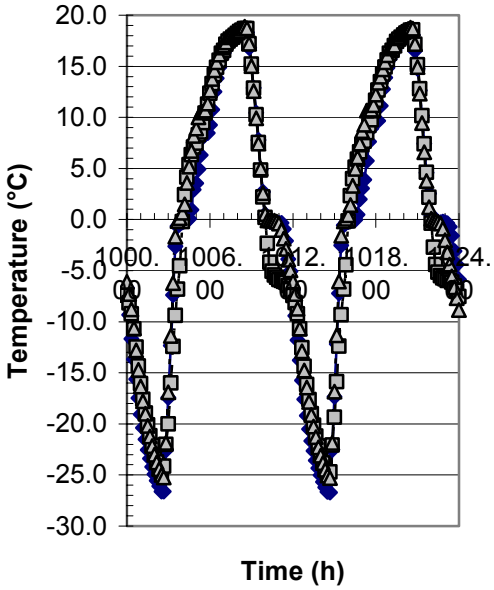

Fig. 5.9 - Freezing rates varying between 8 and 11 °C/h (specimen cast at LTH – internal and salt frost resistance).

5.4 Internal freezing and thawing resistance

5.4.1 Concrete delivered by Vattenfall

Figs 4.8-9 and Appendix 4.1 show that practical concrete with w/b > 0.45 did not fulfil the ASTM 666 requirements as concerns internal loss of FRF, i.e. elastic modulus to be larger than 40% after 300 cycles. Eight of 12 concrete were totally destroyed even before 100 frost cycles. Concrete with anti-wash out powder was not durable to internal freezing and thawing. SCC with w/b = 0.48 and 6% air content exhibited a high grade of internal freezing and thawing resistance.

5.4.2 Concrete cast at LTH

Figs 4.10-11 and Appendix 4.2 show less internal frost resistance of concrete cast at the remote end of the L-box than near the place of casting. Still, all concrete with w/b = 0.35 shows good internal frost resistance both related to FRF (less than 13% losses of FRF after 300 cycles) and scaling (less than 1% loss of weight after 300 cycles). The difference between the frost resistance at the near and the remote end of casting in the L-box clearly indicate that either some segregation took place during the casting or that some air content was washed out during the movement of the air in the water. Indication of the mentioned behaviour may be confirmed by observations of the density of the drilled cores that were used in the tests.

5.4.3 Concrete cast at BTC

Figs 4.12-13 and Appendix 4.3 show good performance of internal frost resistance of concrete with w/b = 0.40 and w/b = 0.45 that were cast at BTC (less than 9% loss of FRF and almost no loss of weight after 100 cycles) [97]. Still larger losses of internal frost resistance were observed at the remote end of the pump – larger losses were observed at the crest of the casting than at the foot. This indication may be a confirmation of segregation of the concrete during the casting process or air leaving the concrete, especially at w/b = 0.35.

5.5 Salt freezing and thawing resistance

Fig. 4.14 and Appendix 4.4 show too large salt frost scaling for all practical concrete delivered by Vattenfall. Concrete with anti-wash out powder was not durable to salt freezing and thawing scaling even through as much as 8 % air content was studied at w/b = 0.45. SCC with w/b varying between 0.35 (1% air content) and 0.45 (8% air content), cast at LTH, exhibited an excellent salt freezing and thawing resistance (less than 0.2 kg/m² of scaling) at the near end of the L-box at casting. At the remote end of the L-box air probably was washed out during the casting which reduced the salt freezing and thawing resistance substantially. At the remote end of the L-box 8% of air content was required for SCC with w/b = 0.35 and w/b = 0.40 in order to fulfil the salt freezing and thawing resistance at casting submerged. For w/c = 0.45 a air content of 8% was not sufficient to fulfil a salt freezing and thawing scaling at the remote end of casting. However, salt freezing and thawing resistance is normally not required in dams, foundations and pillars in fresh water. SCC may probably not be cast submerged in sea water since chloride then will be cast in the concrete causing reinforcement corrosion.

5.6 Density and strength

5.6.1 Concrete cast at LTH

Fig. 4.16 shows a clear effect of the air content on the density of the concrete. However, only a small effect of density on strength was observed, Fig. 5.10. The following formula was obtained for the effect of density on strength, f_c (MPa):

$$f_c = 0.179 \cdot 10^{-12} \cdot \rho^{3.78} \qquad (5.5)$$

ρ denotes the density of SCC ($2200 < \rho < 2500$ kg/m³)

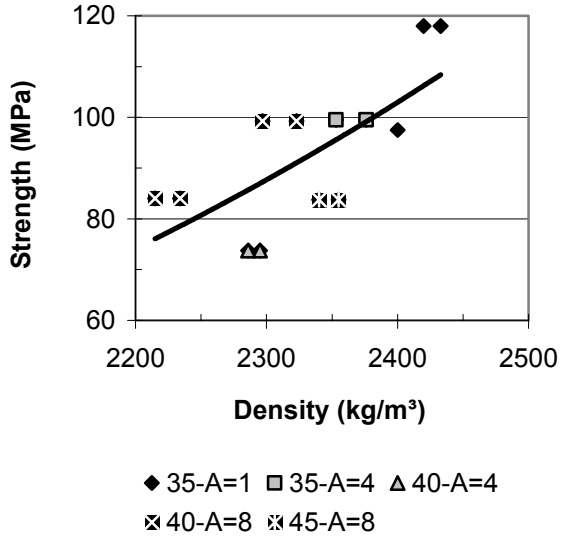

Fig. 5.10 - Strength versus density with varying air content cast at LTH. A = air content (%). C = crest; F = foot; N = near; R = remote.

5.6.2 Concrete cast at BTC

Table 5.2 and Figs. 5.11 show segregation at the crest near the pump almost independent of w/b.

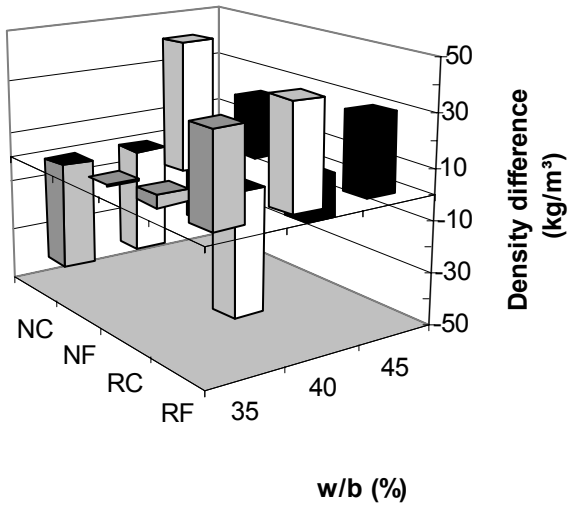

Fig. 5.11 – Difference in density dependent on the position at casting. C = crest; F = foot; N = near the; R = remote.

Table 5.2 - Density difference dependent on the position of the casting versus w/b (kg/m³).

w/b (%)	35	40	45
NC	-41	-40	-35
NF	0	49	23
RC	5	-49	-18
RF	36	40	30

Some coarse aggregate probably was washed away from the crest near the pump towards the remote foot of casting which seems logical. Still the difference in density was small but did substantially affect the strength, Figs. 5.12-5.13.

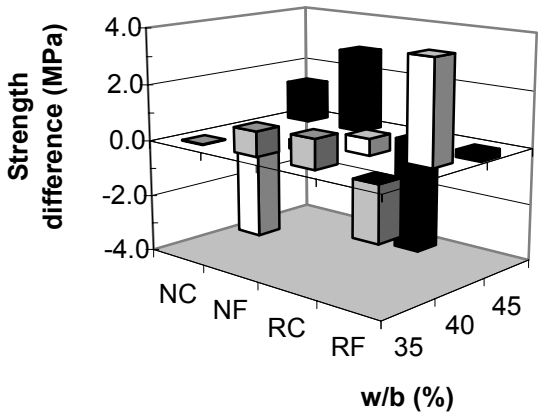

Fig. 5.12 – Strength difference to average (MPa). C = crest; F = foot; N = near the; R = remote.

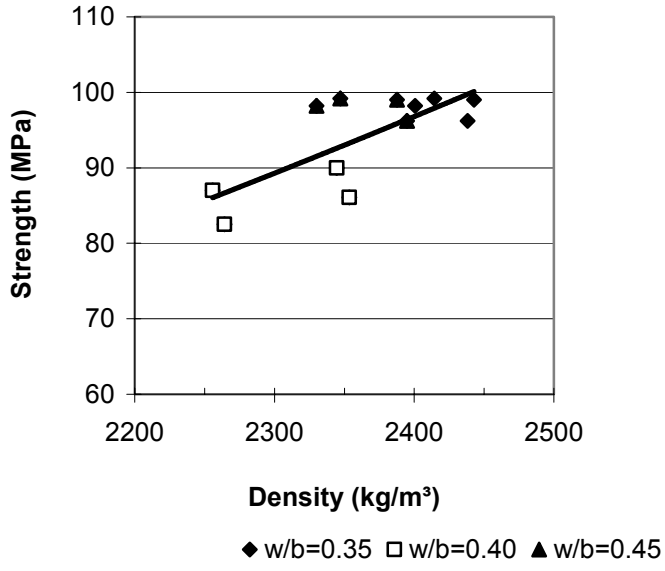

Fig. 5.13 – Strength versus density at different w/b.

The following relationship was obtained between strength and density:

$$f_c = y = 0.370 \cdot 10^{-6} \rho^{1.90} \quad (5.6)$$

f_c denotes compressive strength of SCC (MPa)
ρ denotes the density of SCC ($2200 < \rho < 2500$ kg/m³)

5.7 Internal frost resistance, air content and density

5.7.1 Concrete cast at LTH

The concrete were designed to contain 1%, 4% or 8% air content. Fig. 5.14 shows the change of FRF at the near and the remote end of L-box (4 = 4% air content, 35 = w/b (%)). Especially for concrete 45S8 an increased loss of FRF was observed. The loss of FRF was 9 times as high at the remote end of the L-box as close to the pouring place. As concerns concrete 45S8 the density shown in Fig. 4.16 and the strength given in Appendix 3.2 indicate that the air content performed at the casting of concrete 45S8 was much lower than 8%, probably about 3% air content. Still the difference in density between the near and the remote end of casting was small, Fig. 4.16. If air had left the concrete then the density would increase with 10 kg/m³ per percent of decrease of air. If segregation took place during the casting in the L-box, i.e. more fines were transported to the end of the L-box then the density would decrease. Probably both phenomena took place during casting in the L-box: some air content left the concrete, about 2%, which increased the density with about 20 kg/m³. In parallel some segregation took place in the concrete with w/b = 0.35 and with w/b = 0.45, influencing a change of density of about 30 kg/m³. However, for concrete with w/b = 0.40 and 8% the separation was less, maybe affecting density with 10 kg/m³ only, Fig. 4.16. The results for concrete 45S8 thus resulted in too low air content at the end of the L-box and thus too large loss of internal frost resistance, about 80% loss of FRF. Concrete 45S8 was almost destroyed far from the casting place. Fig. 5.14 shows the change of FRF after 300 cycles in fresh water at the remote end of casting in the L-box. Still, for concrete with w/b = 0.45, the real air content probably was only about 1%, i.e. too low for the concrete 45S8 to resist internal frost. At w/b = 0.35 and at w/b = 0.40 also some self-desiccation took place which caused internal air voids to form and thus internal frost resistance of the concrete [21]. Fig. 5.15 shows the change of FRF after 300 cycles in fresh water at the near end of casting in the L-box. Before segregation of aggregate, which

not took place close to the pouring place in the L-box, and before loss of about 3% air, the air content of concrete 45S8 was sufficiently large for the concrete to withstand internal frost for 300 cycles in fresh water, even at w/b = 0.45. Probably about 3% air content was sufficient for the concrete 45S8 to resist internal frost for 300 cycles, at near end of casting in the L-box.

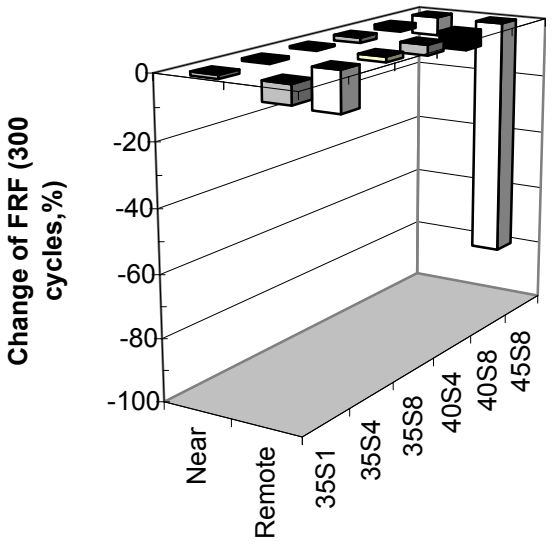

Fig. 5.14 – Change of FRF at near and at the remote end of L-box. 4 = 4% air content, 35 = w/b (%).

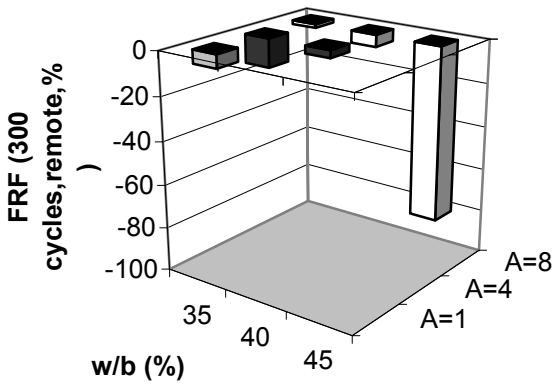

Fig. 5.15 – Change of FRF after 300 cycles in fresh water at the remote end of casting in the L-box.

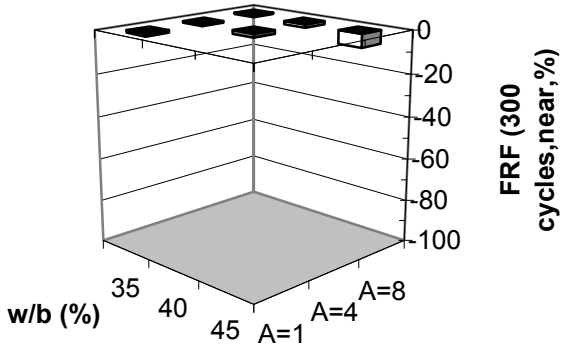

Fig. 5.16 – Change of FRF after 300 cycles in fresh water at the near end of casting in the L-box.

5.7.2 Concrete cast at BTC

All concrete was designed to contain 4% air content. Fig. 5.17 shows the difference in density at the crest of casting. Fig. 5.18 shows the difference in density at the foot of casting. As expected the density diminished at the crest of casting, quit substantially and in the contrary increased at the bottom of the mould due to aggregate separation, probably. The difference in density may also be related to movement of air in the fresh mix, upwards, which then also would increase the density at the bottom of the mould. Generally, the increase of density at the bottom of the moulds was 40 kg/m³, which coincide well with 4% of air content leaving the mix at the bottom of the mould. At the foot of casting also an increase of strength systematically took place, which either was a result of the increasing content of aggregates or the result of a decrease of the air content, Fig. 5.12. Figs. 5.19-5.20 show that the main differences of density in the concrete were observed vertically, i.e. either some aggregate moving downwards or air leaving the bottom of the mixed fresh concrete. Fig. 5.21 shows that the largest decrease of FRF took place at the crest of the casting, which shows that the difference of air content was not the reason for density difference but the segregation of aggregates. If the difference of the density would be related to air leaving the mix at the bottom the air content at the top of the casting would be higher than foreseen and then the decrease of FRF lower than observed. The decrease of FRF was also slightly related to w/b of the con-

crete, larger loss of FRF at low w/b = 0.35 than at w/b = 0.45. Still the decrease of FRF was small, 20 % maximum, i.e. less than the acceptable loss of FRF, which is 60% [94]. Fig. 5.22 shows the decrease of FRF at the remote end of the casting. At the remote end of casting the loss of FRF became much larger than at the near end. At the near end of casting at BTC the losses also were larger than these observed in the L-box at the laboratory tests with concrete, since no vertical segration took place in the L-box but certainly at BTC. This tends to indicate that air also left the mix proportions between casting at the near end and during the transport, horizontally, in the mould also seen in Fig. 5.18, which shows an increase of density at the far end of casting compared with the near end. Two phenomena thus acted in parallel, air leaving the concrete and aggregate segregation. However, aggregate and air separation was related to w/b = 0.45 at which concrete quality it was pronounced – only minor at w/b = 0.35 and w/b = 0.40. Fig. 5.23 shows the change of FRF versus the change of density at the near end of casting. An increase in density resulted in larger decrease of FRF. For the other position of casting no correlation was found between change of density and decrease of FRF, Fig. 5.25-5.26. Large decrease of FRF occurred at no change of density at all, which indicted that the density decreased just as much due to aggregate separation as the density increased due to air content losses.

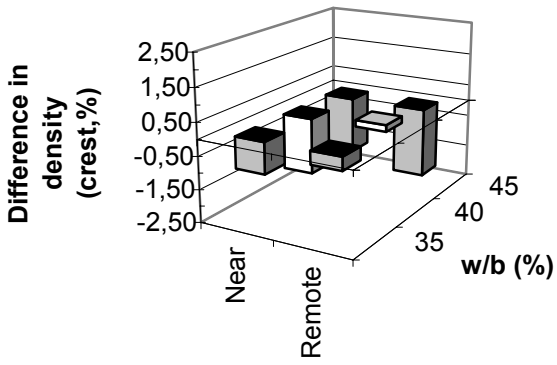

Fig. 5.17 – Difference in density at the crest of casting.

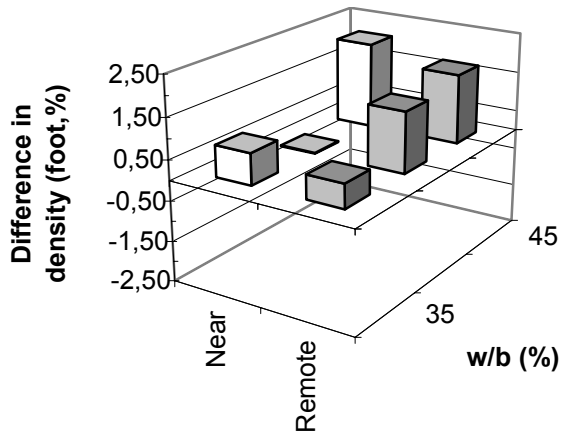

Fig. 5.18 – Difference in density at the foot of casting.

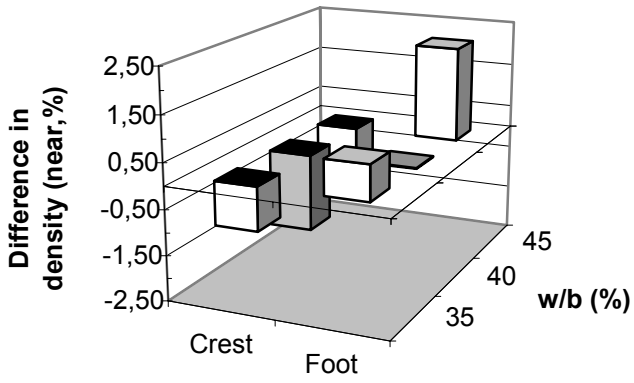

Fig. 5.19 - Difference in density at the near end of casting.

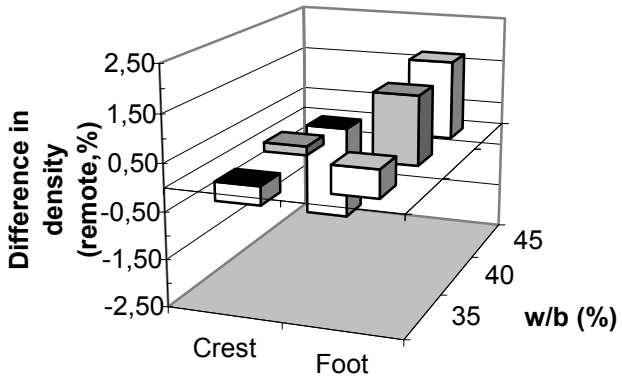

Fig. 5.20 - Difference in density at the remote end of casting.

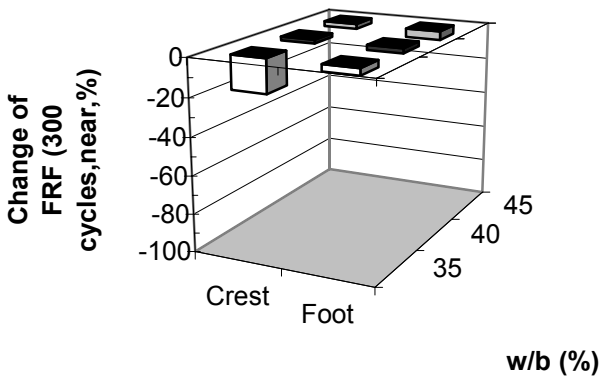

Fig. 5.21 - Decrease of FRF at the near end of the casting.

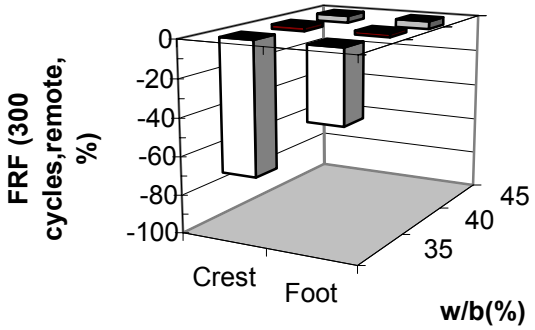

Fig. 5.22 - Decrease of FRF at the remote end of the casting.

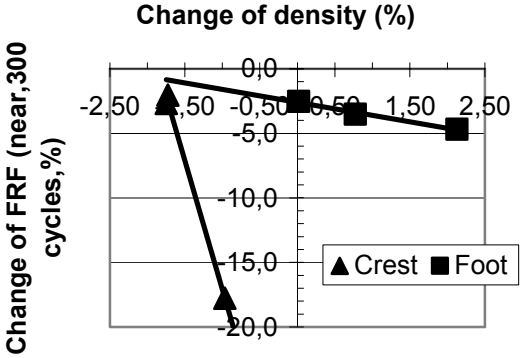

Fig. 5.23 – Change of FRF versus change of density at the near end of casting.

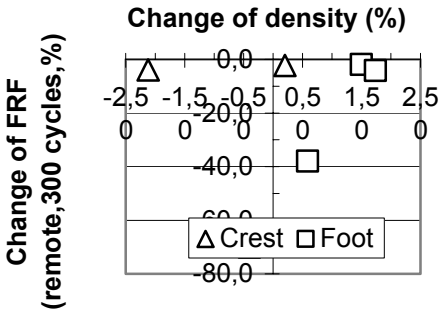

Fig. 5.24 – Change of FRF versus change of density at the remote end of casting.

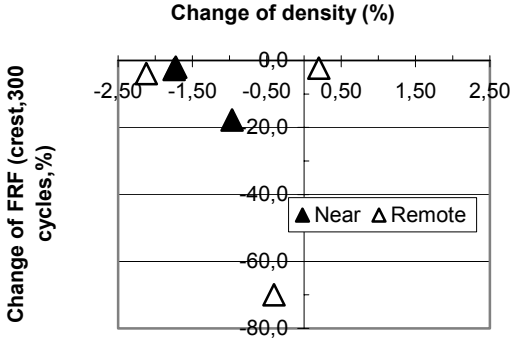

Fig. 5.25 – Change of FRF versus change of density at the crest of casting.

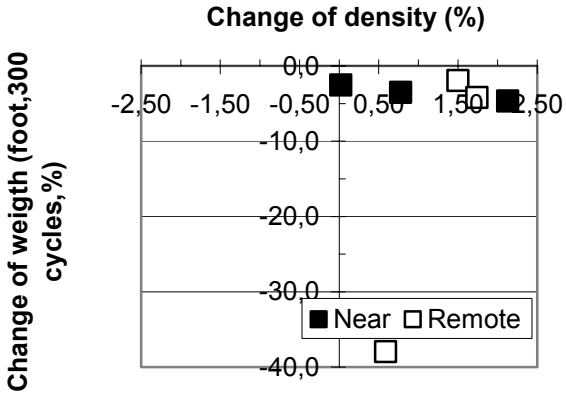

Fig. 5.26 – Change of FRF versus change of density at the foot of casting.

5.7.3 Salt frost scaling, air content and density

Fig. 5.27 shows salt frost scaling at different positions of casting. Together with Fig. 4.16 the result of Fig. 5.27 indicate that aggregate assemble at the near end of casting where no air loss occurred. This combination gave an excellent salt frost resistance. On the other hand more mortar was transported to the remote end of the L-box and also air lost which all together caused about nine times as large salt frost scaling, especially at low

w/b = 0.35. At w/b 0.45 the air content in the cast concrete was probably lower than 8% which after air losses and combined with high w/b was the reason for the extreme large salt frost scaling, 3.2 kg/m², more than 6 times an acceptable level of 0.5 kg/m². Fig. 5.28 shows the salt frost scaling at the near end of casting. Still, concrete with w/b = 0.35 did not show logical salt frost scaling at the near end of the L-box at casting since the largest amount was observed at air content, 4%, about 4 times as large as at air content 1 and 8%. For concrete with w/b= 0.40 the result was more logical, i.e. decreasing salt frost scaling with increasing air content. At air content 4% the salt frost scaling increased with larger w/b, which also was a logical results, no segregation occurring at the near end of the L-box at casting. At the remote end of the L-box at casting the same result as at the near end of the L-box at casting was observed, i.e. concrete with w/b = 0.35 did not show logical salt frost scaling at the near end of the L-box at casting since the largest amount was observed at air content, 4%, about 5 times as large as at air content 1 and 8%. For concrete with w/b= 0.40 the result was more logical, i.e. decreasing salt frost scaling with increasing air content. At air content 4% the salt frost scaling increased with larger w/b, which also was a logical results. Segregation probably occurred at the remote end of the L-box at casting, which in turn increased the amount of salt frost scaling, the mortar content in the concrete being larger. It is the mortar of the concrete that is sensitive to frost damages, not the aggregate. The aggregate withstands frost well.

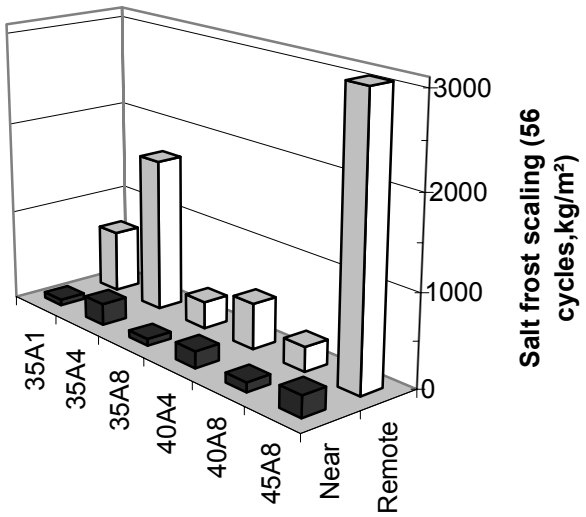

Fig. 5.27 – Salt frost scaling at different positions of casting.

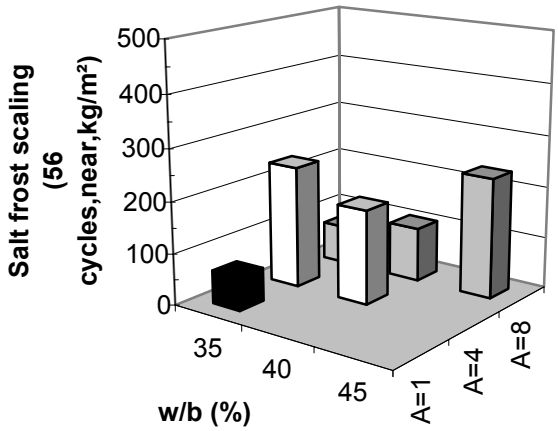

Fig. 5.28 – Salt frost scaling at the near end of the L-box at casting.

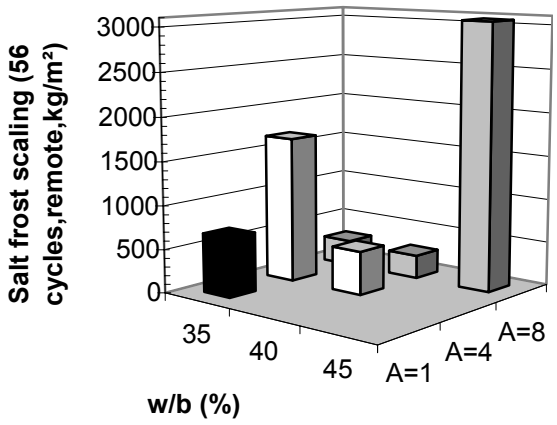

Fig. 5.29 – Salt frost scaling at the remote end of the L-box at casting.

6. SUMMARY AND CONCLUSIONS

6.1 Tested concrete

Studies of the grading curves of the fresh concrete clearly showed that more fines were required in submerged cast SCC than in NC and normal SCC in order to obtain stability of the concrete in the fresh state. With a 1 mm sieve about 38% of the material in the NC mix proportions passed, about 47% of the material of the mix proportions passed 1 mm sieve width with normal SCC and about 53% of the material in the mix proportions passed 1 mm sieve width with submerged cast SCC. It became clear that a large content of air in the concrete in order to avoid frost damage to submerged cast concrete affected the strength results substantially. Increase of the air content (> 8%) as a method to avoid frost damage in concrete with w/b > 0.45 was not feasible as strength became unacceptably low. For concrete cast in the laboratory and in the field with w/b varying between w/b = 0.35 and w/b = 0.45 the strength varied between 100 and 55 MPa at 4% air content. Some effect of the position of the casting on strength was observed in the field, i.e. strength at the crest of the casting became up to 4 MPa lower than average strength and up to 4 MPa higher at the foot of the casting than average strength. The difference in strength due to the position of casting was probably dependent on segregation of aggregate in the fresh mix proportions. Some loss of air also affected strength, i.e. lower air content at the far end of casting increased strength, which acted contrary to an increase of the aggregate content.

6.2 Internal freezing and thawing resistance

Submerged cast SCC with w/b = 0.40 and ≥ 4% air content fulfilled the requirements (7.5% silica fume) of internal freezing and thawing resistance. The freezing rates of the specimens, which were recommended to be 14 °C/h (ASTM 666-92), varied between 6 and 9 °C/h (internal frost resistance) and between 8 and 11 °C/h (salt frost resistance). Still, the freezing rates by far exceeded the maximum values obtained in reality, 3 °C/h. Practical concrete with w/b > 0.45 and anti-washout powder did not fulfil the ASTM 666 requirements for internal loss of FRF, i.e. elastic modulus to be larger than 40% after 300 cycles. Concrete cast in the laboratory exhibited less internal frost resistance at the remote end of the L-box than near the place of casting, Fig. 6.1. The difference between the frost resistance at the near and the remote end of casting in the L-box clearly indicates that either some segregation took place during the casting or that some air content was washed out during the movement of the concrete in the water. Concrete with w/b = 0.45 was not acting acceptably at the remote end at casting in the L-box (80% loss of FRF). Still, all concrete with w/b = 0.35 and w/b = 0.40 showed good internal frost resistance related to FRF (less than 13% losses of FRF after 300 cycles).

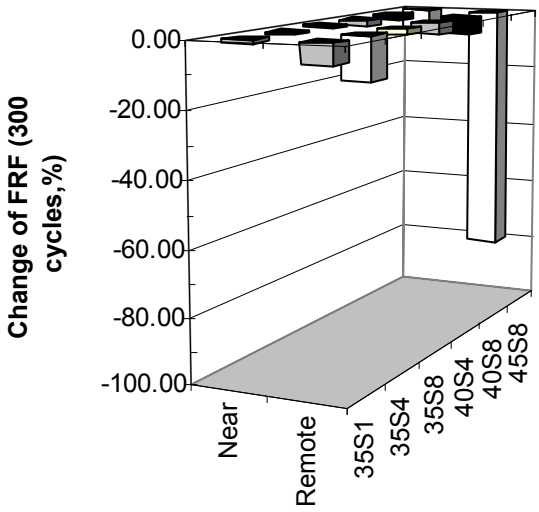

Fig. 6.1 – Alter of FRF of concrete cast in a L-box in the laboratory. 8 = air content (%), 35 = w/b.

Concrete cast in the field with w/b = 0.35 showed poor performance of internal frost resistance of concrete at the remote position of casting (70% loss of FRF at the crest and 40% loss of weight at the foot of casting after 300 cycles), Fig. 6.2. This may be a confirmation of segregation of the aggregate during the casting process of the concrete or may indicate that air was leaving the concrete. Also at the near end a tendency of larger loss of elastic modulus was observed in concrete with w/b = 0.35 than in the other concrete. Concrete with w/b = 0.40 and w/b = 0.45 acted well to frost.

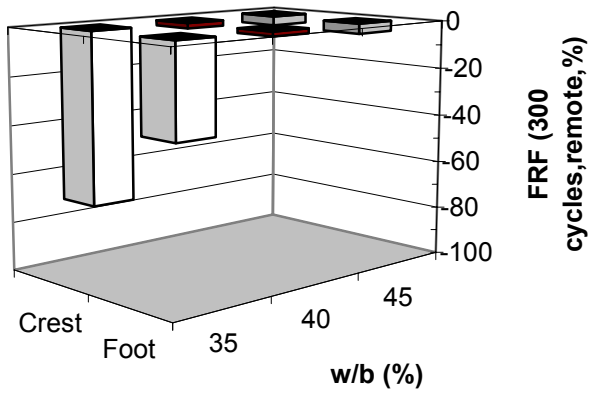

Fig. 6.2 – Alteration of FRF of concrete cast in the field. 35 = w/b. Crest and foot of mould indicated.

6.3 Salt freezing and thawing resistance

Submerged cast SCC with w/b = 0.40 (7.5% silica fume) with ≥ 4% air content fulfilled the requirements of less than 0.5 kg/m² of salt frost scaling. Salt freezing and thawing resistance is normally not required for dams, foundations and pillars in fresh water. SCC may probably not be cast submerged in seawater since cast-in chloride may cause reinforcement corrosion. Too large salt frost scaling for all practical concrete with w/b > 0.45 and anti-washout powder was observed. Concrete with w/b > 0.45 and anti-washout powder was not durable to salt freezing and thawing scaling even though as much as 8% air content was studied. SCC with w/b = 0.35 and w/b = 0.45, submerged cast in the laboratory, showed large salt frost scaling at the remote end of the L-box, Fig. 6.3. Air was probably washed out during the casting process, which reduced the salt freezing and thawing resistance substantially, or aggregate segregation affected the salt frost scaling. Eight percent of air content was required for SCC with w/b = 0.35 and 4% of air content for SCC with w/b = 0.40 in order to fulfil the requirements. For w/c = 0.45 not even an air content of 8% was sufficient to obtain salt frost scaling less than 0.5 kg/m² in the laboratory.

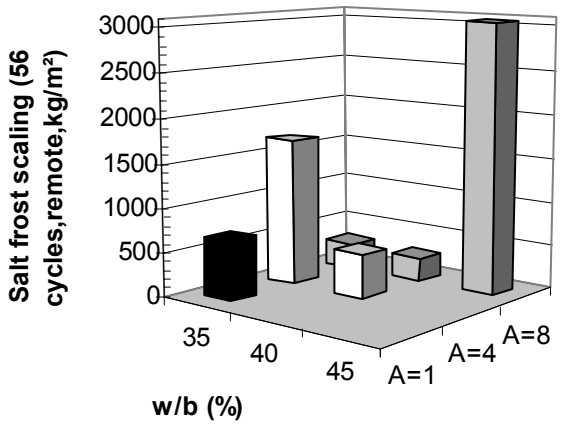

Fig. 6.3 – Salt frost scaling of concrete cast in the laboratory. A = air content (%).

6.4 Density, segregation and strength

A clear effect of the air content on the density of the concrete was observed. Segregation at the crest near the pump, which was almost independent of w/b, was observed in the field concrete. Some coarse aggregate probably segregated both at the near and at the remote end of casting. On the other hand results on frost resistance showed that some of the air content was lost at the remote end of casting, which caused a comparative increase of the density. With larger loss of internal frost resistance almost no change of density was observed at the far end of casting since the segregation of aggregate just compensated for the density change due to the loss of air. Still the difference in density was small and the effect on strength minor, ±4 MPa, Fig. 6.4.

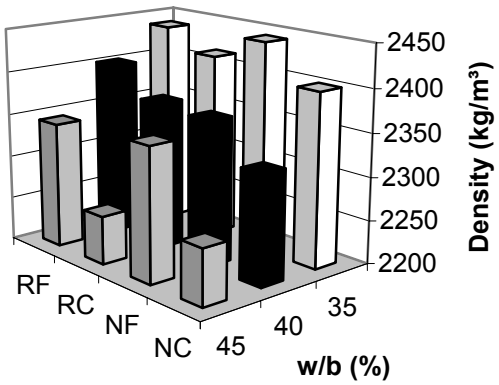

Fig. 6.4 – Concrete density in the field. C = crest, F = foot, N = near end of casting, R = remote end, 35 = w/b.

6.5 Recommendations

Based on previous results, results from the laboratory experiments and from experiments in the field, SCC with w/b = 0.40 (7.5% silica fume) and air content ≥ 4% may be used to fulfil both requirements of internal frost resistance and salt frost scaling.

REFERENCES

1. M. Nilsson, Ö. Petersson. The First Bridge Made of Self-compacting Concrete. Väg- och Vattenbyggaren 2/98 (1998) 28-31.
2. L. Söderlind. Full-scale Tests of Self-compacting Concrete for Dwelling Houses. RILEM Symposium on Self Compacting Concrete. Ed.: Skarendahl and Petersson (1999) 723-728.
3. Trägårdh, J., Very Good Frost Resistance of SCC – A case Study of the Stäket Tunnel. "Mycket god frostbeständighet i självkompakterande betong– en fallstudie från Stäkettunneln." Bygg & Teknik. 2001/07, 26-27.
4. Bergholtz, A., Lundgren, S., Concrete Inner Vault in the Grind Tunnel, "Motgjuten betonginkädnad i tunnel vid Grind", Swedish Road Administration and Scandiaconsult Sverige AB respectively, Rock Mechanics Meeting, Swedish Rock Engineering and National Group of International Society for Rock Mechanics, ISSN 0281-4714, 2000, 227-236.
5. Persson, B., Mix Proportions and Strength of SCC for Production of High Strength Poles, Piles and Pillars. Contribution to "1. Münchener Baustoffseminar Selbstverdichtender Beton" 9 oktober 2001. Ed.: Peter Schiessl. 2001, 31-39.
6. Persson, B., High Performance SCC. Proceedings of the 6th International Symposium on Utilization of High Strength/High Performance Concrete. University of Leipzig. Ed.: König, G., Dehn, F., Faust, T., Leipzig. 2002, 1273-1290.
7. Persson, B., SCC with High Performance. Proceedings of the 18th Symposium on Nordic Concrete Research. Nordic Research Projects, Elsinore, Ed.: Bager, D., Glavind, M., Publisher: The Norwegian Concrete Association. Oslo. 2002, 327-330.
8. Persson, B., SCC, with High Performance, HP, Proceedings of the Congress on Challenges of Concrete Construction, Dundee, Ed.: Dhir, R. K., Publisher: The University of Dundee, Dundee, 2002, 16 pp.
9. Persson, B., A Comparison between Deformations of Self Compacting Concrete and Corresponding Properties of Normal Concrete, CCR, 31, 2001, 193-198.
10. Persson, B., Shrinkage and Creep of High-Performance Self-Compacting Concrete, HPSCC. ACI Journal. 2003, 22 pp. (Accepted for publication.)
11. Persson, B., Mix Proportions and Strength of Self-compacting Concrete for Production of High-Strength Poles, Piles and Pillars. Report U01.05 (assignment for SACAC Ltd, Lenzburg). Division of Building Materials. Lund Institute of Technology. Lund University. Lund. 2001, 11 pp.
12. Persson, B., Shrinkage and Creep of High-Performance Self-Compacting Concrete, HPSCC. Assignment report U02.06. Div. Building Materials. Lund Institute of Technology. Lund, 32 pp.
13. Jepsen, M. T., Predicting Concrete Durability by Using Artificial Neural Network. Nordic Seminar on Durability of Exposed Concrete Containing Secondary Cementitious Materials. Hirtshals. Ed.: D. Bager, 2001, 11 pp.
14. Jepsen, M. T., Mathiesen, D., Munch-Petersen, C., Bager, D., Durability of Resource Saving "Green" Types of Concrete. Durability of Exposed Concrete Containing Secondary Cementitious Materials. Hirtshals. Ed.: D. Bager, 2001, 10 pp.
15. Boubitsas, D., Paulou, K., Self Compacting Concrete for Marine Environment. TVBM-5048. Lund Institute of Technology. Lund University. Lund, 2000, 55 pp.
16. Rougeau, P., Maillard, J. L., Mary-Dippe, C., Comparative Study on Properties of Self Compacting Concrete and HPC Concrete Used in Precast Construction. RILEM Symposium on Self Compacting Concrete. Stockholm. Ed.: Skarendahl and Petersson, 1999, 251-261.
17. Bager, D., Aalborg Portlands Durability Project – 18-year judgement. Durability of Exposed Concrete Containing Secondary Cementitious Materials. Hirtshals. Ed.: D. Bager, 2001, 30 pp.
18. Utgennant, P., Petersson, P.-E., Frost Resistance of Concrete Containing Secondary Cementitious Materials – Experience from Three Field Exposure Sites. Durability of Exposed Concrete Containing Secondary Cementitious Materials. Ed.: D. Bager, 2001, 17 pp.
19. Friebert, M., Durability of High Performance oncrete Containing Fly Ash and Silica Fume. Durability of Exposed Concrete Containing Secondary Cementitious Materials. Ed.: D. Bager, 2001, 11 pp.
20. Auberg, R., Zuverlässige Prüfung des Frost und Frost-Tausalz. Widerstands von Beton mit dem CDF und CIF Test. University of Essen, 1998.

21. Fagerlund, G., Effect of Self-desiccation on Internal Frost Resistance of Concrete. Self-Desiccation and Its Importance in Concrete Technology. Ed.: B. Persson, G. Fagerlund. TVBM-3075. Lund University. Lund, 1997, 227-238.
22. Persson, B., Assessment of Chloride Migration Coefficient, Salt Frost Resistance, Internal Frost Resistance and Sulphate Resistance of Self-Compacting Concrete. Report TVBM-3100 (assignment for SBUF and Skanska AB, Malmö). Division of Building Materials. Lund Institute of Technology. Lund University. Lund. 2001, 86 pp.
23. Persson, B., Internal Frost Resistance and Salt Frost Scaling of Self-Compacting Concrete. Cement and Concrete Research. 33, 2003, 373-379.
24. Persson, B., Self-Compacting Concrete - Chloride Ingress and Frost Resistance. Nordic Mini Seminar. fib Commission 5.5. Gothenburg. 2001.
25. Persson, B., Chloride Penetration and Frost Resistance of Self-compacting Concrete. "Frostbeständighet och kloridinträngning hos självkompakterande anläggningsbetong." Report U00.05 (assignment for Skanska Sverige AB). Division of Building Materials. Lund Institute of Technology. Lund University. Lund. 2000, 5 pp.
26. Persson, B., Self Consolidating Concrete, SCC, subjected to environmental or mechanical loading, ACI Journal, 2003, 21 pp. (Submitted for publication).
27. Persson, B., Sulphate Resistance of Self-Compacting Concrete (SCC). Cement and Concrete Research, 2002, 10 pp. (Accepted for publication).
28. CTH Rapid Test for Determination of D in Concrete, NT BUILD 492 (2000).
29. Tang, L. and Nilsson, L.-O., Modelling of Chloride Penetration into Concrete – Tracing Five Years Field Exposure, Concrete Science Engineering, 2, 2000, 170-175.
30. AASHTO T 271-831, Rapid Determination of Chloride Permeability of Concrete.
31. Geiker, M., Thaulow, N. and Andersen, P. J., Assessment of Rapid Test of Concrete Permeability Test of Concrete with and without Mineral Admixtures, in Durability of Concrete and Components, Brighton, (Chapman & Hall, 1990) 52-61.
32. Persson, B., A Background for the Choice of Mix Design of the Concrete for the Great Belt Link, Report U91.02, Div. Building Materials, Lund Institute of Technology, Lund, 1991, 102 pp.
33. Buenfeld, N., Personal information, Imperial College, London, 2001.
34. Persson, B., Moisture in Concrete Subjected to Different Kinds of Curing, Materials and Structures 30, 1997, 533-544.
35. Persson, B., Self-desiccation and Its Importance in Concrete Technology. Nordic Concrete Research 20, 1998, 120-129.
36. Persson, B., Shrinkage of HPC. in International Conference on early Age Cracking in Concrete, Haifa, Ed.: Bentur, A. (RILEM, 2001) 301-311.
37. Powers, T.G. and Brownyard, T.L., Studies of the Physical Properties of Hardened Portland Cement Paste. PCA 22 1948, 473-488, 845-864.
38. Nilsson, L.-O., Hedenblad, G. and Norling-Mjörnell, K., Suction after Long Time, HPC Handbook, Svensk Byggtjänst, Stockholm, 2000, 209-226. Persson, B., Seven-year Study of the Effect of Silica Fume in Concrete, Advance Cement Based Materials 7, 1998, 139-155.
39. Castel, R., Francois, G. and Arliguie, A., Clarification of Corrosion of Reinforcement in Concrete Structures Exposed to Chloride Environment, in fib Meeting and the Nordic Mini Seminar, Gothenbourg, 2001, 10 pp.
40. Collepardi, M., et al., The Kinetics of Chloride Ions Penetration in Concrete, Il Cemento 67, 1970, 157-164.
41. Tuutti, K., Corrosion of Steel in Concrete, Report 4:82, CBI, Stockholm, 1982.
42. Tang, L. and Nilsson, L.-O., Rapid Determination of Chloride Diffusivity of Concrete by Applying an Electric Field, ACI Material Journal 49 (1), 1992, 49-53.
43. Maage, M., Helland, S. and Carlsen, J. E., Chloride Penetration in HPC Exposed to Marine Environment, RILEM Workshop on Durability, Ed.: H. Sommer (1994) 194-207.
44. Poulsen, E., Predict. Models STAR 53, Danish Road Direct., Ed. Nilsson, L.-O., 1996.
45. Persson, B., Thirteen-year Pozzolanic Interaction between Portland Cement and Silica Fume in Concrete. Eight CANMET/ACI International Conference on Fly Ash, Silica Fume, Slag and Natural Pozzolans in Concrete. Ed.: V.M. Malhotra. 2003 (Submitted for publication).
46. Persson, B., Thirteen-year Effect of Silica Fume in Concrete. "Trettonårig effect av silikastoft i betong. Asignment of Cementa and Elkem, Norge. Report U03.02. Division

of Building Materials. Lund Institute of Technology. Lund University. Lund. 2003, 25 pp. (In English with Swedish summary.)
47. Persson, B., Thirteen-year Studies Shows That Silica Fume Makes Concrete more Durable. “13 års studier visar att silikastoft gör brobetong mera beständig.” Husbyggaren 3/2003, 40-49 (In Swedish).
48. Persson, B., Silica Fume Concrete after 13 Years, Materials and Structures, 2003, 20 pp. (Submitted for publication).
49. Persson, B., Silica fume concrete – after 13 years. “Silikastoftbetong – efter 13 år.” Bygg & Teknik2003/07 (In Swedish).
50. Persson, B., Silica fume concrete – after 13 years. “Silikastoftbetong – efter 13 år.” Bygg & Teknik2003/08 (In Swedish).
51. Persson, B. Hydration, Structure and Strength of High-Performance Concrete. “Högpresterande betongs hydratation, struktur och hållfasthet.” TVBM-1009. Lund University. Lund. 1992. 400 pp.
52. Persson, B. Drying of Concrete after Different Kinds of Curing; Materials and Structures, Vol. 30, 1997, 533-544.
53. ASTM E 104-85. Standard Practice for Maintaining Constant Relative Humidity by Means of Aqueous Solutions; ASTM, 1985, pp. 33-34, 637.
54. Persson, B. Hydration and Strength of High Performance Concrete; Advanced Cement Based Material, 1996, pp. 107-123.
55. Byfors, J. Plain concrete at early ages; Doctoral thesis. Report FO 3:80. The Swedish Cement and Concrete Institute, Stockholm, 1980, 40-43.
56. Hassanzadeh, M., Fracture mechanical properties; Report M4:05, Lund Institute of Technology, Div. of Building Materials, Lund, 1992, 8-13.
57. Persson, B. Hydration, structure and strength of High Performance Concrete; Report TVBM-7011. Lund University, Lund, 1992, pp 38.
58. Persson, B., Seven-year Study of the Effect of Silica Fume. ABCM 7, 1998, 139-155.
59. Persson, B., Self Consolidating Concrete, SCC, subjected to environmental or mechanical loading, ACI Journal, 2003, 21 pp. (Submitted for publication).
60. Bertil Persson, Self-Compacting Concrete, SCC, affected by creep, Materials and Structures, 2003, 20 pp. (Submitted for publication
61. Ingvar Nilsson. Sprickfri kringgjutning vid reparation av Ölandsbrons pelare. SBUF. 1995, 70 sid.
62. Persson, B., Ideal Distribution of Particles in Concrete, Concrete 03, Stockholm, 1995, 6-8, 39.
63. Dieden, C., SCC for House Production – Composition, Strength and Shrinkage, Report TVBM-5040, Lund Institute of Technology, 1999, 50 pp.
64. Andersson, R., Sjökvist, L.G., SCC for the Element Industry – Technical Analyses, Report TVBM-5039, Lund Institute of Technology, Lund, 1999, 48 pp. Odman, S.T.A., Effect of variations in volume, surface area exposed to drying, and composition of concrete on shrinkage, RILEM Colloquium on Shrinkage, Madrid, 1968.
65. Pujol (Hugas), A., Mix Proportions and Properties of Self-Compacting Concrete. “Sammansättning och egenskaper hos självkompakterande betong.” Report TVBM-5041. Division of Building Materials. Lund Institute of Technology. Lund University. Lund. 1999, 56 pp.
66. Charkas, M., Fayli, W., Self-Compacting Concrete with Glass Filler – Studies on Aspects on Materials and Production. “Material- och produktionstekniska studier av självkompakterande betong med glasfiller.” Report TVBM-5042. Division of Building Materials. Lund Institute of Technology. Lund University. Lund. 1999, 80 pp. (In Swedish with English summary.)
67. Persson, B., Shrinkage and Creep of SCC, Proc. 17th Symposium on Nordic Concrete Research, Reykjavik, Ed: Wallevik, O., 1999, 55-57.
68. Persson, B., Creep, Shrinkage and Elastic Modulus of SCC, RILEM 1st Symp. on Self-compacting Concrete, Ed: Skarendahl and Peterson, 1999, 239-250.
69. Troxell, G.E., Raphael, J.M., Davis, R.E., Long-term creep and shrinkage tests of plain and reinforced concrete, ASTM 58, 1958, 1101-1120.
70. Neville, A.M., Dilger, W.H., Brooks, J.J., Creep of Plain and Structural Concrete, Conctruction Press, London/New York, 1981.
71. Persson, B., Quasi-instantaneous and Long-term Deformations of HPC with Some Related Properties, Report TVBM-1016, Lund Institute of Technology, Lund, 1998.
72. EB Bulletin d’Information, 199, Comité Euro-International du Béton, Lausanne, 1990.
73. CEB-fib Model Code 1990, CEB Bulletin d’Information, No. 213/214, Lausanne, 1993.
74. European Committee for Standardisation (CEN), ENV 1992-1, Design of Concrete

Structures, Part 1: General Rules and Rules for Buildings, 1991.
75. Müller, H.S., "Zur Vorhersage der Schwindenverformungen von Bauteilen aus Beton", On the Prediction of Shrinkage of Concrete, Salutation Paper for Prof. Reinhardt, 1999.
76. Müller, H.S., Küttner, C.H., Kvitsel, V., Issue for RFGC – ACI Workshop, Paris, 1999.
77. Müller, H.S., Kvicel, V., Creep and Shrinkage Model for Vibrated concrete and HPC – concept for a uniform code-type approach, Issue for RFGC – ACI Workshop, Paris, 2000.
78. Persson, B., Validation of Fédération International de Béton, fib, 2000 Model for Shrinkage in Normal and HP Concrete, Report TVBM-7157, Lund Institute of Technology, Lund, 1999, 108 pp.
79. Persson, B., Justification of Fédération International de Béton, fib, 2000 Model for Elastic Modulus of Normal and HP Concrete, TVBM-7159, Lund Institute of Technology, Lund, 1999, 24 pp.
80. Persson, B., Deviation of the fib 2000 Model for Creep of Normal and HP Concrete and Laboratory Measurements, TVBM-7160, Lund Institute of Technology, Lund, 1999, 343 pp.
81. Persson, B., Validation of the fib 2000 Model for Shrinkage in Normal and HPC, CONCREEP6, Ed. F-J Ulm, Z Bazant and F.H. Whittmann, Elsevier, 2001, 741-746.
82. Persson, B., Justification of Fédération International de Béton, fib, 2000 Model for elastic modulus of normal and High-Performance Concrete, HPC, Cement and Concrete Research, 2001, 13 pp. (Accepted for publication).
83. Persson, B., Justification of Fédération International de Béton, fib, 2000 Model for elastic modulus of normal and High-Performance Concrete, HPC, Cement and Concrete Research, 2001, 13 pp. (Accepted for publication).
84. Neville, A.M., Brooks, J.J., Concrete Technology, Addison Wesley Longman Ltd, Edinburgh Gate, Harlow, Essex CM20 2JE. 1987, 290.
85. Björkenstam, E., A Study on Submerged Cast Concrete with Anti-washout Powder Mainly on Fresh Properties and Frost Resistance, "En studie av undervattensbetong med antiutvaskningsmedel med tyngdpunkt på de färska egenskaperna och frostbeständigheten". Elforsk rapport 02:XX och Vattenfall Utveckling. Älvkarleby. 2002, 60 pp.
86. Concrete Constructions, Part 4, Chapter 46, Bro 2002, The Swedish Road Administration, 2002.
87. The Swedish Road Administration Publication 2002:51.
88. Design and Performance of Submerged Concrete, Appendix 3, Norwegian Concrete Association, 1994.
89. McLeish, A., Underwater concreting and Repair, Chapter 5, 1994.
90. Bartos PJM., Ceza M., Assessment of washout resistance of a fresh concrete by the MC-a test, 1996.
91. Bartos, PMJ., Khayat, KH., Sonebi, M., Assessment of washout resistance of underwater concrete: A comparison between CRD C61 and new MC-1 tests, Materials and structures vol 32, may 1999 p 273-281.
92. Khayat, K.H., Sonebi M., Bartos PJM., Ceza M., Assessment of washout resistance of a fresh concrete by the MC-a test, 1996.
93. Khayat, K.H., Frost Durability of Concrete Containing Viscosity-Modifying Admixtures, ACI Materials Journal, Nov.- Dec., 1995, 625-633.
94. ASTM C 666-92, Freezing and Thawing Resistance, 1992.
95. ASTM C 672 – 76, Scaling Resistance, 1976.
96. Bertil Persson. Consequence of Cement Constituents, Mix Composition and Curing Conditions for Self-Desiccation in Concrete. Materials and Structures 33. 2000, 352-362
97. Saleh, I., Testing of compressive strength, "Provning av tryckhållfasthet", SBUF report 11056, Skanska Asfalt & Betong, Farsta, 2002.
98. Lindmark, L., Mechanisms of Salt Frost Scaling of Portland Cement-bound Materials: Studies and Hypotheses. TVBM-1017. Lund University, 1998, 266 pp.
99. Persson, B., Self-Compacting Concrete at Fire Temperatures. Report TVBM-3110. Division of Building Materials. Lund Institute of Technology. Lund University. Lund. 2003, 200 pp.

APPENDIX 1 – SECTION THROUGH PILE CAP IN SCC

APPENDIX 2

Appendix 2.1 – Mix composition of SCC.

Material/mix composition	D	F	G	RO II	T
Crushed aggregate Bålsta 8-16	496	494	580	876	495
Natural sand Bålsta 0-8	699	728	800	727	714
Natural sand SÄRÖ 0-2	505	465	220	149	521
Fly ash	89	55			
Glass filler			60		
Cement Aalborg (CEMI)	375				
Cement Degerhamn (CEMI)		440	420	438	
Slag cement (CEMIII, 68% slag)					470
Silica fume Elkem (granulate)	35	18	21		
Air-entrainment (wet, g, 10% dry)	0.498	0.501	0.500	482	0.498
Superplasticiser (wet, 35% dry)	5.25		4.24	5.92	3.52
Water	191	172	162	171	183
w/b	0.38	0.38	0.37	0.39	0.39
Slump (flow) (mm)	690	725	720	150	737
Flow time until diameter 500 mm (s)	7	8	8		6.5
Density	2247	2300	2306	2368	2281
Aggregate content (>0.125, % vol.)	0.64	0.64	0.60	0.66	0.65
Air content (%)	6.4	6.2	6.3	6.1	5.7
28-day cube strength (100 mm, MPa)	61	70	64	63	79

Notations: D = flash mix composition; F = optimum fly ash mix composition; G = glass filler; RO II = normal concrete mix composition, second; T = slag mix composition

Appendix 2.2 – Mix composition and frost resistance of NC and SCC.

Material, cement type, w/c	SCC3	SCC5	NC
Coarse aggregate 6-14 mm	267	267	
Sand 3-6 mm	543	544	
Sand 0-4 mm	886	887	
Limestone powder	101	100	
Cement CEMI 52.5 R	352	350	323
Plasticiser	3.2	5.0	
Superplasticiser	2.3	0.9	
Water	197	190	
w/c	0.56	0.54	
Water-powder ratio, w/p	0.44	0.42	
Aggregate content (>0.125 mm, % vol.)	0.64	0.64	
Slump flow (mm)	600	580	
28-day strength (MPa)	56	58	72
Decrease of internal transversal resonance (%):			
150 frost cycles	0	13	100
300 frost cycles	7	18	-
Increase of length (%): 150 frost cycles	0.01	0.13	0.39
300 frost cycles	0.01	0.22	-
Salt frost scaling (kg/m²): 28 frost cycles	0.9	1.3	1.8
56 frost cycles	0.9	1.4	3.7

Appendix 2.3 – Mix composition and properties of NC and SCC.

Material/mix composition	KN	KOB	KN8	KO	KOT	SO	RO	ROII
Crushed aggregate Bålsta 8-16	363	371	355	367	363	402	862	876
Natural sand Bålsta 0-8	853	872	836	864	855	786	715	727
Natural sand SÄRÖ 0-2	316	135	309	320	316	422	146	149
Limestone filler Köping 500	183	375	180	186	184	94	0	
Cement Degerhamn	418	427	409	423	419	416	431	438
Microair (wet, g, 10% dry)	585	213	1203	106	117	125	474	482
Superplasticiser(wet, 35% dry)	2.97	4.13	3.2	3.39	3.69	2.99	7.32	5.92
Water	163	167	160	165	163	162	168	171
w/c	0.39	0.39	0.39	0.39	0.39	0.39	0.39	0.39
w/p	0.27	0.21	0.27	0.27	0.27	0.32	0.39	0.39
Air content (%)	5.6	4.9	8	5.5	6.3	5.6	5.8	6.1
28-day cube strength (MPa)	63	84	50	75	75	61	68	63
Slump (flow) (mm)	720	780	735	620	640	710	110	150
Flow time until 500 mm (s)	5	7	8	10	8	5	-	-
Density	2297	2348	2250	2323	2300	2285	2325	2368

B = increased amount of filler; K = Limus 40 limestone filler; N = new way of mixing (filler last); O = ordinary; R = NC; S = Limus 15 limestone filler; T = 5.5 m hydrostatic pouring pressure, II = second.

Appendix 2.4 – Chemical composition and physical properties of cement (%).

Components	CEM I42.5BV/SR/LA Degerhamn
CaO	65
SiO_2	21.6
Al_2O_3	3.5
Fe_2O_3	4.4
K_2O	0.58
Na_2O	0.05
MgO	0.78
SO_3	2.07
Ignition losses	0.47
CO_2	0.14
Clinker minerals: C_2S	21
C_3S	57
C_3A	1.7
C_4AF	13
Water demand	25%
Initial setting time	145 min.
Density	3214 kg/m^3
Specific surface	305 m^2/kg

Appendix 2.5 – Mix composition and properties of NC and SCC.

Mix	Cement, c	Type	Silica fume, s	w/b=w/(c+s)	Sand filler	Air (%)	Strength
SCC27	500	SL	50	0.24	50	1.3	141
NC 32	389	N		0.32	106	12	55
SCC38	400	N		0.38	145	1.4	86
SCC50	340	N		0.50	165	3.5	61
SCC80	260	N		0.80	185	1.9	27

Notations: N = CEMI42.5R Slite Std; SL = CEMI42.5BV/SR/LA Degerhamn.

Appendix 2.6 – Mix composition and properties of NC and SCC.

Material/mix- water-binder ratio (%)	1-40	1-50	H40	2-40
CEMI42.5BV/SR/LA Degerhamn	420	370	399	420 (Slite Std)
Silica fume			21	
Water	168	185	168	168
Air content (% vol.)	6	6.4	5.9	6.2
Aggregate	1692	1684	1685	1675

Appendix 2.7 – Number of specimen in study of silica fume concrete.

Parameter	1 m	3 m	5 m	15 m	90 m	155 m
f_c	144	144	72	144	144	72
f_{ct}	72	72	-	72	72	72
Hydration	144	144	72	144	144	72
RH	72	72	-	72	18	72
Salt freezing and thawing resistance						72
Total	432	432	180	432	378	360

m = month

Appendix 2.8 – Mix proportions and strength of specimen in study of silica fume concrete.

Material/w/c	0.22	0.25	0.24	0.33	0.36	0.47	0.48	0.58
Quartzite 8-12 mm	1360	1310	1310	1210	1160	1150	1150	1150
Gravel 0-8 mm	525	630	549	723	730	846	825	812
Cement, low-alkaline	484	456	476	400	389	303	298	299
Silica fume	48	-	48	-	39	-	30	-
Superplasticizer	13.3	8.84	7.78	3.35	3.07	3.01	2.13	-
Density	2530	2510	2500	2470	2460	2440	2450	2420
Aggregate content	0.71	0.74	0.75	0.75	0.73	0.71	0.73	0.70
Air content (%)	0.95	1.5	0.8	1.4	1.1	1.1	0.95	0.75
Workability (vebe)	29	34	13	25	12	9	12	15
Strength – 1 month (MPa)	114	93	112	77	93	58	65	38
- 3 months	128	104	128	91	100	70	76	45
- 15 months	142	121	139	105	104	78	81	51
- 90 months	139	121	131	106	106	74	79	49
- 155 months	141	129	142	114	117	80	94	56

Appendix 2.9 – Mix proportions (kg/m³) and fresh properties of concrete for shrinkage and creep tests.

Material	NC	SCC35	SCC35SF	SCC35Ø55	SCC40
Pea gravel 4-8 mm	904	475	498	475	467
Crushed stone 0-4 mm	904	627	664	627	615
Crushed stone 2-4 mm	0	206	221	206	203
Quartzite sand 0.1-1 mm	0	303	332	303	299
Limestone powder 40 µm	0	140	0	140	148
CEMII/A-D-52.5	452	466	498	466	447
Water	149	168	169	168	179
w/b	0.33	0.36	0.34	0.36	0.40
Polycarboxylic ether		9.08	11.94	9.08	11.02
Viscosity agent					2.50
Melamine formaldehyde	6.33				
Density	2414	2394	2393	2394	2368
Aggregate content including limestone powder	0.75	0.73	0.72	0.73	0.73
Slump flow until 500 mm diameter, T_{50} (s)	-	7	10	7	9
Slump flow (mm)	(400)	740	650	740	570
V-funnel (s)	-	12	20	12	18
Separation ratio of aggregate	-	0.96	1.01	0.96	0.97
L-box ratio	-	1	0.75	1	0.8
28-day 100-mm cube strength (MPa)	91	111	96	111	85

NC = normal concrete; SCC = self-compacting concrete; SF = silica fume; 35 = w/b; Ø = diameter of cylinder.

Appendix 2.10 – Development over time of elastic modulus and creep coefficient of concrete 35SF.

Time (days)	Compliance (millionths/MPa)	E-modulus	Loading	Unloading
0.002	25.9	38.7	0.00	0.00
0.005	26.09	38.4	0.01	0.01
60	44.19	22.7	0.71	0.80
125	48.99	20.4	0.89	1.01
315	51.890	19.3	1.00	1.14
550	54.09	18.5	1.09	1.24
550	31.39	44.0	1.21	1.38
556	26.3	36.0	1.02	1.16

Appendix 2.11 - Constants in equation (2.2)

Type of cement and concrete strength	s
Slowly hardening, concrete strength ≤ 60 MPa	0.38
Normal or rapid hardening cement, concrete strength ≤ 60 MPa	0.25
Rapid hardening high-strength cement, concrete strength ≤ 60 MPa	0.20
All types of cements, concrete strength > 60 MPa	0.20

Appendix 2.12 - Constants in equations (2.10) and (2.11)

Type of cement	α_{as}	α_{ds1}	α_{ds2}
Slowly hardening	800	3	0.13
Normal or rapid hardening cement	700	4	0.12
Rapid hardening high-strength cement	600	6	0.12

Appendix 2.13 - Mix proportions and properties of concrete (kg/m³).

Material	32G	32H	32N	40G	40H	40N	45G	45H	45N
Cement, c	448	448	448	400	399	401	360	358	356
Water	143	148	143	160	159	160	166	161	162
Sand	555	551	555	704	701	705	749	746	742
Gravel	1202	1193	1202	1040	1035	1040	1039	1035	1028
AEA (‰/c)	3.22	4.56	1.19	1.15	1.08	0.31	1.29	5.57	0.19
Superplast. (%/c)	2.95	2.95	1.03	1.15	1.38	0.6	0.92	2.01	0.45
VMA (%/c)	0.06	0.08		0.08	0.15		0.1	0.26	
DAA (‰/c)		0.075			0.123			0.31	
Air content (fresh)	0.063	0.057	0.057	0.07	0.073	0.07	0.06	0.065	0.068
Density	2364	2352	2354	2310	2300	2308	2320	2310	2290
Slump (mm)	180	190	160	200	230	190	180	190	170
Strength (34 d,MPa)	54.1	52.3	57.4	49.8	50.2	50.9	46.3	40.8	44.1
Air content (hard.,%)	0.05	0.04	0.046	0.042	0.059	0.058	0.042	0.086	0.04
Spacing factor, L (mm)	0.178	0.25	0.241	0.234	0.168	0.256	0.377	0.152	0.336
Elongation, 300 c. (‰)	0.765	0.491	0.666	0.861	0.973	0.404			
Salt-frost 50 c. (kg/m²)	2.17	2.39	1.45	1.93	1.63	0.81	4.9	2.95	4.82

Notations: d = days' age, AEA = air-entraining admixture, DAA = de-airing- admixture, G = vela gum, H = hydroxypropyl methylcellose, HPMC, N = normal concrete, VMA = Viscosity-Modifying Admixtures, 32 = w/c.

APPENDIX 3

Appendix 3.1 – Mix composition and properties of NC cast by Vattenfall.

Appendix 3.2 – Mix composition and properties of SCC cast at LTH.

Appendix 3.1 – Mix composition (kg/m³) and properties of NC and SCC. (kg/m³)

w/c – U=submerged concrete – S=SCC – air content (%)	45U8	46U11	48U4	48S6	48U4	49U3	49V6	50U3	51U4	52U1	55V2	78U2
Notations	AUV1%	AUV2%	UVNorm	SCC	AUV	AUVrefv	K40	AUV 32	AUV16	UVN	BOR	AUV
Date	5-apr.	4-apr.	27-feb.	8-okt.01	28-feb.	4-apr.	27-feb.	11-okt.01	11-okt.01	27-sept.01	?	8-okt.01
Total aggregate	1654	1537	1745	1639	1743	1742	1757	1741	1783	1749	1780	1666
Limestone powder				173								
CEM I42.5BV/SR/LA	402	374	405	371	404	404	395	414	384	405	350	386
Air-entrainment (fir oil, g/m³)	4000	7500		370			200					
Air-entrainment (%/binder)	1	2		0			0.5					
Anti-wash out additive	2	2			2	2		2	2		2	8
Water	182	173	194	179	194	196	192	205	194	206	192	302
Superplasticiser I				4.8								
Superplasticiser I (%/binder)				1.3								
Superplasticiser II	6.40	6.00	4.70		7.40	6.50	5.90	6.60	5.80	6.10	4.20	6.80
Superplasticiser II (%/binder)	1.59	1.60	1.16		1.83	1.61	1.49	1.59	1.51	5.80	1.20	1.76
Retarder			2.4		2	2			1.9	2.4		
Air content (%)	7.5	11	4	6	3.9	3	6	3	3.8	1	1.9	1.8
Slump (mm)	245	255	140	260	225	240	50	250	230		275	235
Slump flow (mm)	460	500	480	570	370	450	350	510	500		530	460
L-box	0.20	0.43									0.93	0.28
w/b	0.45	0.46	0.48	0.48	0.48	0.49	0.49	0.50	0.51	0.51	0.55	0.78
w/p	0.45	0.46	0.48	0.33	0.48	0.49	0.49	0.50	0.51	0.51	0.55	0.78
Density	2238	2084	2344	2365	2341	2342	2344	2360	2361	2360	2322	2354
Aggregate/Cement	4.11	4.11	4.31	4.42	4.31	4.31	4.45	4.21	4.64	4.32	5.09	4.32
Aggregate/Density	0.74	0.74	0.74	0.69	0.74	0.74	0.75	0.74	0.76	0.74	0.77	0.71
Aggregate/Powder	4.11	4.11	4.31	3.01	4.31	4.31	4.45	4.21	4.64	4.32	5.09	4.32
Strength, 28 days (MPa)	50.5	27.5	63.0	76.0	61.4	59.3	60.0	68.0	65.0	59.0	33.6	26.0

Appendix 3.2 – Mix composition and properties of SCC cast at LTH.

w/b – air content (%)	35S1	35S4	35S8	40S4	40S8	45S8
Date	2002.04.17	2002.06.05	2002.05.22	2002.08.30	2003.02.27	2003.03.11
Lenzhard 4-8 mm	480	464	452	457	444	446
Lenzhard 0-4 mm	633	612	596	602	585	588
Crushed stone 2-4 mm	208	201	196	198	192	193
Quartzite sand 0.1-1 mm	306	295	288	291	283	284
Limestone powder Köping 500	141	136	133	177	172	214
Blended cement Fortico 5R	470	454	442	405	393	354
Microair	0.0000	0.045	0.124	0.150	0.252	0.244
Water	169	164	159	162	157	159
Glenium 51 (wet)	9.17	8.86	8.63	8.72	8.48	8.52
Glenium 51 (%/powder)	2.0	2.0	2.0	2.2	2.2	2.4
Density	2419	2335	2275	2301	2236	2248
Air content (%)	1.1	3.9	7.0	5.0	7.9	7.4
Slump flow Ø (mm)	750	735	735	740	750	750
L-box	0.72	0.53	0.88	0.93	0.94	0.68
Strength (MPa)						
2 days	57.0	69.0	62.0	47.5	43.5	38.0
	60.5	67.5	61.0	43.5	47.0	36.5
2 days, average	58.8	68.3	61.5	45.5	45.3	37.3
28 days	117.5	95.0	97.0	70.5	81.5	85.5
	118.5	104.0	101.5	77.0	86.5	82.0
28 days, average	118.0	99.5	99.3	73.8	84.0	83.8
90 days	126.0	116.0	101.0	91.5	85.50	90.50
	105.0	114.5	85.0	89.0	95.00	90.50
90 days, average	115.5	115.3	93.0	90.3	90.25	90.50

APPENDIX 4

Appendix 4.1 – Internal freezing and thawing resistance for concrete delivered by Vattenfall

Appendix 4.2 – Internal freezing and thawing resistance for concrete cast at LTH

Appendix 4.3 – Internal freezing and thawing resistance for concrete cast BTC.

Appendix 4.4 – Salt freezing and thawing scaling for concrete from Vattenfall or cast at LTH

Appendix 4.1 – Internal freezing and thawing resistance for concrete delivered by Vattenfall

Concrete	Concrete	Sort	Start value			Average	100 cycles			Estimation	300 cycles			Estimation
45U8	AUV1%	(Hz)	6410.0	6350.0	6280.0	6346.7	6050.0	5860.0	1450.0	-29.8	1490.0	1470.0	1360.0	-77.3
45U8		(g)	672.0	671.0	673.0	672.0	655.9	645.3	520.0	-9.7	631.6	592.4	444.0	-17.3
46U11	AUV2%	(Hz)	5850.0	5730.0	5770.0	5783.3	5520.0	5310.0	5440.0	-6.2	5250.0	5000.0	5040.0	-11.9
46U11		(g)	629.0	622.0	630.0	627.0	613.2	602.6	613.4	-2.8	595.4	580.5	591.7	-6.0
48U4	UVNorm	(Hz)	6940.0	6890.0	6900.0	6910.0	0.0	0.0		-100.0				-100.0
48U4		(g)	694.0	701.0	700.0	698.3	0.0	0.0	0.0	-100.0				-100.0
48S6	SCC	(Hz)	6810.0	6860.0	6820.0	6830.0	6720.0	6750.0	6640.0	-1.9	6660.0	6650.0	6260.0	-4.5
48S6		(g)	684.3	685.6	683.2	684.4	683.8	685.2	683.2	0.0	678.0	679.0	677.0	-0.9
49U3T	AUVreft	(Hz)	6490.0	6540.0	6420.0	6483.3	0.0	0.0	0.0	-100.0				-100.0
49U3T		(g)	691.0	692.0	686.0	689.7	0.0	0.0	0.0	-100.0				-100.0
49U3V	AUVrefv	(Hz)	6600.0	6640.0	6600.0	6613.3	0.0	0.0	0.0	-100.0				-100.0
49U3V		(g)	695.0	693.0	694.0	694.0	0.0	0.0	0.0	-100.0				-100.0
49V6	K40	(Hz)	7020.0	6840.0	6850.0	6903.3	1500.0	6500.0	1500.0	-54.1	2410.0	1560.0	1510.0	-73.5
49V6		(g)	678.0	687.0	682.0	682.3	662.1	678.1	666.4	-2.0	647.9	666.6	639.5	-4.5
50U3	AUV32	(Hz)	6830.0	6750.0	6170.0	6583.3				-100.0	0.0	0.0	0.0	-100.0
50U3		(g)	700.6	697.6	703.0	700.4	281.0	451.0	299.0	-50.9	0.0	0.0	0.0	-100.0
51U4	AUV16	(Hz)	6750.0	6760.0	6580.0	6696.7				-100.0	0.0	0.0	0.0	-100.0
51U4		(g)	689.2	692.4	690.1	690.6	207.0	264.0	250.0	-65.2	0.0	0.0	0.0	-100.0
52U1	UVN	(Hz)	6660.0	6650.0	6620.0	6643.3	1540.0	1730.0	1490.0	-76.1	0.0	0.0	0.0	-100.0
52U1		(g)	685.4	689.0	693.3	689.2	668.9	662.9	674.7	-3.0	0.0	0.0	0.0	-100.0
55V2	BOR	(Hz)	6800.0	6810.0	6790.0	6800.0	0.0	0.0	0.0	-100.0				-100.0
55V2		(g)	697.0	689.0	701.0	695.7	0.0	0.0	0.0	-100.0				-100.0
78U2	AUV	(Hz)	5540.0	5440.0	5440.0	5473.3	0.0	0.0	0.0	-100.0	0.0	0.0	0.0	-100.0
78U2		(g)	656.9	658.2	653.5	656.2	207.0	264.0	250.0	-63.4	0.0	0.0	0.0	-100.0

S = SCC; U=submerged concrete; 2 = air content (%)45 = w/c (%); 2% = 2% anti washing-out compound.

Appendix 4.2 – Internal freezing and thawing resistance for concrete cast at LTH

Concrete	Concrete	Sort	Start value			Average	100 cycles			Estimation	300 cycles			Estimation
35S1N	HPSCC	(Hz)	7400.0	7400.0	7410.0	7403.3	7380.0	7430.0	7380.0	-0.1	7260.0	7360.0	7330.0	-1.2
35S1N		(g)	724.4	724.6	726.5	725.2	724.1	724.3	726.0	-0.1	723.3	724.2	724.5	-0.2
35S1R	HPSCC	(Hz)	7450.0	7406.0	7420.0	7425.3	7440.0	7270.0	7310.0	-1.1	7330.0	6760.0	6830.0	-6.1
35S1R		(g)	727.9	727.6	723.7	726.4	727.2	727.1	722.9	-0.1	726.4	724.3	719.9	-0.4
35S4N	HPSCC	(Hz)	7390.0	7300.0	7340.0	7343.3	7300.0	7270.0	7320.0	-0.6	7350.0	7250.0	7270.0	-0.7
35S4N		(g)	716.5	714.3	717.0	715.9	716.6	719.1	716.1	0.2	715.6	713.7	716.5	-0.1
35S4R	HPSCC	(Hz)	7380.0	7280.0	7180.0	7280.0	7290.0	7050.0	6990.0	-2.3	7000.0	6160.0	5830.0	-13.0
35S4R		(g)	712.8	714.2	716.4	714.5	711.3	712.7	715.5	-0.2	708.7	709.4	710.5	-0.7
35S8N	HPSCC	(Hz)	7060.0	7040.0	7200.0	7100.0	7030.0	7000.0	7170.0	-0.5	7003.0	7010.0	7170.0	-0.5
35S8N		(g)	689.2	686.0	689.3	688.2	688.6	686.7	688.8	0.0	687.7	685.7	687.8	-0.2
35S8R	HPSCC	(Hz)	7090.0	7030.0	7160.0	7093.3	6980.0	7000.0	7080.0	-1.0	6970.0	6920.0	7020.0	-1.7
35S8R		(g)	689.3	687.5	690.7	689.2	688.6	686.7	689.8	-0.1	687.3	686.0	688.1	-0.3
40S4N	HPSCC	(Hz)	7040.0	6980.0	7030.0	7016.7	7000.0	6870.0	6920.0	-1.2	6880.0	6900.0	6910.0	-1.7
40S4N		(g)	688.6	684.7	690.4	687.9	687.8	683.8	689.6	-0.1	684.5	682.0	686.5	-0.5
40S4R	HPSCC	(Hz)	7050.0	7000.0	7000.0	7016.7	6910.0	6880.0	6830.0	-2.0	6790.0	6790.0	6750.0	-3.4
40S4R		(g)	689.0	688.8	684.2	687.3	687.2	683.2	687.7	-0.2	683.9	679.2	684.3	-0.7
40S8N	HPSCC	(Hz)	6980.0	6990.0	6830.0	6933.3	6910.0	6940.0	6780.0	-0.8	6830.0	6880.0	6770.0	-1.5
40S8N		(g)	662.0	670.5	667.1	666.5	661.5	670.0	666.9	-0.1	656.9	666.0	662.9	-0.7
40S8R	HPSCC	(Hz)	6920.0	6870.0	6930.0	6906.7	6850.0	6790.0	6740.0	-1.6	6710.0	6590.0	6290.0	-5.5
40S8R		(g)	665.7	663.3	662.7	663.9	665.8	662.5	662.6	0.0	663.0	658.5	655.6	-0.7
45S8N	HPSCC	(Hz)	7190.0	7150.0	7270.0	7203.3	7090.0	7050.0	7220.0	-1.2	6840.0	6480.0	6960.0	-6.2
45S8N		(g)	705.6	700.6	698.0	701.4	704.1	699.8	693.9	-0.3	695.2	693.3	686.6	-1.4
45S8R	HPSCC	(Hz)	7130.0	7220.0	7220.0	7190.0	5960.0	6890.0	6980.0	-8.1	1500.0	1310.0	1590.0	-79.6
45S8R		(g)	697.8	703.1	700.2	700.4	685.2	700.9	698.4	-0.8	662.4	691.7	686.9	-2.9

35 = w/c (%); S = 7.5% silica fume; 4 = air content (%).

Appendix 4.3 – Internal freezing and thawing resistance for concrete cast at BTC.

Concrete	Concrete	Sort	Start value			Average	100 cycles			Estimation	300 cycles			Estimation
35S4NC	C3	(Hz)	6800.0	6700.0	6760.0	6753.3	6760.0	6620.0	6740.0	-0.7	5050.0	5670.0	5940.0	-17.8
35S4NC		(g)	599.2	596.6	594.9	596.9	598.7	596.4	594.4	-0.1	598.5	597.0	594.0	-0.1
35S4NF	C4	(Hz)	6920.0	6970.0	6920.0	6936.7	6820.0	6860.0	6840.0	-1.4	6630.0	6700.0	6750.0	-3.5
35S4NF		(g)	608.4	607.4	606.4	607.4	608.0	606.9	605.8	-0.1	607.2	605.0	604.4	-0.3
35S4RC	C1	(Hz)	6800.0	6810.0	6810.0	6806.7	6230.0	6430.0	5890.0	-9.2	1160.0	1550.0	3430.0	-69.9
35S4RC		(g)	597.6	602.6	600.7	600.3	598.4	603.1	602.1	0.1	598.4	603.2	600.7	0.1
35S4RF	C2	(Hz)	6880.0	6930.0	7000.0	6936.7	6850.0	6730.0	6030.0	-5.8	6550.0	5880.0	482.0	-38.0
35S4RF		(g)	602.6	603.8	612.4	606.3	602.3	603.4	613.2	0.0	600.7	601.7	611.5	-0.3
40S4NC	B3	(Hz)	6410.0	6660.0	6620.0	6563.3	6370.0	6520.0	6550.0	-1.3	6290.0	6480.0	6520.0	-2.0
40S4NC		(g)	566.4	584.7	581.0	577.4	565.2	583.8	580.0	-0.2	561.9	576.8	581.4	-0.7
40S4NF	B4	(Hz)	6780.0	6630.0	6700.0	6703.3	6650.0	6540.0	6550.0	-1.8	6540.0	6510.0	6550.0	-2.5
40S4NF		(g)	590.5	585.4	585.8	587.2	589.5	584.3	584.3	-0.2	586.8	582.1	581.0	-0.7
40S4RC	B1	(Hz)	6650.0	6800.0	6820.0	6756.7	6640.0	6690.0	6660.0	-1.4	6610.0	6590.0	6610.0	-2.3
40S4RC		(g)	581.6	589.4	593.9	588.3	580.4	588.9	593.2	-0.1	576.4	586.8	590.8	-0.6
40S4RF	B2	(Hz)	6840.0	6770.0	6770.0	6793.3	6750.0	6700.0	6700.0	-1.1	6710.0	6620.0	6650.0	-2.0
40S4RF		(g)	597.4	596.3	594.1	595.9	596.7	595.7	593.4	-0.1	593.3	593.6	590.5	-0.6
45S4NC	A3	(Hz)	6160.0	6200.0	6020.0	6126.7	6050.0	6160.0	5950.0	-1.2	6050.0	6020.0	5820.0	-2.7
45S4NC		(g)	517.2	511.8	510.2	513.1	515.2	509.6	508.4	-0.4	511.5	505.1	502.6	-1.3
45S4NF	A4	(Hz)	6490.0	6410.0	6480.0	6460.0	6340.0	6180.0	6340.0	-2.7	6250.0	6080.0	6140.0	-4.7
45S4NF		(g)	531.3	537.6	531.0	533.3	529.4	535.5	528.7	-0.4	524.9	531.7	523.6	-1.2
45S4RC	A1	(Hz)	6040.0	6130.0	6260.0	6143.3	5900.0	6000.0	6050.0	-2.6	5750.0	6020.0	5940.0	-3.9
45S4RC		(g)	508.3	517.3	512.1	512.6	506.4	516.6	510.3	-0.3	501.7	513.0	505.6	-1.1
45S4RF	C3	(Hz)	6440.0	6530.0	6360.0	6443.3	6240.0	6360.0	6250.0	-2.5	6150.0	6220.0	6150.0	-4.2
45S4RF		(g)	528.3	535.8	529.7	531.3	526.6	533.0	527.7	-0.4	521.2	527.8	521.6	-1.5

35 = w/c (%); S = 7.5% silica fume; 4 = air content (%); C = crest; F = foot; N = near the; R = remote.

Appendix 4.4 – Salt freezing and thawing scaling for concrete (g/m²)

		Start				28 Cycles			Estimation	56 Cycles			Estimation	112 Cycles			Estimation
	Specimen	1	2	3	av.	1	2	3		1	2	3		1	2	3	
35SRef	HPSCC	757	770	745	757	756	769	745	26	756	769	745	34	756	768	745	40
35S1N	HPSCC	736	710	702	716	735	710	701	32	735	709	700	65	731	706	698	165
35S1R	HPSCC	680	683	686	683	676	659	684	381	675	639	683	677	673	612	681	1083
35S4N	HPSCC	644	643	655	648	637	641	654	139	632	640	653	236	626	638	649	385
35S4R	HPSCC	634	644	627	635	592	637	623	696	525	634	620	1673	449	626	616	2823
35S8N	HPSCC	660	668	643	657	659	667	642	43	659	666	641	75	657	665	640	131
35S8R	HPSCC	655	645	652	651	646	643	650	161	639	642	648	294	633	641	645	424
40S4N	HPSCC	614.5	611.8	640.0	622	611.9	609.2	638.8	85	610.0	606.5	636.0	183	607.4	604.0	634.4	271
40S4R	HPSCC	628.8	629.6	632.6	630	615.8	627.1	629.4	245	603.5	623.0	626.5	499	589.5	618.3	621.2	814
40S8N	HPSCC	604.9	581.6	581.6	589	603.7	580.1	580.0	57								
40S8R	HPSCC	591.3	590.1	590.7	591	587.4	587.5	587.5	130								
45S8N	HPSCC	619.8	623.8	613.5	619	616.8	621.1	610.8	113								
45S8R	HPSCC	619.6	621.7	607.4	616	612.8	616.8	567.4	693								
45U8	AUV1%	672	679	687	679	634	647	651	1327	594	609	602	2918	523	548	521	5272
46U11	AUV2%	621	618	605	615	615	613	601	198	604	605	595	499	594	596	585	816
49U3T	AUVreft	639	665	647	650	490	473	445	6769	0	0	0	24323	0	0	0	23064
49U3V	AUVrefv	684	695	696	692	620	649	639	2082	463	500	369	9263	0	0	0	24530